



Volcanogenic features of IOCG deposits of North Carajás, Brazil, and related constraining evidence

Sérgio Luiz Martini^{1*} , Ana Maria Dreher¹ 

¹Independent geologist. Rua Pedro Weingartner 168/601, Rio Branco - Porto Alegre - Brazil, CEP: 90430-140

Abstract

The magnetitic Cu-Au (IOCG) deposits of north Carajás, Amazonian Craton, Brazil, are hosted in the Neoproterozoic (2.76 Ga), dominantly basaltic-greywacke Itacaiúnas metavolcanic-sedimentary sequence that evolved in a continental rift setting. The mainstream interpretation of these deposits is that they are epigenetic, though they do show common features observed in syngenetic deposits of volcanogenic affiliation. The features include hosting tectonic and geological settings with coeval granitic and mafic heat sources; evidence of syn depositional faulting, exemplified by intraformational fragmental rocks; attending hydrothermal alteration represented by extensive Na-Ca, spilitic and chloritic alteration along with deposit-scale magnesian (chlorite, dalmatianite), potassic (biotite) and aluminous (andalusite, sillimanite) products; strata-bound morphology, with ore hosted in banded oxide-silicate facies iron-formations and debris flow breccia bodies located at eruptive breaks, where quiescent waning volcanic conditions favorable to ore deposition prevail; and near-deposit exhalites, for instance, oxide iron-formation, metachert and laminated quartz-amphibole-tourmaline-garnet rocks, that may extend laterally away from the deposits constituting ore-equivalent horizons. This altogether suggests that the deposits are intrinsic components of the stratigraphic package they are hosted in and constitute syngenetic hydrothermal products. Regarding constraining evidence – as represented by fluid inclusion, stable isotope and geochronological data – the available information does not rule out syngeneses. Fluid inclusions reveal highly saline mineralizing fluids that explain the low sulfur content of ore. Sulfide sulfur signature is near zero per mil, usually found in Archean volcanogenic deposits. Available stable C, O, H and B isotopic data can to a good extent be explained in connection with syngenetic systems, with particular reference to the evaporitic boron isotopic signature of tourmaline constituting firm argument against granite-related epigenesis, whereas evidence of metamorphism is exiguous. Pb-Pb ages on sulfides usually coincide with the age of the volcanic-sedimentary host unit, whereas supposedly robust epigenesis supporting ages have been considered doubtful due to, for example, problematic dating of granitic sources and/or geological inadequacy through contradicting dated contact relationships. Considering this scenario, we maintain here our former position that the scrutinized deposits represent synvolcanic IOCG hydrothermal systems. Metamorphism- and deformation-related complexity mar the unraveling of this metallogenic connection, blurring detail features and nourishing misinterpretation. The large-scale geological integrity of the deposits, however, has been greatly preserved, as per the coherent stratigraphic distribution, strata-bound morphology and typological attributes. Unexpectedly, they consist of disseminated sulfides, with magnetite taking the place of the usual pyrite of VMS deposits, a peculiar aspect that is nonetheless shared by other volcanogenic deposits.

Article Information

Publication type: Review Article
Received 30 August 2023
Accepted 26 February 2024
Online pub. 8 March 2024
Editor: Carlos Spier

Keywords:
Carajás
IOCG
Metallogeny
Economic Geology
Ore deposit
Typological features

*Corresponding author
Sérgio Luiz Martini
E-mail address: martini.s@uol.com.br

1. Introduction

This paper deals with the main magnetitic Cu-Au (IOCG) deposits of the north Carajás Province, hosted in the Neoproterozoic metavolcanic-sedimentary rocks of the Itacaiúnas Group, with particular emphasis on their deposit-scale geologic setting. The work was designed specifically to the study of volcanogenic features and related constraining evidence and therefore a general description of the geology

of these deposits is not included. We suggest the interested readers to look for further details in the sources mentioned in the article. The deposits dealt with are Pojuca, Salobo, Igarapé Bahia, Gameleira, Igarapé Cinzento (GT-46), Furnas and Grota Funda. The discovery of the first deposits dates back to the second half of the 1970s and, based in the consultancy work of R.W. Hutchinson (1977, 1979), the early findings – Pojuca and Salobo – were characterized straightforwardly as volcanogenic deposits, based essentially



on an empiric geological features (Hirata et al. 1982; Farias and Saueressig 1982; Docegeo 1988; Vieira et al. 1988). The deposits, however, are not standard volcanogenic massive sulfides (VMS) of the type usually found hosted in subaqueous volcanic sedimentary packages. They are instead “massive oxide” deposits (Hutchinson 1979) in which sulfides occur disseminated in a magnetite-rich rock similar to a mixed oxide-silicate facies iron-formation. Based on this aspect, inter alia, the syngenetic interpretation shifted in time towards the epigenetic side as they were compared with so-called IOCG deposit group (Winter 1994; Huhn and Nascimento 1997; Tallarico et al. 2005; Xavier et al. 2017). The acronym refers pragmatically to the main metallic content (iron oxide-copper-gold) of the deposits, which are found in a variety of geologic environments (Hitzman 2000; Williams et al. 2005). The shift took place in connection with the application of laboratory studies involving particularly fluid inclusions, stable isotopes, litho geochemistry and geochronology (Lindenmayer et al. 2001; Pimentel et al. 2003; Silva et al. 2005; Requia and Fontboté 2000; Requia et al. 2003; Tallarico et al. 2005; Toledo et al. 2017, 2019; Melo et al. 2017, 2019a,b), whose results have been almost entirely interpreted from the epigenetic standpoint. However, part of these results is in agreement with the syngenetic side, leading several authors to keep aligned with this genetic view (Almada and Villas 1999; Villas and Santos 2001; Dreher and Xavier 2001; Dreher 2004; Dreher et al. 2008, 2018; Schwarz and Frantz 2013). Moreover, the fact is that drawbacks and ambiguities may occur in connection with the general interpretation of results of the mentioned studies (Huston 1999; Heinrich et al. 2000; Marshall et al. 2000; Franklin et al. 2005; Suzuki et al. 2000, 2001; Dreher et al. 2008; Nouzaki et al. 2014; Trunfull et al. 2020; Zhang and Audétat 2023), emphasizing therefore the significance of using empirical observation and geological reasoning in their interpretation.

Considering this altogether, the scope of the present paper is to compile volcanogenic features of the Itacaiúnas-hosted iron oxide Cu-Au deposits of north Carajás and scrutinize the data obtained from the mentioned laboratory studies regarding their capacity to discriminate between syngenetic versus epigenetic origins. This task is exercised through an oriented review of the literature using the tools presented in the section below.

At this point, it must be reemphasized that the work was oriented to the search for volcanogenic features rather than to describing the deposits. Descriptions would make the article unnecessarily longer and additionally would not impart the adequate emphasis on volcanogenic features, which is the main scope of the study.

2. Methodology

Geologic information on the deposits has been compiled following the concept of *gitology*, which prescribes an essentially descriptive study of mineral deposits themselves and their related geologic environment, based on quality fieldwork. This anatomy-based approach is still the main current approach used in the prospection for base and precious metals, and is bound to remain so for long (Jébrak and Marcoux 2014, p. 531-532). The descriptive approach has been used to define deposit types, i.e., groups of deposits that share a significant amount of common geologic features,

and, perhaps more importantly, to achieve an anatomical understanding of a mineral deposit system (Blondel 1955; Routhier 1963, 1983; Dixon 1979; Eckstrand et al. 1996; Martini 2002; Goodfellow 2007; Jébrak and Marcoux 2014, p. 41-44). According to this approach, the descriptive information on the Itacaiúnas-hosted Cu-Au deposits of north Carajás is compiled from the literature with particular reference to critical or essential attributes of volcanogenic deposits. These attributes include mainly magmatic heat sources, regional hydrothermal alteration zones, synvolcanic faulting evidence, deposit-scale alteration, and associated exhalites, cap rocks and ore-equivalent horizons (Sangster 1972; Large 1992; Franklin et al. 2005; Dubé et al. 2007; Galley et al. 2007; Gibson et al. 2007). The compilation is presented in itemized form for each of the mentioned deposits.

The above approach represents a more pragmatic and factual counterpart to a process-based approach, focused on the systemic analysis of critical aspects in the genesis of deposits with the aid of continuously more efficient analytical tools (Jébrak and Marcoux 2014), which is obviously also useful in exploration targeting (cf. mineral system concept, McCuaig and Hronsky 2014). Genetic aspects are also to be considered in the present exercise, particularly in connection with interpretation of results of the above-mentioned laboratory studies, which may constrain or reinforce the validity of geologic observation.

The laboratory results considered here have been also compiled from the literature and are mostly focused on ore and mineralization-related materials. This constraining evidence is displayed through tables for each deposit showing fluid inclusion, stable isotope and geochronological data. The interpretation background is based on reviews such as those of Huston (1999), Shanks III (2014), and Jébrak and Marcoux (2014) as well as from general literature information. Our tenets in the present study are that interpretation of laboratory results benefit from, and should therefore take into account, the deposit related features and that there must be a common bottom line between the field and laboratory data sets.

3. Regional geology and metallogeny

The area treated herein constitutes the northern portion of the Carajás tectonic province in the SE border of the Amazon Craton (Fig. 1, inset), the largest basement unit of the South America Platform in central-northern Brazil and adjacent countries (Almeida et al. 1981; Cordani et al. 2000; Tassinari et al. 2000). The Amazon Craton was stabilized at the end of the Mesoproterozoic Era (ca. 1 Ga) with the Carajás Province consisting essentially of a Meso to Neoproterozoic basement and a platform cover. It shows a general W-NW tectonic trend abutting the N-S-trending Neoproterozoic Araguaia fold belt to the east (Fig. 1).

The Carajás Province has been divided into the Rio Maria Domain to the south and the Carajás Domain to the north (Vasquez et al. 2008). The former consists of a Mesoarchean granite-greenstone terrain with a Neoproterozoic platform cover and Paleoproterozoic cratogenic granites. The latter, described in more detail below, is essentially Neoproterozoic in age and shows as main characteristic a significant metallic endowment, particularly in the form of world-class volcanic-sedimentary-hosted iron and copper-gold, sedimentary cover-hosted manganese and lateritic nickel deposits (Hutchinson

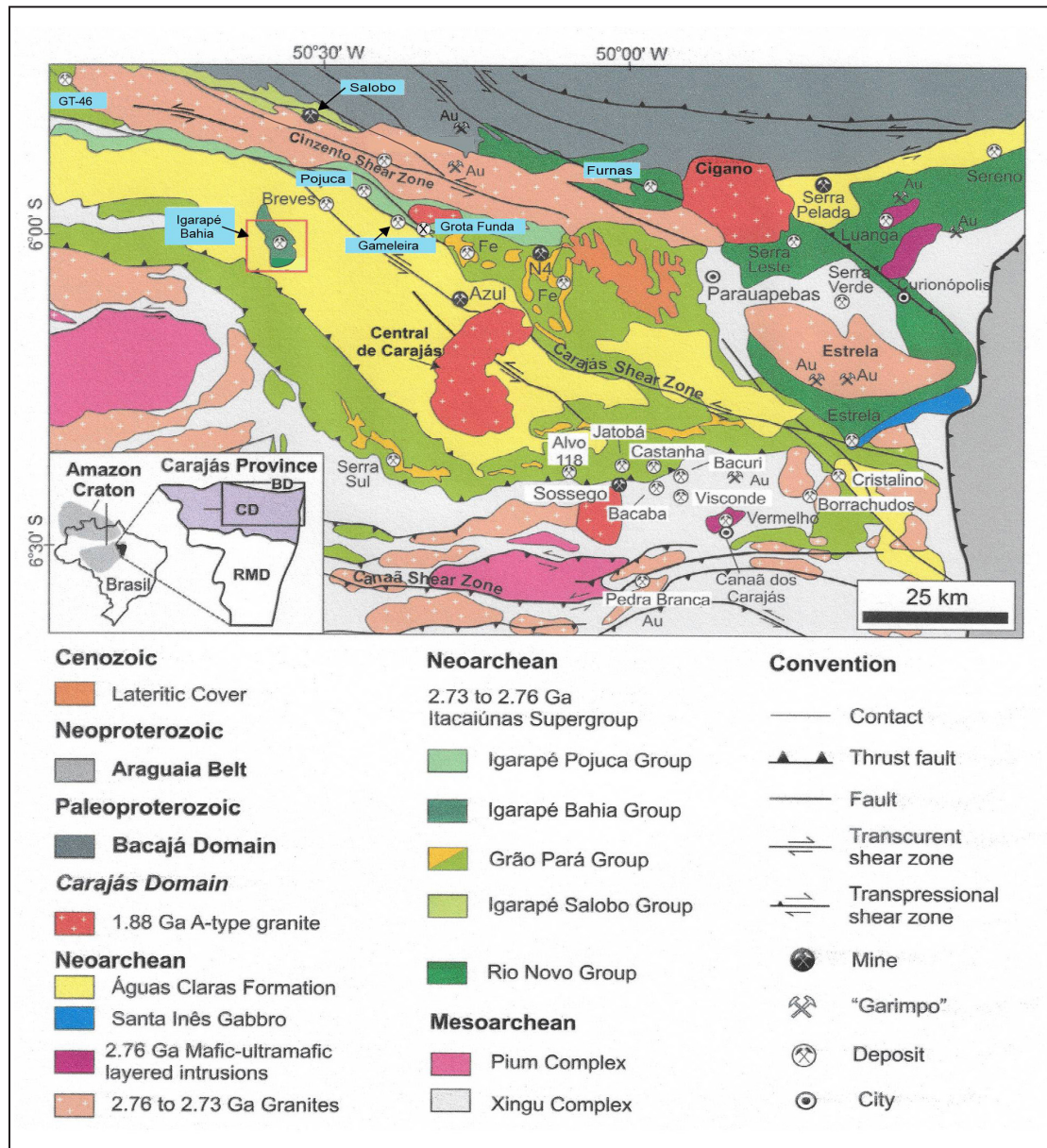


FIGURE 1. Geological map and mineral deposits of the central and eastern Carajás mineral province with the IOCG deposits studied in this paper marked in blue and the Igarapé Bahia camp squared off in red (from Melo et al. 2019a, based on Docegeo 1988 and Vasquez et al. 2008). The limits of the Carajás Domain (CD), Rio Maria Domain (RMD) and the Bacajá Domain (BD) are shown in the inset at the lower-left side of the figure.

1979; Bernardelli et al. 1982; Docegeo 1988; Xavier et al. 2017). North of the Carajás Domain lies the Bacajá Domain, which encompasses mainly Archean / Paleoproterozoic granitoids and granulites with few greenstone belt strips.

The main geological units of the Carajás Domain, according to Vasquez et al. (2008), are basement gneisses of the Xingu Complex and granulites and norites, exemplified by the Pium Complex; the Itacaiúnas and Rio Novo groups of greenstones; deformed A-type granites (e.g., the Estrela and Igarapé Gelado batoliths); the extensive Águas Claras platform sedimentary cover; and a number of Paleoproterozoic anorogenic granites (e.g., the Central and Cigano stocks).

The Itacaiúnas Supergroup of greenstones and the foliated granites are of utmost importance regarding the deposits dealt with here. The former hosts, and has a parental genetic connection with, the strata-bound Cu-Au deposits treated

herein (Dreher 2004; Dreher et al. 2008; Villas et al. 2001; Villas and Santos 2001; Dreher and Xavier 2001; 2005; Almada and Villas 1999), whereas the latter may have contributed heat and some of the mineralizing fluids themselves to the generation of the strata-bound deposits (Requia et al. 2003; Tallarico et al. 2005).

The Itacaiúnas greenstones consist of metabasalts overlain by iron-formation and turbidites or other siliciclastic rocks that were likely deposited in an extensional continental rift setting and submitted to greenschist to granulite facies metamorphism (Hirata et al. 1982; Docegeo 1988). They return robust depositional ages, for instance, U-Pb from zircons of volcanic rocks of 2.73 to 2.76 Ga (Vasquez et al. 2008). The metamorphism, to which some authors have related the mineralization (Winter 1994; Toledo 2017), is poorly constrained in terms of age. Available ages are limited

and include 2.73 Ga and 2.76 Ga for the Pojuca and Salobo deposits, respectively (Machado et al. 1991).

The foliated granites of north Carajás have geochemical traits of A-type granites (Barros et al. 2009; Dall'Agnol et al. 2012), and their geochronological results record nearly the same range of the Itacaiúnas units (Barros et al. 2001; Trunfull et al. 2020). Of particular significance is the Igarapé Gelado granite (2.73 Ga, Barbosa et al. 2001; 2.76 Ga, Melo et al. 2017), which covers an area of approximately 200 km x 10 km and which is central to all deposits included in this study, except for Igarapé Bahia (Fig. 1). A lesser group of small and localized deformed granites returns younger Neoproterozoic ages, as represented by the Old Salobo and Itacaiúnas granites of ca. 2.57 Ga (Machado et al. 1991; Souza 1996; Melo et al. 2017). Important strata-bound Cu-Au mineralization has been interpreted as genetically linked with these granites (Requia et al. 2003; Tallarico et al. 2005). However, Barros et al. (2001) and Toledo et al. (2021), based on the defective zircons used in the determinations, interpret the above age as a minimum one and consider this group of granites as part of the above-described 2.73-2.76 Ga regional granitic manifestation. Therefore, these authors turn down the mentioned epigenetic ca. 2.57 Ga granite-related metallogenic episode.

Overlying unconformably the Itacaiúnas greenstones and their strata-bound Cu-Au deposits (Barreira et al. 1999; Siqueira et al. 2001) is the Águas Claras Formation (Fig. 1), which represents a siliciclastic marine-fluvial platform cover (Araújo Filho 2018). Its age is constrained by basic intrusive bodies - of ca. 2.65 Ga (Pb-Pb, zircon, Dias et al. 1996), to 2.67 Ga (Pb-Pb xenocrystic zircon, Tallarico et al. 2005), to 2.71 Ga (U-Pb, zircon, and Pb-Pb, sulfides, Mougeot et al. 1996a,b) and by siliciclastic rocks of 2.68 Ga (U-Pb, synvolcanic zircon, Trendall et al. 1998) and 2.76-2.78 Ga (U-Pb, youngest identified detrital zircons, Mougeot et al. 1996a, Melo et al. 2019a). In addition, Mougeot et al. (1996b) reported ages on sulfides of 2.06 Ga and 1.88 Ga, linking them, respectively, to sulfide remobilization related to an undetermined regional event and to the anorogenic granitic magmatism of Carajás dealt with below.

A further significant episode of felsic intrusive magmatism is represented by anorogenic stocks of ca. 1.88 Ga (Dall'Agnol et al. 1994, 1997), including the Central and Cigano granites (Fig. 1). They also formed epizonal Cu-Au mineralization (Tallarico et al. 2004; Xavier et al. 2005a), which may be hosted in the older units and superimpose the Neoproterozoic strata-bound Cu-Au deposits (Soares et al. 1999; Botelho et al. 2005; Schwarz and Frantz 2013; Pollard et al. 2019).

Structure is dominated by W-NW trending lineaments representing systems of strike slip fault zones (Fig. 1). Two main WNW-ESE-trending transcurrent systems, Cinzento and Carajás, dominate the regional structural scenario of the Carajás Domain (Pinheiro and Holdsworth 2000). They have been characterized as transpressional (ca. 2.7 Ga) and transtensional (ca. 2.6-2.5 and 1.8 Ga) reactivation systems whose general trace was inherited from the mylonitic Itacaiúnas shear zone, with associated metamorphism and upright folding, that developed earlier (ca. 2.8 Ga) in the granitoid-granulitic basement (Pinheiro and Holdsworth 2000). An intervening (ca. 2.76 Ga?) extensional episode responsible for the implantation of the Grão Pará basin took place, creating tectonic conditions compatible with the development of exhalative hydrothermal systems. Pinheiro

and Holdsworth (2000) also adduce that protracted brittle processes and related increased fault-zone permeability occurred during tectonic reactivation, allowing for extensive circulation of mineralizing fluids. Similarly, Tavares et al. (2018) indicated a prolonged complex structural history for the northeast sector of the Carajás domain. This aspect seems to have been taken into consideration in the interpretation of geochronological signatures shown by some of the strata-bound deposits of north Carajás (Melo et al. 2017; Toledo et al. 2017, 2019; Trunfull et al. 2020).

4. Pojuca Corpo 4

4.1. Volcanogenic features

Since the early accounts by Hutchinson (1977,1979), Pojuca Corpo 4 (Fig. 1) has been studied by several authors, including Hirata et al. (1982), Beisiegel and Farias (1978), Farias et al. (1984), Medeiros Neto (1986a,b), Docegeo (1988), Saueressig (1988), Winter (1994), Schwarz and Frantz (2013) and Dreher et al. (2018). According to these sources, the likely volcanogenic-related features and aspects of Pojuca Corpo 4 include the following ones (Fig. 2): (1) Early recognition of the volcanogenic nature of the Pojuca mineralization based on, inter alia, geological setting, strata-bound and stratiform morphology, identification of stringer ore, slump-related and soft sedimentary syndepositional folds, typical anthophyllite-cordierite alteration rocks, exhalites like ore-bearing iron-formation and metachert, debris-flow nature of mineralized fragmental rocks, and magnetite-rich sulfide-poor ore mineralogy, leading to the denomination 'volcanogenic massive oxide' (Docegeo geologists, Hutchinson 1977, 1979). (2) Occurrence of a 1 to 2 km-wide gabbro body just NE of the deposit (Schwarz and Frantz 2013), associated with coarser metabasalts occurring northeast of the deposit (Fig. 2), suggestive of an intrusive synvolcanic mafic magma body contributing to the heat source necessary for the development of a robust exhalative hydrothermal cell. (3) Evidence of synvolcanic fault activity in the form of slump structures and intra-formational breccias (mineralized "xistos fragmentos", see below) indicative of tectonic instability-related syndepositional deformation and debris-flow products (Farias et al. 1984; Medeiros 1986a; Winter 1994). (4) Copper-depletion of Pojuca metabasalts (Winter 1994, p. 6-18), a feature usually found in the mafic rock piles underlying volcanogenic deposits and originated through the stripping metal effected by a synvolcanic convective hydrothermal cell. (5) Synsedimentary tectonic activity also indicated by clasts of metachert embedded in lower horizons of the clastic metasedimentary package stratigraphically overlying the deposit (Dreher et al. 2018). (6) Sedimentary debris-flow origin of the fragmental schists also suggested by the observation of rough graded bedding (Schwarz and Frantz 2013). (7) Magnesian hydrothermal alteration in the form of cordierite-anthophyllite-cummingtonite-bearing metabasaltic rocks (cf. dalmatianites, Sangster 1972, Beatty and Taylor 1982), as early acknowledged by Docegeo geologists (Farias et al. 1984; Saueressig 1988) and corroborated by Dreher et al. (2018). (8) Masses of biotitic / chloritic rock and ore-related garnet-feldspar-andalusite-muscovite-quartz schist (Saueressig 1988), suggestive, respectively, of magnesian and aluminous alteration, with andalusite-muscovite-bearing schists being

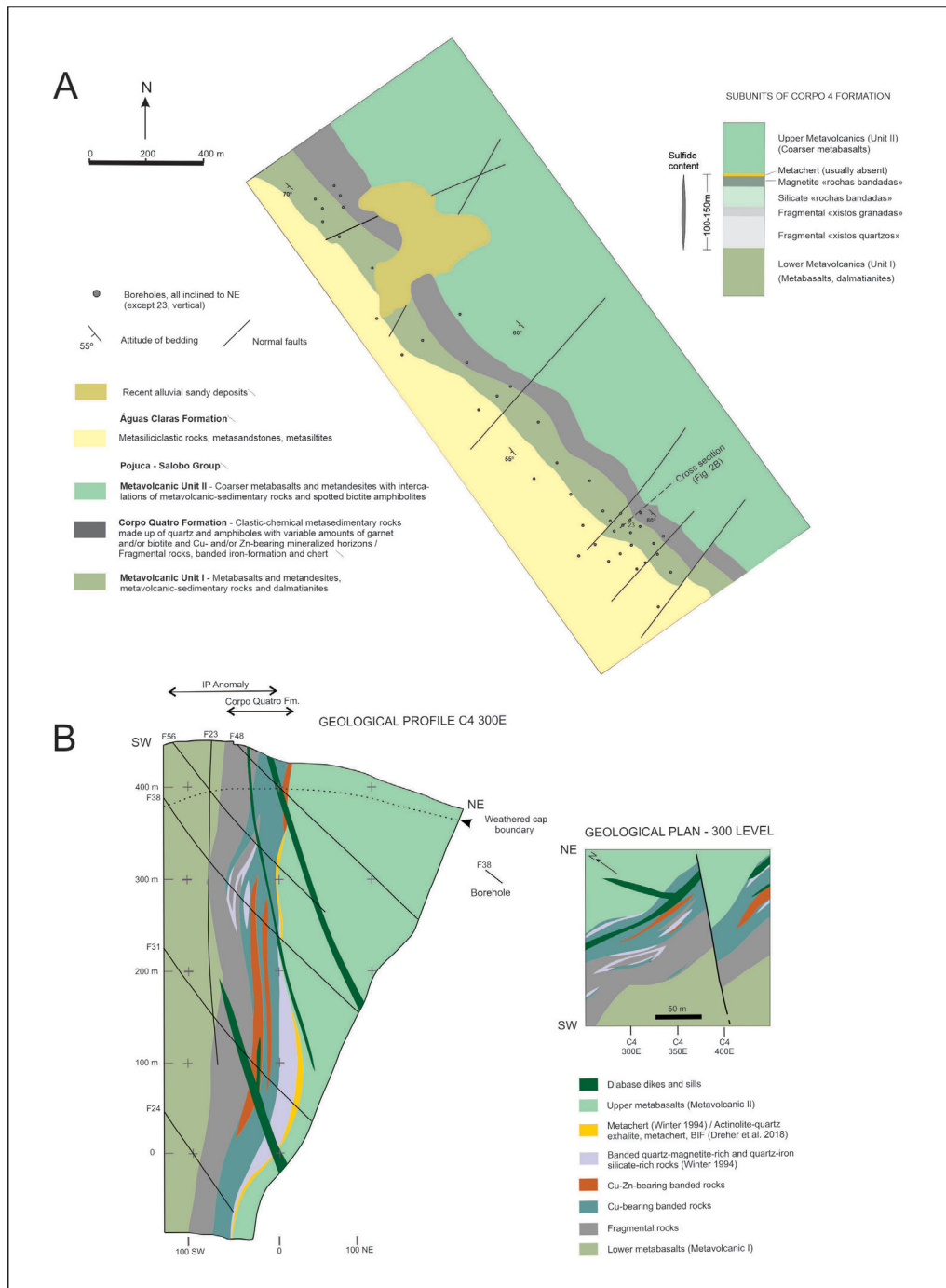


FIGURE 2. A- Geologic map of the Pojuca Corpo 4 deposit (from Saueressig 1988) and stratigraphic column of the Corpo 4 Formation (based on Winter 1994). B- Cross-section and 300 Level plan of Pojuca Corpo 4 (from and Farias et al. 1984). Note the relative position of dalmatianites (an anthophyllite rock spotted with cordierite, Sangster 1972, Beaty and Taylor 1982), fragmental rocks, BIFs and metachert-exhalites suggestive of inverted bedding facing up northeast, as acknowledged by Schwarz and Frantz (2013) and Dreher et al. (2018).

the main copper-bearing lithology in the nearby C2 prospect (Farias et al. 1984). (9) Albitic alteration zones, up to 15 m in width, affecting lower and upper metabasalts around the Corpo 4 deposit, associated with the main mineralization stage of Winter (1994) and constituting a feature found in Besshi-type volcanogenic deposits (Slack 1993). (10) The suggestion of a footwall position for the dalmatianites, according to the volcanogenic model, and therefore of local inverted stratigraphy (Hutchinson 1977; Dreher et al. 2018), an interpretation

however not universally accepted (see Farias et al. 1984; Medeiros Neto 1986a; Winter 1994). (11) Main mineralized unit, named “rochas bandadas” by Winter (1994), described as made up of conspicuously banded rocks of metasedimentary, predominantly chemical nature, with siliceous-iron silicate-oxide compositions denoted by its mineralogy including, among others, quartz, grunerite, almandine, magnetite, iron-bearing sulfides disposed along millimeter- to centimeter-wide bands. (12) Mineralization in “rochas bandadas”

occurring mainly in the form of recurrent banding-controlled disseminations and lesser massive strips of Fe-Cu-Zn sulfides (Medeiros Neto 1986a; Winter 1994), with abrupt variations in metal content, e.g., from 300 ppm to 8% Cu in adjacent bands (Beisiegel and Farias 1982). (13) Disseminated ore also in fragmental rocks ("xistos fragmentos", Winter 1994) made up of elongated quartz aggregates / metachert set in a matrix of hornblende-biotite or amphibole (cummingtonite-grunerite, tremolite-actinolite, hastingsite), quartz, plagioclase and/or cordierite, possibly representing mixed chemical, clastic and tuffaceous material. (14) Mineralization also described as 'fracture sulfide', common throughout the banded oxide and silicate iron-formation as well as in the fragmental rock, and consisting of up to 3-4 mm wide and 5 cm long sulfide veinlets with mainly chalcopyrite and pyrrhotite (Winter 1994, p. 3-22), which may indicate stringer ore as initially acknowledged by Hutchinson (1977, 1979). (15) Vertical stratigraphic cyclic zonation of stratiform ore with zinc enrichment relative to copper towards the top of each mineralized horizon as well as laterally along strike zonation with relative zinc concentration in the central portion of the orebody (Medeiros Neto 1986a). (16) Reference to abundant pyrite and sphalerite in the fragmental rocks relatively to banded oxide and silicate banded iron-formation (Winter 1994, p. 3-37), suggesting also an originally stratigraphic controlled zonation. (17) Discontinuous layers of metachert and oxide-facies banded iron-formation ("rochas bandadas", metaexhalites) associated with strata-bound mineralization (Fig. 2), and distinctly banded actinolite metacherts intercalated with or overlying the mineralized horizon (Dreher et al. 2018). (18) Fragments of aggregates of sulfides and magnetite accompanying, and finely laminated sulfides bordering, chert clasts in the fragmental rocks (Medeiros Neto 1986a, p. 1543), indicating early deposition of these ore minerals. (19) Metamorphism and deformation of the ore evidenced by distribution and elongation of ore minerals parallel to foliation, concentration of sulfides in fold hinges, sulfide intergrowth with metamorphic iron-amphiboles as Fe-hastingsite and grunerite, and development of metamorphic textures in sulfides, such as annealing and *durchbewegung* (Medeiros Neto 1986a, p. 1544). (20) Gahnite as a common phase of sphalerite-rich horizons (Saueressig 1988), and strong correlation between zinc and cadmium (Medeiros Neto 1986a). (21) The association of fragmental schists, exhalites and iron-formation conforming to an ore-equivalent or favorable ore horizon of exhalite settings (Sangster 1972; Large 1992), with fragmental schists and particularly almandine-rich rocks ("xistos granadas", Winter 1994) used by Docegeo geologists as ore-tracer horizons in exploration for copper and zinc (Farias et al. 1984; Saueressig 1988; Winter 1994). (22) General interpretation of Pojuca as a classical volcanogenic association of an underlying altered zone with stockwork / stringer ore, covered by chemical layers containing Cu-Zn sulfides and terminating with an exhalite horizon with BIF plus chert at the cap (Hutchinson 1979; Almada and Villas 1999; Schwarz and Frantz 2013; Dreher et al. 2018).

4.2. Constraining evidence

Constraining evidence for Pojuca C4 is restricted to fluid inclusion studies by Medeiros Neto (1986b) and Winter (1994). Among these, data of direct interest from the syngenetic standpoint are those of Winter (1994) specifically obtained

from quartz grains of the mineralized oxide-silicate-facies BIF ("rochas bandadas") and from the main ('Q2') quartz veins, which occur predominantly in the form of a strata-bound set in the "rochas bandadas" (cf. Appendix 1).

Regarding these data, the following aspects are considered relevant: (1) Fluid inclusion results concerning "rochas bandadas" and Q2 veins indicate the involvement of mainly two aqueous fluids in the mineralization process, with salinities of 4-34 wt% eq. NaCl (mean 19.7%) and 15-41 wt% eq. NaCl (mode 30%). (2) Based on this, and on a novel metallogenic interpretation of the deposit, Winter (1994) envisaged the mineralization of Pojuca as resulting from a two-step regressive metamorphic epigenetic process, involving sequentially the two above-mentioned fluids (Table 1), with metal transportation as chloride complexes. (3) The first stage would have promoted strata-controlled ore deposition via sulfidation of magnetite, with attending Ca-Na metasomatism of Fe-amphiboles of the banded rocks and generation of secondary hornblende, plus albittization of metabasalts, and the second stage generated quartz-biotite-sulfide veins, with accompanying retrograde biotitization of garnet and hornblende and further deposition of ore sulfides. (4) The model includes a magmatic connection via heat source from a 2.53 Ga granitic magmatism (cf. Old Salobo event). Alternatively, a purely magmatic origin via a direct granitic hydrothermal fluid input is not discarded (Winter 1994, p. 6-16, Fig. 6.2 therein). (5) In agreement with this interpretation, Winter (1994) compares Pojuca C4 with epigenetic, iron oxide-copper-gold (IOCG) deposits, with particular reference to the metamorphogenic deposits associated with coeval granites of the Cloncurry district and the eastern Mount Isa block, Australia, for instance, the magnetite ironstone-hosted replacement mineralization at the Starra deposit (Williams et al. 2005). (6) As geological background to her epigenetic interpretation, Winter (1994, p. 3-27) indicates that ore materials of Pojuca show no evidence of metamorphism and deformation, lacking, for instance, ductile remobilization, *durchbewegung* textures, pressure-induced twinning and typically metamorphic triple junctions at grain boundaries. (7) Additionally, Winter (1994, p. 6-10 to 6-14) refutes that several features of Pojuca are related to synvolcanic mineralization, with particular reference to the stringer ore, the magnesian hydrothermal alteration and the metal zonation, denying therefore a volcanogenic connection for the deposit.

Winter's interpretation evidently is in entire disagreement with the syngenetic view intrinsically attached to section 4.1. Regarding this, it can be argued that: (1) The age proposed for mineralization by Winter (1994) is much younger than the age of 2.76 Ga proposed for the metamorphism of Pojuca by Machado et al. (1991) and even a 2.53 Ga granitogenesis in north Carajás has been considered doubtful since defective zircons were used on age determinations (Barros et al. 2001; Toledo et al. 2021). (2) Nevertheless, Winter's work configures the first application of an epigenetic model to the Itacaiúnas-hosted Cu-Au deposits of Carajás, then unanimously considered volcanogenic, and, in fact, there is no further constraining evidence so far, to contradict an epigenetic interpretation for Pojuca, though geological attributes (section 4.1) configure strong support to syngeneses. (3) Fluid inclusions are in general significantly modified by metamorphic conditions and, therefore, become virtually inefficient for defining the origin of metamorphosed

deposits, particularly in the absence of other constraining methods (Marshall et al. 2000; Marshall and Spry 2000, p. 46). (4) Metamorphogenic base-metal deposits have been considered very rare and difficult to characterize with respect to genesis (Heinrich et al. 2000; Cartwright and Oliver 2000). However, the situation is modified if metamorphism involved highly saline fluids, as exemplified by the eastern Mount Isa terrane (Cartwright and Oliver 2000) and Pojuca itself. This topic is retaken in the discussion item (section 11).

5. Furnas

5.1. Volcanogenic features

The large-tonnage, low-grade Furnas Cu-Au deposit (Fig. 1) repeats largely the typology of Pojuca Corpo 4. Furnas is also hosted in metavolcanic-sedimentary rocks of the Itacaiúnas Supergroup and the main features sustaining a volcanogenic origin for it are the geological setting, the strata-bound nature of the ore as well as the presence of exhalites and typical alteration zones (Dreher et al. 2018). According chiefly to these authors, with few additional information from Santos (2014), Jesus (2016) and Alves and Monteiro (2019), volcanogenic features of Furnas include (Figs. 3 and 4): (1) In terms of geologic setting, the location of the deposit precisely at a major contact between a volcanic and a clastic-chemical sedimentary package, similar to, for example, Igarapé Bahia. (2) Features similar to those found in the admittedly volcanogenic deposit of Pojuca Corpo 4, including hydrothermal alteration zones and associated exhalites, as per the following items. (3) The stratigraphic base to the ore comprising alteration rocks derived in their majority from ancient basalts with development of cordierite-cumingtonite-anthophyllite alteration assemblages. (4) Hydrothermal chlorite chemistry showing an increase in the Fe/(Fe+Mg) ratio towards the mineralized zone (Jesus 2016), similar to the case of Igarapé Bahia, this representing chemical zonation from recharge to discharge zones normally observed in volcanogenic hydrothermal deposits (Zang and Fyfe 1995, cf. section 6.1). (5) Most of the ore associated with a thick oxide-silicate facies BIF horizon made up mainly of grunerite, almandine, magnetite ± quartz, with disseminated chalcopyrite, pyrrhotite, pyrite, bornite, chalcocite and molybdenite. (6) A package of laminated metaexhalites stratigraphically above the BIF horizon consisting of alternating beds of chert, tourmaline and garnet, which grades into an impure metachert and transitions into clastic metasedimentary rocks. (7) Stratigraphically upper clastic metasedimentary rocks (Fig. 4) containing in their lower levels chert fragments derived from the underlying cherty exhalites, a feature suggestive of synvolcanic tectonic instability and growth faulting. (8) Upper metasedimentary layers including rocks rich in garnet, andalusite and sillimanite, with staurolite, quartz and biotite, this constituting a mineralogy suggestive of strong aluminous alteration found in association with exhalative deposits. (9) Interpretation of this alteration by Dreher et al. (2018) as a metamorphic equivalent of advanced argillic alteration usually identified in association with auriferous volcanogenic deposits, produced by strongly acidic hydrothermal magmatic fluids incorporated in the seawater of evolving hydrothermal exhalative systems (Galley et al. 2007; Dubé et al. 2007; Ronde et al. 2005).

(10) In connection with the former item, the occurrence of the Furnas granite near the Furnas deposit, considered by Jesus (2016) similar to the Igarapé Gelado granite (2.76 Ga, Pb-Pb in zircon, Melo et al. 2017, Fig. 1), suggesting or indicating the presence of a sustained heat source for the development of a robust exhalative hydrothermal system. (11) Very significant spatial coincidence of high- and low-grade ore zones with the iron- and silica-rich rocks, respectively (cf. Fig. 4 and Santos 2014). (12) Accordingly, rock types formerly interpreted as alteration products by Santos (2014) and Jesus (2016), e.g., silicified quartz mylonite and magnetite-grunerite-almandine iron metasomatites, showing compositional banding and mineralogy compatible with metacherts and BIFs, and reinterpreted as metaexhalites by Dreher et al. (2018) (Fig. 4).

5.2. Constraining evidence

Constraining evidence for Furnas is restricted to a few isotopic sulfur and boron data. Results and interpretations include the following aspects: (1) Sulfur signature from pyrrhotite of -0.37‰ to 1.72‰ $\delta^{34}\text{S}$, interpreted as indicative of a magmatic source for sulfur, e.g., from fluids of Neoproterozoic A-type granites and from leaching of ultramafic rocks, that is, sulfur either derived directly from magmas or leached from igneous rocks (Alves and Monteiro 2019). (2) Boron isotope studies in tourmaline, carried out conjointly with the Igarapé Bahia, Salobo and Igarapé Cinzento deposits (Melo et al. 2021), implying or suggesting an exhalative connection for the Furnas mineralization (cf. section 6.2.4). (3) Still regarding sulfur, both fluid sources mentioned above – magmatic input and rock leaching – may in fact contribute to convective cells of exhalative systems and, as isotopic sulfur compositions near zero per mil are common in Archean volcanogenic deposits (Franklin et al. 2005; Huston 1999; Huston et al. 2010), the available sulfur isotopic signature actually comes in support of a synvolcanic origin for Furnas. This is indicated convincingly by geological features and at least partially corroborated by the boron isotopic data. (4) Nevertheless, Jesus (2016) defends an epigenetic interpretation for the Furnas mineralization, arguing that the attending hydrothermal alteration begins with intense silicification coeval with mylonitization (that is, syndeformation), followed by potassic alteration (biotitization, chloritization) of ore hosting rocks, which is succeeded by boron alteration (tourmaline) and schistosity-parallel iron metasomatism (magnetite, grunerite, almandine). (5) However, as already stated before, several rock types referred to by Jesus (2016) as quartz mylonites and iron metasomatites are in fact conspicuously banded (cf. several illustrations therein) and could correspond to metacherts and iron-formations. These rocks were considered by Dreher et al. (2018) as metaexhalites instead of epigenetic alteration products, which implies a syngenetic ore deposition.

6. The Igarapé Bahia camp

The Igarapé Bahia IOCG Camp (Fig. 1) contains the best-studied IOCG deposits of north Carajás. Consequently, the following sections are inevitably long in order to cover the subject with the detail the authors consider adequate for the purposes of the present exercise.

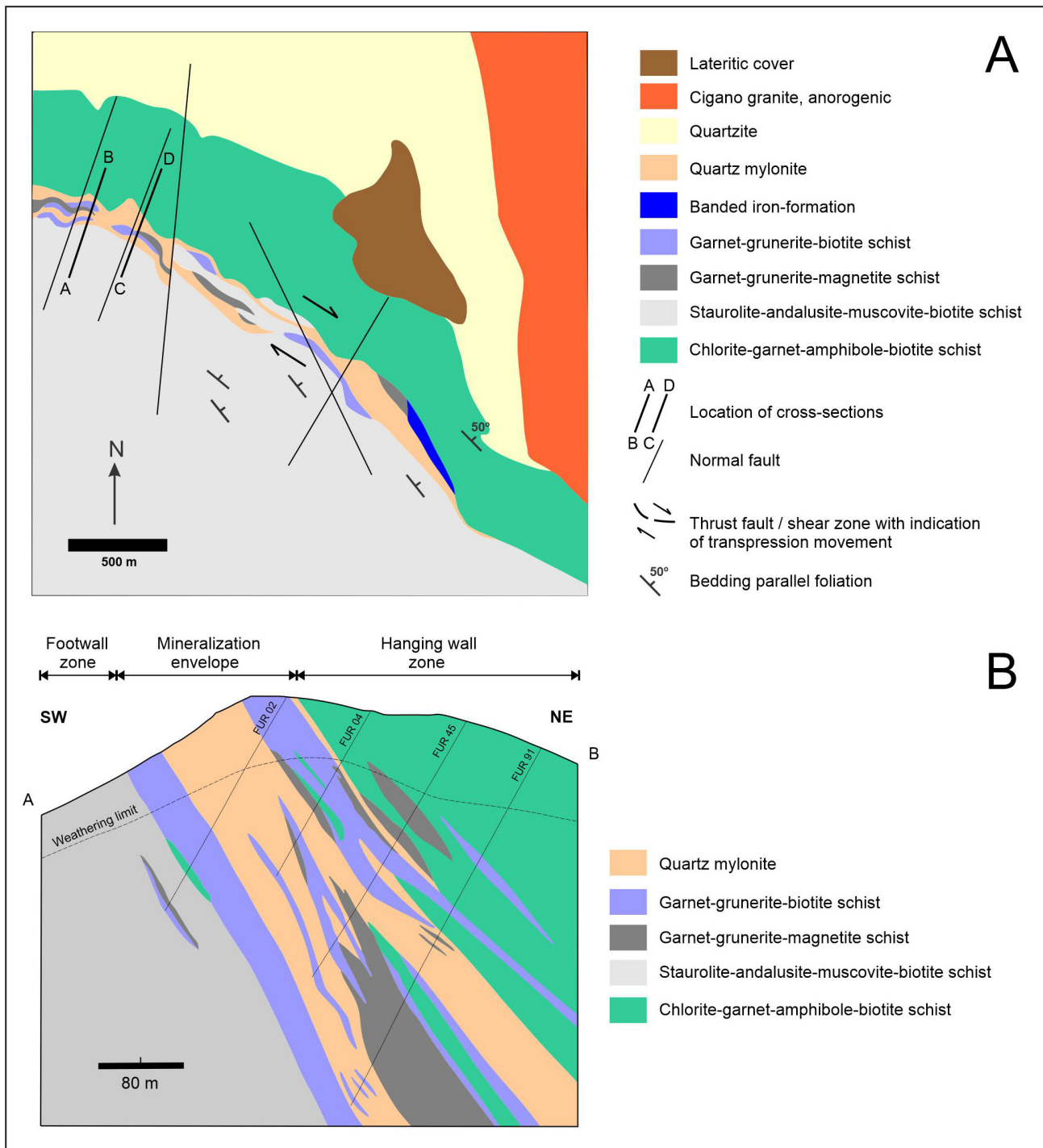


FIGURE 3. A- Geologic map of the southeast portion of Furnas and B- cross-section of the deposit (from Jesus 2016 and Santos 2014, based on Vale 2010 and 2012). Units along the shear zone within the mineralization envelope interpreted as products of hydrothermal alteration with unspecified protoliths.

6.1. Volcanogenic features

The Igarapé Bahia camp is made up of three outcropping deposits, namely, Acampamento Sul, Acampamento Norte and Furo Trinta, plus their blind Alemão extension, which constitutes the western down faulted portion of the ensemble (Fig. 5).

Since the early suggestion by Hutchinson (1977), many authors have interpreted Igarapé Bahia as a whole as a volcanogenic deposit, with particular reference to Zang and

Fyfe (1995), Almada and Villas (1999), Villas and Santos (2001), Villas et al. (2001), Galarza Toro (2002), Dreher (2004) and Dreher and Xavier (2001, 2005, 2006) and Dreher et al. (2005, 2008), whereas several others, cf. Soares et al. (1999), Tazava and Oliveira (2000), Ronzê et al. (2000), Tallarico et al. (2000, 2005) and Williams et al. (2005), have come in support of an epigenetic, granite-related origin for the deposit. Despite this divided opinion, a significant number of attributes underpin the synvolcanic argument. Based particularly on the above-mentioned work led by Villas and by Dreher, the

attributes encompass (Fig. 5): (1) Hosting sequence unit consisting essentially of a lower basaltic-dominated unit and an upper metaturbiditic package, both carrying subordinated oxide-facies BIF and chert, with the four deposits occurring systematically at this volcanic-sedimentary contact (Fig. 5), and this altogether conforming to a common geologic setting and locus for volcanogenic deposits, particularly those of the Besshi type (Almada and Villas 1999; Villas and Santos 2001). (2) Reference to intense spilitization of underlying metabasalts (Melo et al. 2021), as per the reservoir zone alteration of VMS deposits (Franklin et al. 2005). (3) The deposits and the hosting volcanic-sedimentary contact forming an up-right roughly sub-circular feature around the stratigraphically underlying basalt, this constituting a feature suggestive of a related volcanic core control. (4) The orebodies occurring in the form of a strata-bound breccia interpreted as an intraformational debris-flow deposit, showing gradational contacts (Villas and Galarza Toro 2001; Dreher and Xavier 2001) and containing angular to subrounded fragments mostly derived from stratigraphically adjacent or underlying rock units such as basalt, oxide-facies BIF and, chert, as well as some clasts from the upper sedimentary metarythmite section, as emphasized by Santos and Villas (2001) and Dreher (2004). (5) Breccia located in a geological situation similar to mineralized synsedimentary

breccias found as a subsurface facies of exhalative deposits (Goodfellow et al. 1993; Lydon 1995). (6) The matrix consisting of an assemblage of chlorite, magnetite, siderite, quartz and dravitic tourmaline, considered altogether as hydrothermal alteration products, commonly found in synvolcanic deposits. (7) Increase in chlorite content and in the Fe/(Fe+Mg) ratio of chlorite in country rocks, e.g., metabasalts, towards the deposit, this constituting a feature consistent with change in alteration pattern from reaction to discharge zones of volcanogenic hydrothermal systems, as interpreted by Zang and Fyfe (1995). (8) Tourmaline in particular, characterized as Mg-rich dravite commonly with Fe/(Fe+Mg)<0.5, similar to those occurring characteristically, although not exclusively, in sulfide deposits formed in submarine-hydrothermal systems and interpreted as products of mixing of Fe-rich hydrothermal fluids with Mg-rich seawater (Villas and Galarza Toro 2001; Xavier et al. 2005b). (9) Occurrence of pyrosmalite in the mineralized breccia matrix, a rare chlorine-rich (up to 5% Cl in weight) mineral generated from saline solutions found in a number of volcanogenic and sedex deposits, an association accepted for the case of Igarapé Bahia by most authors (Tazava et al. 1998; Tazava and Oliveira 2000, p. 211; Dreher 2004; Dreher and Xavier 2006) but denied by others (magmatic origin, Tazava et al. 1999). (10) Occurrence in the matrix of

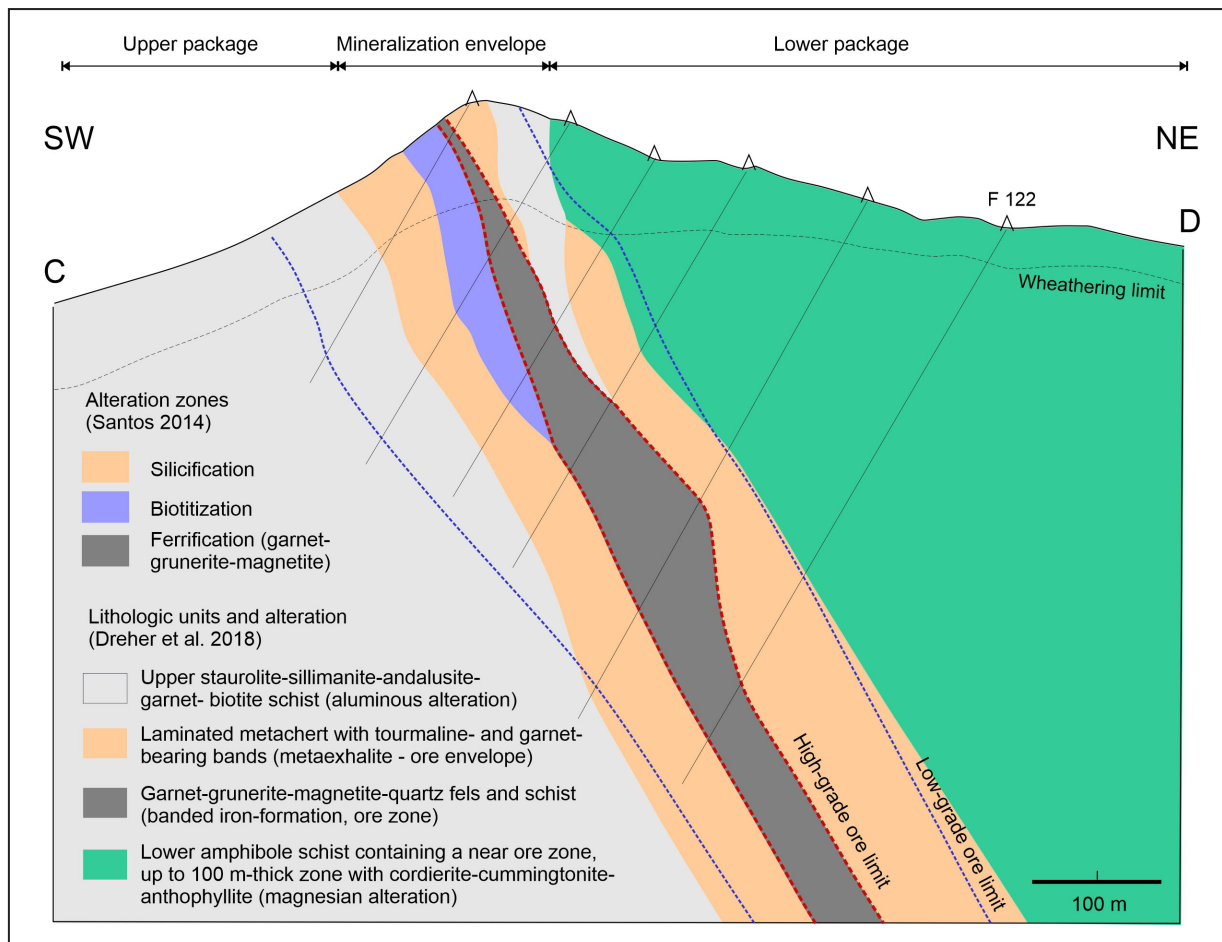


FIGURE 4. Cross-section of the Furnas deposit showing alteration zones and high- and low-grade ore limits from Santos (2014, based on Vale 2012) and the reinterpretation of Dreher et al. (2018). The latter indicates an inverted, SW-facing, mineralized package consisting of an iron-rich (BIF) orebody inserted in a metachert horizon as opposed to NE-facing mineralized hydrothermal alteration zones of Santos (2014) and Jesus (2016).

mineralized breccias of amphiboles (hastingsite, Fe-actinolite) associated with stilpnomelane and magnetite, constituting a paragenesis found in oxide-silicate iron-formation metamorphosed to medium greenschist to amphibolite facies (Dreher 2004). (11) Similar record of an iron-rich chlorite (chamosite), also commonly found in iron-formations and allowing for interpretation of location relative to hydrothermal discharge sites (Zang and Fyfe 1995; Dreher 2004). (12) The presence of chlorine in amphiboles and chlorites (Dreher 2004), as known in some volcanogenic deposits (Hannington and Kjarsgaard 2002, p. 109). (13) Evidence of an angular discordance between strata-bound ore and platform cover at the Alemão orebody (Barreira et al. 1999; Siqueira et al. 2001, Fig. 6), pointing to a minimum age for the deposit, as constrained by zircon U-Pb dating (2.65-2.71 Ga) of a swarm of mafic dykes transecting the ore, host rocks and cover units (cf. section 6.2.5). (14) Occurrence of massive sulfide ore, as per a remarkable 40 m @ 25% Cu drilling intersection at Alemão reported by Barreira et al. (1999) and Ronzê et al. (2000). (15) Occurrence of thin mineralized stratiform sulfide lenses and nodules following bedding planes in the overlying metarhythmites, a feature clearly indicative of early, syngenetic sulfide deposition. (16) Occurrence of massive sulfide clasts in

a conglomerate in overlying metasedimentary rocks (Santos and Villas 2001, p. 324), constituting another feature indicative of early deposition of sulfides in the local stratigraphic package. (17) Along the same line, the occurrence of pelitic rip-up clasts containing lenticular chalcopyrite in the hanging wall metagreywacke package (Xavier et al. 2017, Fig. 7). (18) Mineralized breccia exhibiting elongated fragments as well as penetrative foliation (Soares et al. 1999; Ronzê et al. 2000; Dreher and Xavier 2001; Dreher 2004) and incidence of greenschist metamorphism (Almada and Villas 1999; Tallarico et al. 2000; Dreher and Xavier 2001), this altogether also suggesting an early pre-deformational/metamorphic, probably synsedimentary formation for the rock. (19) Mineralized breccia exhibiting rough graded bedding (Villas et al. 2001), similarly to the fragmental unit of Pojuca, this constituting another feature pointing to the synsedimentary nature of this rock. (20) Mineralized breccia exhibiting gradational contacts, suggestive of its link with the volcanic-sedimentary environment. (21) Dreher (2004) and Dreher et al. (2005, 2008) envisaging a deep marine environment for Igarapé Bahia, in conformity with the setting of turbiditic sediments, mafic flows and absence of recognizable pyroclastic products; and considering the mineralized breccias as a sedimentary

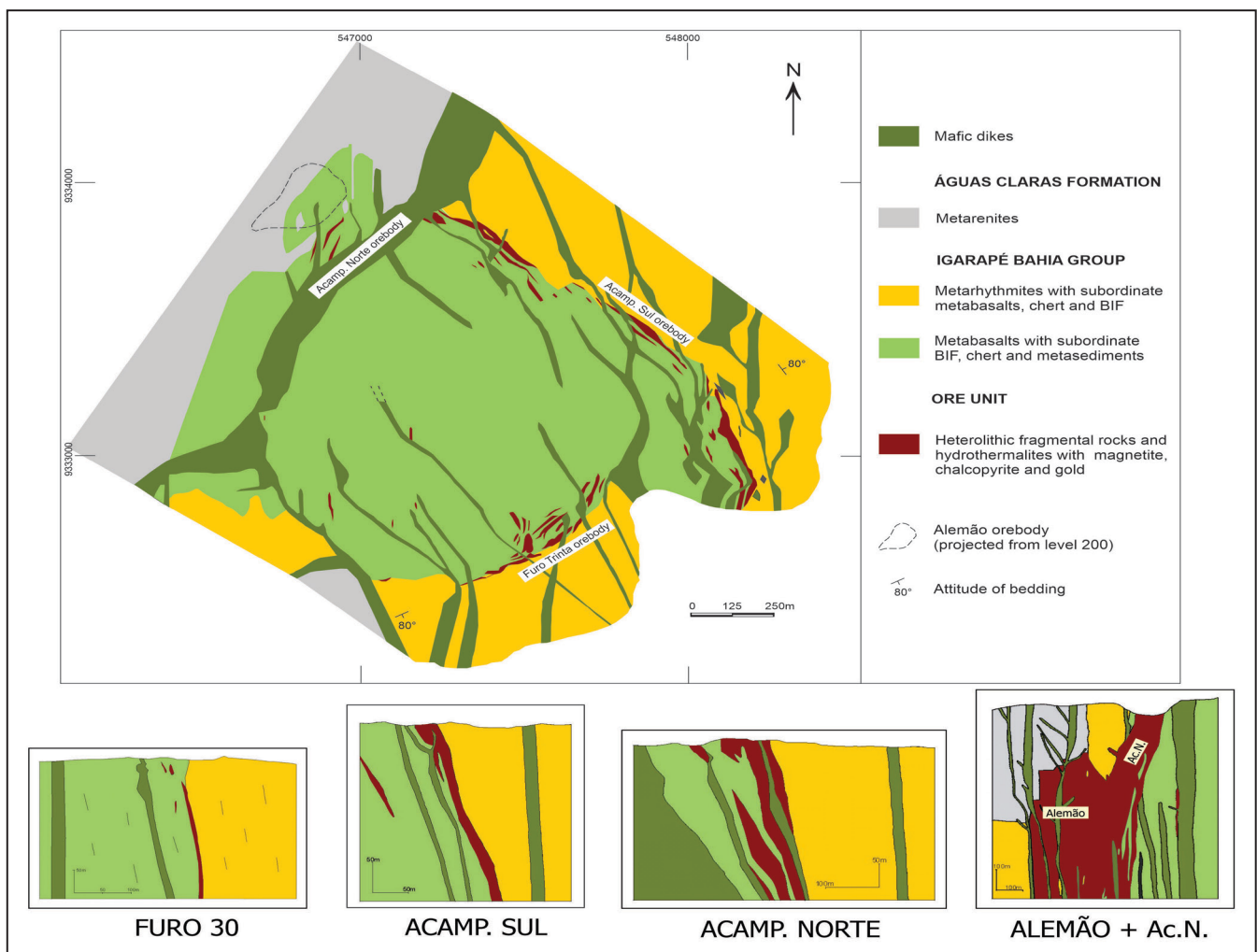


FIGURE 5. Geology of the Igarapé Bahia camp and cross-sections of deposits (from Dreher 2004, after CVRD 2000, with profiles from Barreira et al. 1999, Santos 2002 and Dreher 2004). Note the location of orebodies along a roughly circular volcanic-sedimentary contact.

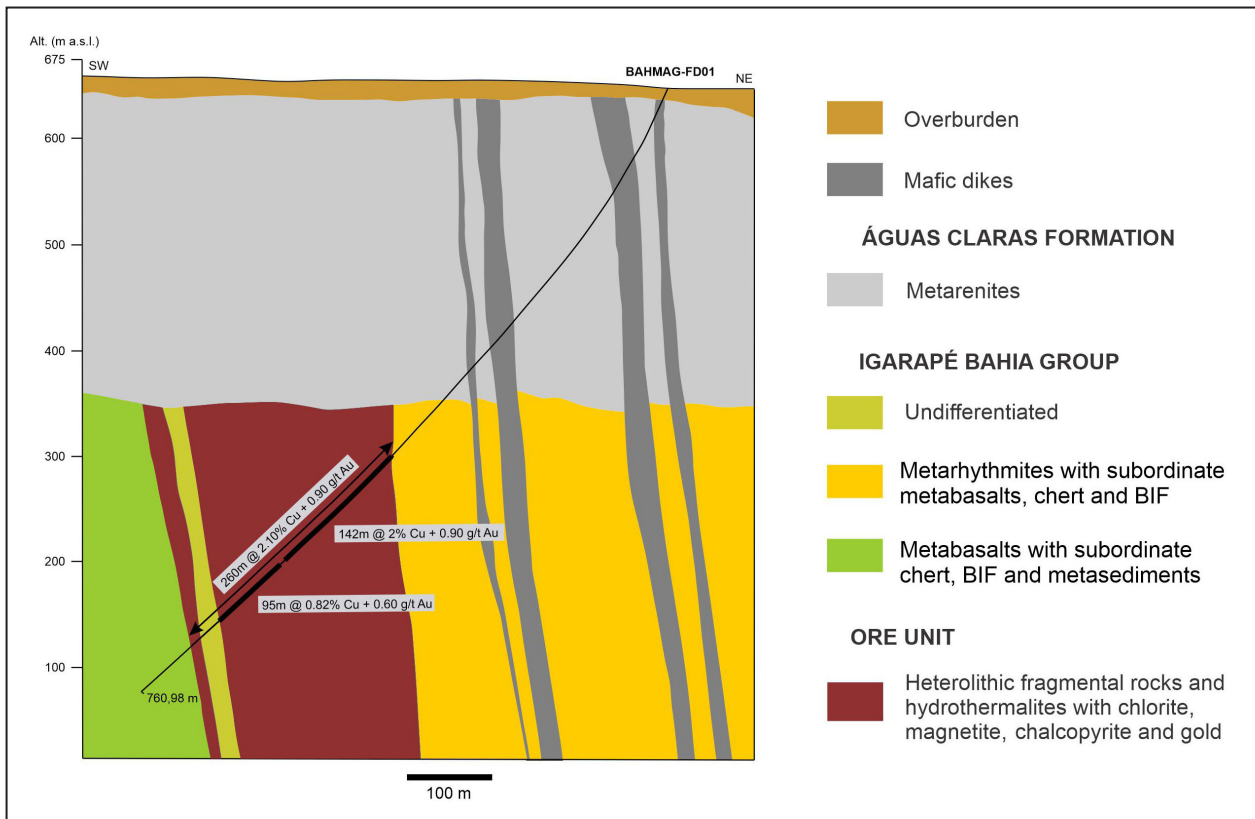


FIGURE 6. Cross-section of the Alemão orebody (Barreira et al. 1999; Santos 2002; Dreher 2004; Dreher et al. 2008). Note the stratigraphic relations implied by the angular unconformity and the crosscutting dikes.

debris-flow deposit, formed in connection with growth-faults. (22) The important organic link of synvolcanic growth faulting, breccia generation and mineralization, strongly consistent with the volcanogenic model, made by the above-mentioned authors (Fig. 8). (23) The interpretation by Dreher (2004, p. 107), of the Alemão deposit as a vent facies of a synvolcanic hydrothermal system, based on the high Fe/(Fe+Mg) ratio of chlorite (chamosite), which is corroborated by the massive, brecciated and discordant nature of a part of the deposit, and in agreement with Santos (2002), who considered Alemão located along an important hydrothermal conduit.

6.2. Constraining evidence

6.2.1. Fluid inclusions

Data obtained from fluid inclusions of Igarapé Bahia of direct interest here, i.e., those obtained from quartz of the mineralized breccia, are summarized in Appendix 2.1. According to these data, main points and interpretation on breccia-related fluid inclusion studies of Igarapé Bahia are: (1) General agreement that strata-bound mineralizing solutions involved three main types of fluids, namely, aqueous, aqueous-carbonic and carbonic. (2) Aqueous fluids consisting of two types, one representing evolved seawater from a convective synvolcanic cell (up to 24% NaCl) and another from a granitic source (29-41% NaCl), with an additional, purely carbonic fluid, from volcanic emanations of a mantelic source (Almada and Villas 1999). (3) The different inclusions identified representing co-existing fluids in evolved seawater of an exhalative cell, with high salinity obtained from either

magmatic input or a predominantly evaporitic source plus a carbon contribution from the breccia host rock (Dreher 2004; Dreher et al. 2008). (4) The indication by these last authors that their sampled fluid inclusions failed in characterizing early, higher temperature fluids of the deposit, so that results are actually incomplete. (5) The additional aspect that the low metamorphic grade of the deposit warrants that the fluid inclusion retained their pre-metamorphic characteristics and therefore are adequate for the characterization of syngenetic metalliferous solutions (Marshall et al. 2000). (6) The low Cl/Br ratio of highly-saline fluid inclusions interpreted as indicative of mineralizing fluids sourced from residual marine evaporative bittern brines, discarding an origin specifically from dissolution of marine evaporites (Xavier et al. 2009, 2013), but nevertheless still indicating the involvement of a marine evaporitic environment in the hydrothermal system. (7) The low salinity aqueous-carbonic inclusions coexisting with brines suggesting anew a magmatic fluid contribution to the hydrothermal cell (e.g., Xavier et al. 2013).

6.2.2. Sulfide sulfur isotopes

Sulfide sulfur isotopic results and interpretations available for Igarapé Bahia are summarized in Appendix 2.2, with the main points to be emphasized being: (1) $\delta^{34}\text{S}$ data from chalcopyrite of the matrix of the mineralized breccia, ranging from -2.1 to 5.6 per mil, correlated with exhalative systems, with the sulfur source being the disseminated sulfides of the underlying volcanic pile (Villas et al. 2001; Galarza Toro 2002; Dreher 2004). (2) A limited although important contribution of reduced biogenic sulfur to the mineralized system indicated by

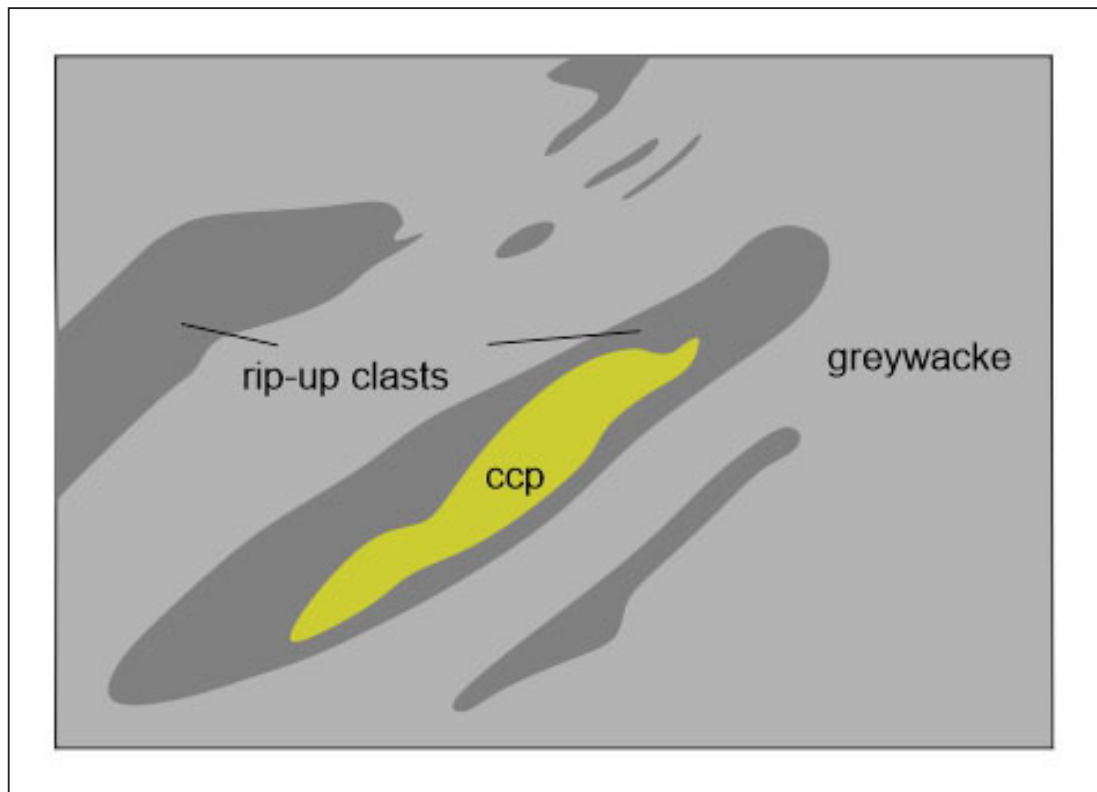


FIGURE 7. Lenticular chalcopyrite (ccp) inside a pelitic rip-up clast set in greywacke of the Igarapé Bahia / Alemão deposit. Clast is a few centimeters long. Drafted after a drill core illustration shown in Xavier et al. (2017, p. 900).

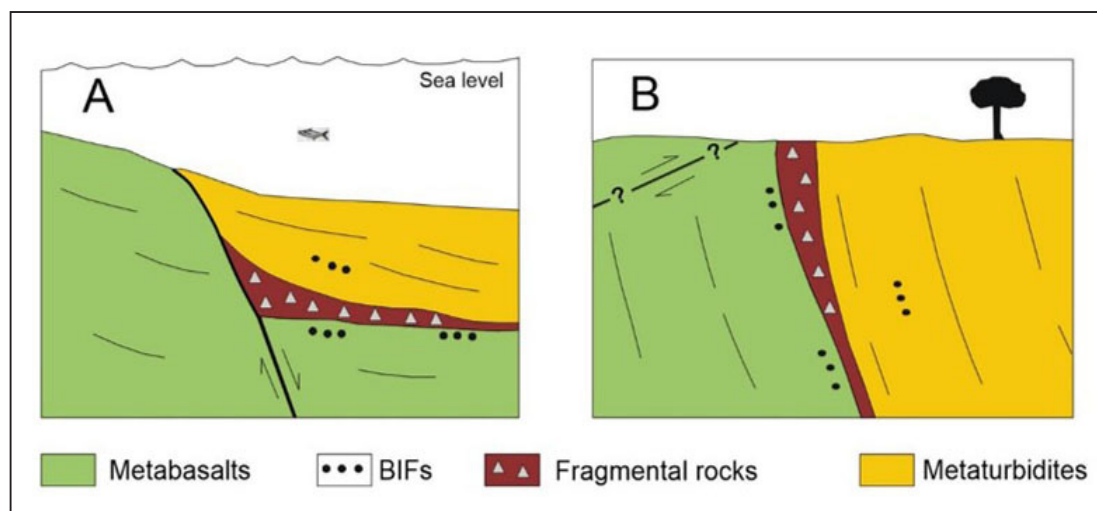


FIGURE 8. Model of generation and evolution of the fragmental rocks of Igarapé Bahia (A) During the Archean; (B) Present situation (from Dreher 2004 and Dreher et al. 2005) with fragmental rocks and turbidites corresponding, respectively, to proximal debris flow and distal turbidity current products developed in association with syndimentary growth faulting (Dreher 2004 after geological model of Einsele 1991). Not to scale..

the anomalous $\delta^{34}\text{S}$ result of -10.8 per mil obtained from sulfide ore by Dreher (2004). (3) The interpretation of a volcanic sulfide source for the sulfur also forwarded by Santiago (2016) to explain near zero $\Delta^{33}\text{S}$ results also obtained from chalcopyrite of the ore. (4) This interpretation used by Melo et al. (2019a) but applied only for the $\delta^{34}\text{S}$ signature of sulfidic nodules and layers of chalcopyrite found in metaturbidites of the upper portion of the local volcanic-sedimentary stratigraphy (cf.

section 6.1). (5) In the case of the IOCG breccia ore, Melo et al. (2019a) consider similar $\delta^{34}\text{S}$ sulfide sulfur results of ca. 1 to 5 per mil as related to an epigenetic magmatic hydrothermal source, with part of it, however, incorporated from seawater via dissolved sulfate reduction during the deposition of the sedimentary pile, representing therefore a syngenetic process. (6) Perhaps a more realistic interpretation to this situation would be that a syngenetic hydrothermal system

inherited its sulfur mainly from scavenging the underlying volcanic pile and less so from a direct magmatic contribution, as proposed, for instance, by Franklin et al. (2005), Slack (1993) and Huston (1999). (7) Moreover, according to these authors, inter alia, isotopic sulfide sulfur values close to zero have been obtained from sulfides of Archean volcanogenic deposits and thus the available sulfur isotopic data of Igarapé Bahia constitute support for a syngenetic rather than epigenetic origin for the deposit.

6.2.3. Carbon, oxygen and hydrogen isotopes

Carbon, oxygen and hydrogen isotopic data for Igarapé Bahia are summarized in Appendix 2.3, and the following points are worthwhile stressing in connection with its content: (1) Agreement among practically all authors indicating that carbon isotope composition obtained from siderite of the mineralized breccia reflects a deep-seated magmatic input of CO₂ to the hydrothermal system, with particular reference to a carbonatitic source (Villas et al. 2001; Villas and Santos 2001; Galarza Toro 2002). (2) Disagreement, however, of Dreher (2004) and Dreher et al. (2008), through making the point that the range of carbon isotopic results of the hydrothermal siderite of Igarapé Bahia is similar to that of Precambrian iron-formations (see discussion in section 11.2), and that carbon may have a source connected with the organic matter possibly contained in the mineralized breccia of Igarapé Bahia; remarkably, organic matter in the form of graphite has also been observed in Pojuca (Winter 1994) and Salobo (Guimarães 1987; Vieira et al. 1988). (3) Various authors defending oxygen and hydrogen isotopic signatures of Igarapé Bahia as resulting from mixing of magmatic with meteoric fluids. (4) Melo et al. (2019b) suggesting also the possibility of involvement of metamorphic fluids and Dreher (2004) and Dreher et al. (2008) interpreting the oxygen isotopic signature of magnetite and quartz of the mineralized breccia as due to interaction of the hydrothermal fluid with sedimentary rocks. (5) The carbon, oxygen and hydrogen isotopic signatures leading to the acceptance of a magmatic contribution to the hydrothermal system of Igarapé Bahia, and, on the other hand, permitting to consider reasonable that the magmatic fluid permeated an evolving synvolcanic hydrothermal cell. (6) The natural candidate for this magmatic input being the foliated granites, coeval with the early, depositional stage of the Itacaiúnas basin (cf. Igarapé Gelado batolith, regional geology section).

6.2.4. Boron isotopes

Boron isotope results from hydrothermal tourmaline of the ore breccia of Igarapé Bahia are summarized in Appendix 2.4 and principal related aspects to be pointed out are: (1) Main $\delta^{11}\text{B}$ result range of 12 to 26 per mil interpreted by Xavier et al. (2005b, 2008, 2013) and Dreher and Xavier (2006) as strong evidence that the highly saline fluids involved in the mineralization (cf. item 6.2.1) originated from marine evaporites, precluding a magmatic hydrothermal connection for the mineralization. This evaporitic connection had already been advanced by Dreher (2004) and soon after confirmed by Xavier et al. (2005b) and Dreher and Xavier (2005, 2006). (2) The above non-magmatic scenario reinforced by the boron results obtained from tourmalines of dravitic composition,

which are commonly found associated with volcanogenic deposits (Slack 1993; Slack and Trumbull 2011). (3) Boron isotopic results from tourmalines of metachert fragments of the breccia of the Acampamento Sul orebody returning the same range of those of tourmalines of the breccia matrix (Xavier et al. 2008). In our view, this indicates that the metachert incorporated a boron contribution from the same evaporitic fluid that deposited the hydrothermal tourmaline of the breccia, and implies that the latter is also syngenetic. (4) Melo et al. (2021) finding heavier and lighter boron isotopic composition in cores and rims of zoned tourmalines at Igarapé Bahia and several other IOCG deposits of north Carajás, and interpreting that the heavier boron cores were inherited from 2.76 Ga exhalative systems whereas the lighter boron of rims originated from a magmatic-hydrothermal source. (5) According to Melo et al. (2021), an initial volcano-sedimentary system played a fundamental role as a source for boron and metals that later on were leached by magmatic-hydrothermal fluids to form the IOCG epigenetic deposits of the Carajás Province, that is, a scenario of epigenetic magmatic fluids scavenging metals from a significantly older exhalative source. (6) However, it is difficult to accept that the older lithified source rock had its permeability restored to account for the en masse leaching required to enabling the above process (Dreher and Xavier 2001). (7) The isotopic boron zoning should perhaps be best seen as a syngenetic process because lighter boron is also found in tourmalines of volcanogenic deposits (Shanks III 2014).

6.2.5. Geochronology

Age data of Igarapé Bahia are summarized in Appendix 2.5, showing that two data sets have been obtained to date, ensuing different lines of interpretation. Main points regarding these data are: (1) Age of ca. 2860 ± 65 Ma for the mineralization from an early U-Pb and Pb-Pb study on sulfides of Igarapé Bahia (Mougeot et al. 1996b). (2) A series of Pb-Pb ages on chalcopyrite and gold that matches those produced by Pb-Pb on zircons of host rocks (ca. 2750-2770 Ma), implying a syngenetic synvolcanic origin for the mineralization but with the obvious drawback of large analytical errors (Villas et al. 2001; Galarza Toro 2002; Galarza et al. 2006). (3) A further series of Pb-Pb evaporation data on sulfide and sulfide-associated gold showing mineralization ages of 2540 to 2575 Ma, but still with relatively large analytical uncertainty possibly related to lead contamination (Santos 2002). Anomalous ages at 3455 Ma and 2200 Ma were also obtained. (4) Robust ages of 2575 Ma (Pb-Pb SHRIMP II) and 2560 Ma (U-Pb) on ore-associated monazites of Acampamento Sul and Alemão, respectively (Tallarico et al. 2005; Melo et al. 2019a), interpreted as indicative of epigenetic, granite-related mineralization (cf. Old Salobo granite). (5) Re-Os result on molybdenite of Alemão of ca. 2630 Ma (Perelló et al. 2023) reinforcing the epigenetic standpoint but somewhat narrowing the host rock – mineralization age gap and relating the mineralization in this case with mafic intrusive magmatism. (6) The above-indicated disparity of results indicating the unsuccessfulness of constraining the age of mineralization through geochronology with this definition, consequently, remaining uncertain.

The picture above makes room for the following comments, which are further dealt with ahead in the coming

discussions: (1) The possibility of isotopic resetting of monazite by alteration, recrystallization or even neof ormation related to hydrothermalism and/or metamorphism, suggesting geochronological inadequacy of monazite, as suggested by Dreher (2004) and Dreher et al. (2008), and reinforced more recently by Trunfull et al. (2020). (2) The situation emphasizing the significance of geologic attributes in unravelling the origin of the deposit, a point in fact also made by Dreher (2004) and Dreher et al. (2008), through arguing that the age of the mineralized breccia is constrained by the geologic relation and geochronology of the Águas Claras siliciclastic cover and the associated mafic dike swarm. (3) The Águas Claras Formation overlies unconformably the breccia unit (Fig. 6) and the mafic bodies have a minimum age of ca. 2650-2670 Ma (evaporation Pb-Pb, zircon, Dias et al. 1996, SHRIMP II Pb-Pb, zircon, Tallarico et al. 2005) or 2710 Ma (U-Pb, zircon and Pb-Pb, sulfides, Mougeot et al. 1996a,b). This indicates a minimum age for the siliciclastic cover and consequently for the unconformably underlying orebodies, which are themselves crosscut by the mafic bodies. (4) The mineralization age is also directly constrained by geochronological data of the Águas Claras Formation itself at 2680 Ma (U-Pb, synvolcanic zircon, Trendall et al. 1998) and maximum 2780-2763 Ma (U-Pb, youngest identified detrital zircon, Mougeot et al. 1996a, Melo et al. 2019a, respectively). The 2680 Ma age in particular offsets the possible constraining significance on the mineralization of younger ages of the mafic dike swarm of ca. 2580 Ma (Tallarico et al. 2005, SHRIMP II Pb-Pb), 2577 Ma (Ferreira Filho 1985, Rb-Sr, total rock) and 2310 Ma (Santos 2002, evaporation Pb-Pb, zircon). (5) In short, the above geological relations and ages of the mafic dike swarm and the siliciclastic cover imply a minimum age of ca. 2650-2680 Ma for the Igarapé Bahia orebodies, which supplants largely the mentioned monazite and molybdenite ages used to characterize epigenetic mineralization.

7. Salobo

7.1. Synvolcanic features

Salobo, the sole IOCG deposits located in the northern limb of the Igarapé Gelado batolith (Fig. 1), also exhibits features similar to those that have been considered in the literature essential to volcanogenic deposits. Main ones taken mainly from sources directly involved in exploration and development of the deposit are (Fig. 9): (1) Similarly to the case of Pojuca, early recognition of the volcanogenic nature of Salobo being based on, inter alia, geological setting, strata-bound and stratiform morphology, magnetite-rich ore-bearing iron-formation and a distal, sediment-dominated environment as compared with Pojuca (Docegeo geologists; Hutchinson 1977, 1979). (2) Magmatic heat source represented by the adjacent and regionally extensive Igarapé Gelado granite whose age specifically in the Salobo area is constrained at 2763 Ga (Melo et al. 2017), overlapping that of the ore-hosting volcanic-sedimentary Salobo Group (cf. Section 3 and Fig. 1). (3) Evidence of synsedimentary growth faulting suggested by the occurrence of fragmental rocks in the form of a 200 m x 6 km "siliceous horizon" occurring SW of the mineralized zone and consisting of 70-80% of quartz fragments plus 10-20% plagioclase (Vieira et al. 1988; Souza and Vieira 2000). (4) A strike-parallel shear zone running northeast of the deposit

possibly representing an original synvolcanic fault (Fig. 9) associated with the early development of the Cinzento fault system (Fig. 1). (5) Finely laminated, strongly sheared and altered almandine-ferrous amphibole-quartz-biotite 'Type 5' schist of, e.g., Souza and Vieira (2000) - commonly found at the base of the Igarapé Salobo package along the contact with the Xingu Complex basement gneisses - also possibly developed in connection with synvolcanic faulting. (6) Important potassic, biotite-bearing alteration zones (Souza and Vieira 2000; Requia and Fontboté 2000; Burns et al. 2019), representing an alteration phase found in volcanogenic deposits submitted to progressive medium-high grade metamorphic rank (Bonnet and Corriveau 2007; Shanks III 2012; Dreher A.M, personal comm.). (7) Strong albitic alteration imprinted in upper gneisses containing 40-60% albite, besides 15-20% retrograde chlorite and accessory sillimanite and cordierite (Martins et al. 1982; Farias and Saueressig 1982). (8) Magnesian alteration possibly indicated by retrogressed chlorite schist bodies closely associated with the above-mentioned strata-bound breccia (item 3), representing, according to Souza and Vieira (2000), conduits of hydrothermal solutions. (9) Also probable magnesian and aluminous alteration represented by the occurrence of garnet, cordierite, anthophyllite, sillimanite and gedrite in quartz-almandine-fayalite-biotite-amphibole schist associated with the mineralized horizon (Martins et al. 1982). (10) The bulk of the copper mineralization contained in banded rocks with high proportion of magnetite (up to >50%) and iron-rich silicates forming metric to decametric horizons within the Salobo Group schist package (Martins et al. 1982; Docegeo 1988; Vieira et al. 1988). (11) Banded iron-rich rocks with mineralogy consisting of magnetite, fayalite, grunerite-cumingtonite and almandine, constituting a metamorphosed oxide-silicate-facies iron-formation (Lindenmayer 1998; Lindenmayer and Teixeira 1999; Requia 1995; see also Martins et al. 1982 for petrographic details). (12) Occurrence in the mineralized oxide-silicate iron-formation of pyrosmalite (Martins et al. 1982; Tazava et al. 1999), a rare chlorine-rich mineral commonly found in a number of volcanogenic and sedex deposits, also identified as a volcanogenic product in Igarapé Bahia (Tazava et al. 1998; Dreher 2004). (13) Interpretation of the ore host rock as an Algoma-type iron-formation submitted to progressive high-grade metamorphism and subsequently retrograded to amphibolite and greenchist facies (Guimarães 1987). (14) Silicate-oxide mineralized iron-rich rock grading upwards to an aluminous variant and from this to metagreywackes and quartzites (Lindenmayer 1998), the ensemble representing a facies change from a chemical precipitate of hydrothermal origin to a mixed rock of chemical-clastic, and to a frankly clastic sequence. (15) Reinforcing the above picture, reference to gradational contacts between different units of the Salobo Group suggesting or indicating a coeval package, including those of the main mineralized iron-rich rocks (cf. rock unit descriptions by Souza and Vieira 2000, Fig. 9). (16) Strata-bound and stratiform ore with relationships between sulfides and host rocks indicating syngenesi s, e.g., disseminated sulfides (80-85% bornite + chalcocite, subordinate chalcopyrite) hosted in the above-described magnetite-rich schists and occasionally constituting millimeter-to centimeter-wide massive bands parallel to original planar structures (Martins et al. 1982; Farias and Saueressig 1982). (17) Reference to ore mineral assemblage forming stringers, stockworks and massive accumulations (Burns et al. 2019,

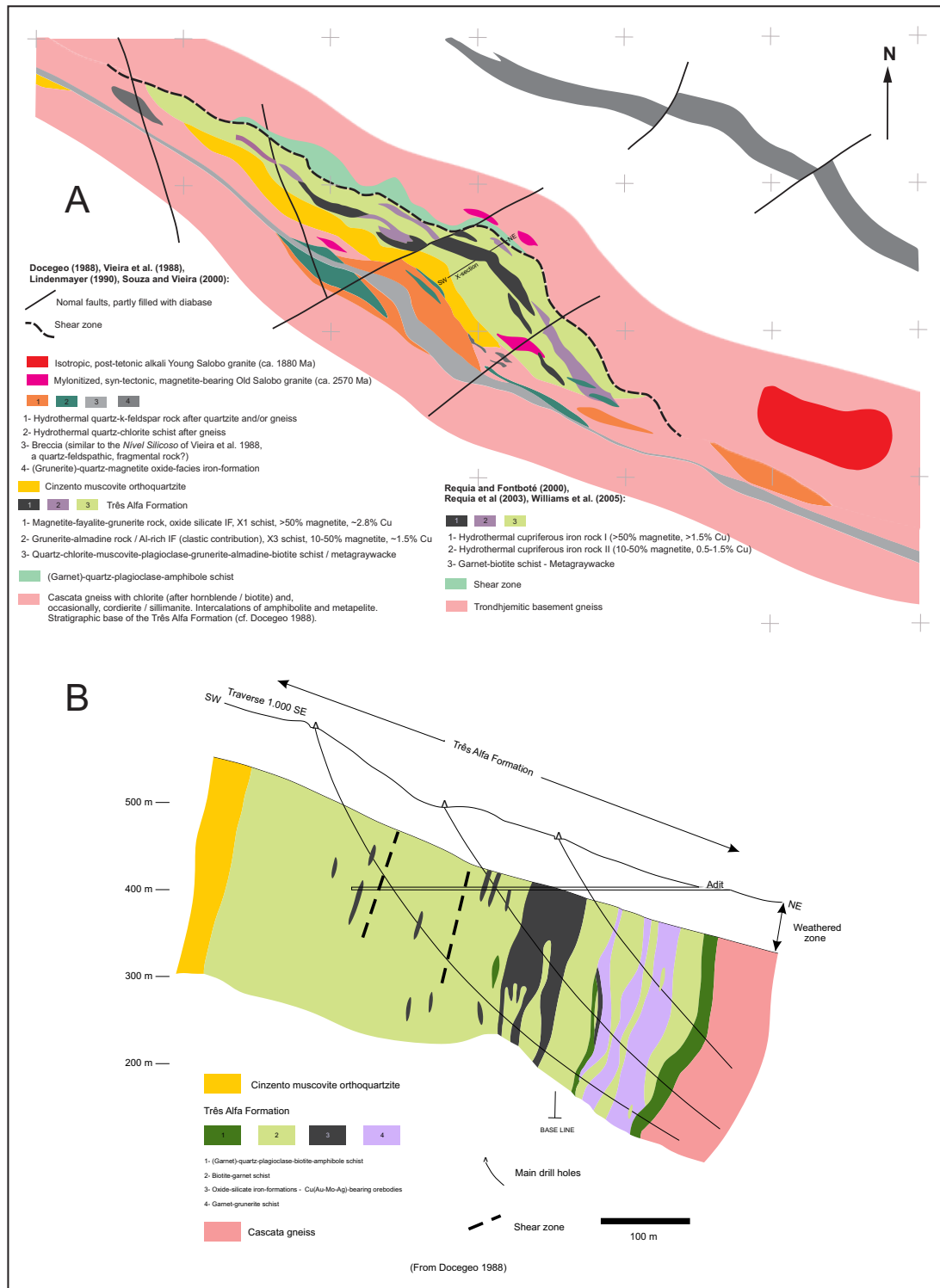


FIGURE 9. A- Geologic map of the Salobo 3 Alfa deposit and environs compiled from different authors referred to in the legend, and incorporating data from the 250 Level. B- Cross-section view of the Salobo deposit showing main lithologic units according to the mining geological model (from Burns et al. 2019, based on CVRD and SMSA 2003, modified).

based on CVRD and SMSA 2003), suggestive of similarity with ore styles of VMS deposits. (18) Despite deformation and remobilization, lithological control still preserved, as per the mentioned preferential association of sulfides and gold with iron-formation within a volcano-exhalative environment suggesting syngenetic concentration (Vieira et al. 1988). (19) Associated volcanogenic exhalites in the form of oxide-silicate facies BIF horizons up to 30 m thick and 300 m long usually

occurring at, but also stratigraphically above, the contact of the ore-bearing schist package with overlying gneiss (Vieira et al. 1988) and including a large, about 100 m-wide, horizon of BIF located ca. 1 km NE of the deposit (Souza and Vieira 2000, Fig. 9). (20) Ore-equivalent horizon represented by the package of oxide iron-formation and hydrothermal chlorite schist occurring immediately above the orebody, with the possible inclusion of the fragmental siliceous quartz-plagioclase horizon of Vieira

et al. (1988) and the mylonitized quartz-plagioclase breccia of Souza and Vieira (2000) extending for several kilometers along strike away from the deposit area (Fig. 9).

7.2. Constraining evidence

7.2.1. Fluid inclusions

Results of fluid inclusion studies for Salobo are shown in Appendix 3.1, being restricted to the work of Requia 1995) and Requia and Fontboté (2000, 2001) and Requia et al. (2003) and Siqueira and Xavier (2001). Main aspects regarding these data, following particularly Requia (1995) and Requia and Fontboté (2000), are: (1) Interpretation of the highly saline fluids (30-58 wt% eq. NaCl) as responsible for copper and gold remobilization, via chloride complexes, during a hydrothermal event associated with greenschist facies retrometamorphism. (2) Interpretation of the low to moderately saline aqueous fluids (1-26% wt% eq. NaCl) as probably representing meteoric solutions, which promoted progressive dilution of the highly saline fluids, cooling, decrease of chlorine activity and metal deposition. (3) Carbonic fluids interpreted as generated or re-equilibrated under metamorphic conditions of high amphibolite facies. (4) Probable source of the highly saline aqueous inclusions considered to include magmatic, formational and meteoric waters, the latter acquiring high salinity through retrograde metamorphic hydration reactions. (5) Following Requia (1995), Requia and Fontboté (2000, 2001) and Requia et al. (2003), in turn, aqueous fluid inclusions in general envisaged as representing a hydrothermal system developed in connection with either medium-high grade metamorphism or a magmatic source, with particular reference to the Old Salobo granite. (6) Recognition of a metamorphic greenschist-facies link for the low to moderate salinity fluid contained in deformed fluorite and, consequently, for the associated subsidiary sulfide mineralization (Siqueira and Xavier 2001). (7) Taken jointly, the above interpretations for fluid inclusion results of Salobo still reflecting doubt between a metamorphic and a granitic connection for the mineralization of Salobo, as already apparent from the work of Winter (1994) in Pojuca.

7.2.2. Stable isotopes

Available stable isotope data for Salobo are shown in Appendix 3.2, and the following comments apply: (1) Oxygen and hydrogen isotopic signature interpreted mainly as evidence of an important magmatic component in the mineralizing fluid of the deposit, having the Old Salobo granite (ca. 2550 Ma) as the ultimate epigenetic fluid source without discarding a metamorphogenic connection (Requia and Fontboté 2000). (2) A magmatic source also suggested for the sulfide sulfur based on the $\delta^{34}\text{S}$ and the $\Delta^{33}\text{S}$ results close to zero (Melo et al. 2019b; Rodriguez et al. 2019) without reference to the possibility of similar results to be produced through the extraction of sulfur from underlying volcanic rocks by convecting seawater. (3) On the other hand, a $\Delta^{33}\text{S}$ ratio near zero interpreted as indicative of involvement of crustal or surface reservoirs (Bhün et al. 2012) and as a signature similar to that of VMS deposits with sulfur leached from basement or supracrustal rocks (Santiago 2016). (4) The syngenetic view reinforced by boron isotopic composition of sulfide-associated tourmaline indicating a marine evaporite source for the boron

and, consequently, for the high salinity of the mineralizing fluids of the deposit, dismissing therefore a magmatic connection (Xavier et al. 2005b, 2008; Dreher and Xavier 2005, 2006). (5) A duple interpretation of boron isotopic results obtained from zoned hydrothermal tourmalines, with heavy boron from cores formed in a 2.76 Ga exhalative system and lighter boron from rims and newly-formed crystals reflecting a 2.55 Ga magmatic-hydrothermal source (Melo et al. 2021; see discussion in item 2.6.4, which applies also here). (6) Taken altogether, stable isotope signatures of Salobo reflecting again the dichotomy between syngeneses and epigenesis, with the evolving research seemingly routing to the former.

7.2.3. Geochronology

Available isotopic dating data of Salobo are summarized in Appendix 3.3 and main points emanating from it are: (1) A Neoproterozoic, synvolcanic age (ca 2705 - 2762 Ma) supported by large-error Pb-Pb leaching results of Mellito and Tassinari (1998) and Tassinari et al. (2003). (2) Re-Os results on molybdenite (table 9) revealing ages of 2576 Ma and 2562 Ma, interpreted as main, granite-related, and local shear-related epigenetic mineralization ages, respectively (Requia and Fontboté 2000; Requia et al. 2003). (3) This line reinforced by U-Pb results of ore-associated zircons of 2535 Ma, with monazite returning U-Pb ages almost 100 Ma younger (table 9), interpreted as related to hydrothermal resetting (Melo et al. 2017). (4) The verification of an apparent geochronological support via robust methods applied on zircon (U-Pb) and molybdenite (Re-Os) to a genetic relationship between the mineralization of Salobo and the late Neoproterozoic (2.57 Ga) Old Salobo granite, indicating an epigenetic origin for the deposit. (5) However, as a counter point to this, the late Neoproterozoic ages (2.6-2.5 Ga) of granites of north Carajás in general being questioned by Toledo et al. (2021) on grounds of the inadequacy of the zircon crystals for precise geochronology, with this metallogenic age bracket being actually discarded (cf. section 11.2.3). (6) According to Toledo et al. (2021), the granitic connection for Salobo still holding but related to the ca. 2.73-2.76 Ga-old, Igarapé Gelado batolith (Fig. 1), considering the deposit ca. 200 Ma older and closer to a syngenetic scenario.

8. Gameleira (Pojuca East)

8.1. Synvolcanic features

The Gameleira or Pojuca East (Fig. 1) deposit constitutes the SE extension of the acknowledged syngenetic volcanogenic Pojuca Corpo 4 (cf. section 4.1). Nevertheless, despite this neighbourhood suggestive of similar metallogeny, Gameleira consists of significant vein mineralization (Docegeo 1993, in Galarza and Macambira 2002) and has been interpreted as a Paleoproterozoic, epigenetic, granite-related deposit in the principal papers dealing with it (Lindenmayer et al. 2001; Ronchi et al. 2001; Pimentel et al. 2003). However, this notwithstanding, Gameleira does show disseminated and banded strata-bound mineralization along with a number of features, taken from the above-mentioned sources, that can be viewed from the volcanogenic standpoint. The features – with particular reference to volumetrically important iron-rich rocks - include (Fig. 10): (1) The deposit occurring in the same mafic volcanic-sedimentary package of Pojuca Corpo

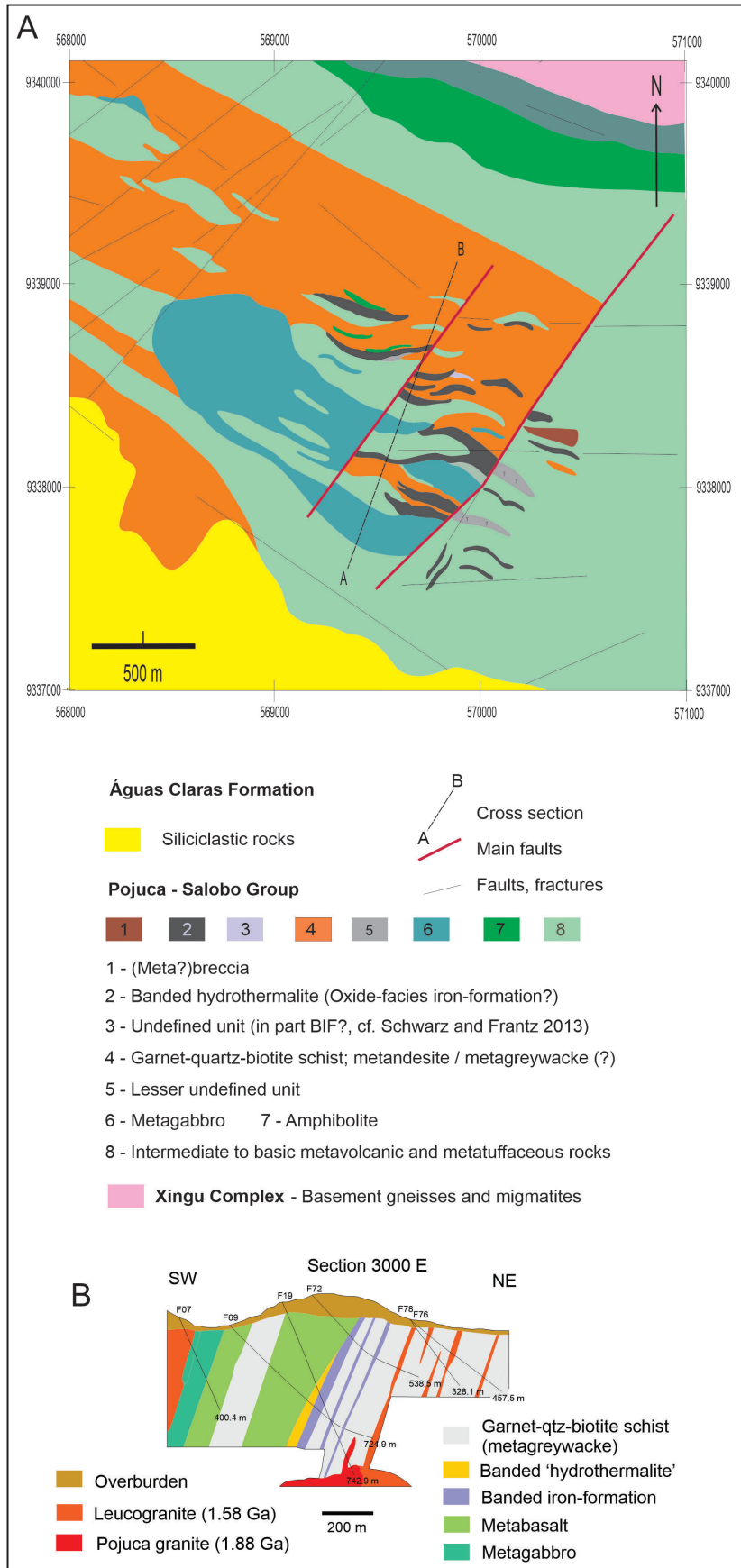


FIGURE 10. A- Geologic map of the Gameleira deposit area (modified from Lindenmayer et al. 2001, after Docegeo 1998). B- Cross-section of Gameleira (from Galarza and Macambira 2002, modified from Docegeo 1997). Note units abutting against main faults, the stretched morphology of the orebodies with local folding, and their habit of occurrence at the contact of a mafic volcanic unit and garnet-quartz-biotite schist.

4 and including an iron-rich banded orebody following, and a set of veins straddling, the contact of volcanic metandesites and a co-magmatic subvolcanic sill of metagabbro. (2) Similar to Pojuca Corpo 4, Gameleira being hosted in a mafic volcanic-sedimentary package, with mention made to biotite schist with fragments remindful of the syngenetic ore-related fragmental rock of Pojuca and possibly representing evidence of synvolcanic growth faulting. (3) The deposit occurring along a regional fault-splay considered the channel for the hydrothermal mineralizing fluid, similar to synvolcanic feeder faults of exhalative systems. (4) The abutting of several units, including hydrothermalites or mineralized iron-formation, against two main faults (Fig. 10A), the configuration suggesting bed morphology controlled by synsedimentary growth faults. (5) The occurrence of near-fault (meta?)breccia, possibly representing an intra-formational coarse-grained deposit related to syndepositional faulting. (6) The observation from the profile by Galarza and Macambira (2002) (Fig. 10B) of a section of metabasalts structurally overlying metagreywackes and intervening mineralized banded iron-formation (and associated hydrothermalite) with the all package suggesting inverted stratigraphy, similarly to the cases of Pojuca and Furnas (Schwarz and Frantz 2013; Dreher et al. 2018). (7) Ore in part strata-bound disseminated in a banded rock composed of quartz, grunerite, magnetite and biotite (Fleck and Lindenmayer 2001), classified as an oxide-silicate iron-formation by Docegeo (1997; in Galarza and Macambira 2002), which are similar to rocks recognized as such, for instance, at Pojuca and Salobo (Hutchinson 1977, 1979; Martins et al. 1982; Guimarães 1987; Docegeo 1988; Winter 1994). (8) This banded host rock, an iron-formation according to several authors, containing tiny, millimeter-wide lenses and disseminations of chalcopyrite in bands of green biotite, magnetite and quartz-grunerite, particularly concentrated in magnetite-rich ones, this altogether suggesting stratiform mineralization in a situation very remindful of synvolcanic ore coeval with an exhalite host rock. (9) The banded quartz-magnetite rock and metavolcanic schists containing, respectively, dravitic tourmaline and amphiboles with high content of chlorine (up to 2%), both mineralogical phases also found in other volcanogenic systems of Carajás, like Igarapé Bahia (see section 6.2.1). (10) Mineralization associated with widespread pervasive potassic (biotite) alteration (Lindenmayer et al. 2001; Galarza and Macambira 2002; Pimentel et al. 2003), a hydrothermal product also found in synvolcanic deposits. (11) Good correlation in the ore between Cr, MgO, CaO and Au as well as the presence of Co-bearing sulfides suggesting that mafic rocks were the source of, and contributed to, the metal budget of the deposit, as would be expected from a hydrothermal synvolcanic cell that permeated andesites and gabbros. (12) Microfolding of the banded host rocks (Fig. 6-I of Lindenmayer et al. 2001) and lenticular and bent morphologies of ore-hosting iron-formations (Fig. 10A) suggesting folded and stretched, i.e., pre-deformation ore-bearing lithological units. (13) The above-mentioned deformation-related morphologic aspect precluding a purely anorogenic, cratonic environment for the orebodies with attending brittle structures and isotropic textures. (14) The reinterpretation of the banded quartz-magnetite rock as a hydrothermalite being based particularly on geochronological evidence, with the rock being denominated a quartz-grunerite vein (Lindenmayer et al. 2001; Pimentel et al. 2003, cf. section

8.2.2 and footnote of appendix 4.2).

8.2. Constraining evidence

8.2.1. Fluid inclusions and stable isotopes

Available data from fluid inclusion and stable isotope studies on mineralized veins of Gameleira are shown in Appendix 4.1. Main points stemming from these sets of data include: (1) Results obtained from fluid inclusions – i.e., large variations in both salinity (up to >50% wt% eq. NaCl) and temperature (150-570 °C) as well as low content or absence of CO₂ (table 10) - indicating a granitic system signature. (2) Reiteration of a magmatic deep-seated source for the hydrothermal fluids of Gameleira via stable isotope results (C, O, S) and, using geochronological support (see next item), a genetic connection of mineralization with Paleoproterozoic (ca. 1.8 Ga) anorogenic granitic magmatism. (3) In contrast, chlorine isotope data and Cl/Br ratios concluding for a significant or dominant evaporitic component in the mineralizing fluids, casting doubt on a purely magmatic epigenetic model for the deposit.

8.2.2. Geochronology

Age data results for Gameleira are summarized in Appendix 4.2 and main points regarding these data are: (1) Results showing clearly a double outcome, namely, a Neoproterozoic (ca. 2600 Ma, Re-Os on molybdenite) and a Paleoproterozoic one (ca. 1800 Ma, Sm-Nd and Ar-Ar on total rock (mineralized vein) and biotite, respectively). (2) This situation coupled with the above-discussed doubtful interpretation of stable isotope data constituting good support for the occurrence of two different, superimposed hydrothermal systems at Gameleira (Pollard et al. 2019). (3) The volume of epigenetic Paleoproterozoic system in the deposit considered significant due to that all rocks are crosscut by veinlets, veins, hydrothermal breccias carrying important amounts of Cu, Au, Mo and F (Galarza and Macambira 2002; Lindenmayer et al. 2001). (4) The metallogenic nature of the Neoproterozoic system remaining uncertain, with Marschik et al. (2002) suggesting mineralization related to regional transpression associated with the late development of the Itacaiúnas basin, and Marschik et al. (2005) favoring an epigenetic connection with granitic magmatism (2.56 – 2.76 Ga) or a syngenetic, Itacaiúnas volcanic affiliation for the mineralization.

9. Grota Funda

9.1. Synvolcanic features

Grota Funda is located a few kilometers southeast of Gameleira and Pojuca (Fig. 1), with which it shares the regional WNW-ESE structural and volcanic-sedimentary trend. Information on Grota Funda is restricted to the accounts by Hunger (2017) and Hunger et al. (2017, 2018) who consider it a representative of the Neoproterozoic epigenetic IOCG deposits of Carajás. Nevertheless, according to these authors, the following features of the deposit are amenable to interpretation from a synvolcanic standpoint (Fig. 11): (1) The same volcanic-sedimentary host setting and structural trend of Pojuca, an acknowledged volcanogenic deposit (section 4.1) (2) Main host rocks of the deposit consisting of strongly and extensively

altered mafic metavolcanic rocks of the Igarapé Pojuca Group that host the homonymous deposit. (3) The occurrence of a similarly strongly altered, and therefore probably subvolcanic, metagabbro unit, making it a candidate to contributor to the magmatic ensemble that provided sustained heat source for a volcanogenic hydrothermal cell. (4) The recognition of an altered dacitic unit carrying blue quartz phenocrysts, a feature found in felsic bodies associated with a number of VMS deposits worldwide (Piercey et al. 2000; Quigley 2016, p. 29; Fredrichs 2017, p. 23; PorterGeo 2018). (5) Banded iron-formations occurring in the vicinities of the deposit, representing exhalite products usually found in association with volcanogenic deposits, and indicating episodic waning phases of the volcanic activity favorable to sulfide deposition. (6) Albite-hastingsite-marialite Na-Ca alteration conceivably corresponding to a variant of the regional sodic-calcic alteration that accompany VMS deposits (cf. spilitization and epidotization). (7) Quartz-magnetite-grunerite-almandine fels, considered by the above authors as early, stage I, ore-related product of iron metasomatism, in fact constituting a variant of mineralized oxide-silicate iron-formation, as suggested elsewhere for other deposits of Carajás. (8) Potassic alteration (biotitization) and chloritization, considered the alteration associated to subsequent stages II and III of the mineralization, as products commonly associated to synvolcanic deposits (Gibson et al. 2007). (9) Alteration chlorite showing iron enrichment, a common chemical characteristic of chlorites occurring at deposit-scale in VMS systems, substituting for Mg-rich alteration chlorites observed further away from the ore

depositional center, as recorded at Igarapé Bahia (Zang and Fyfe 1995) and Furnas (Jesus 2016). (10) Effects of ductile deformation on alteration products such as albite and garnet, suggesting that the products are pre-metamorphic products of an early, perhaps synvolcanic, hydrothermal system. (11) The main ore zone consisting of massive sulfide breccia bodies with up to 70% chalcopyrite, possibly corresponding to brecciated metal-enriched zones reported from vent facies of massive sulfide deposits (Goodfellow et al. 1993), similarly to the Alemão deposit as interpreted by Dreher (2004) (section 6.1). (12) The possibility that the sequential and overlapping three-stage picture of alteration and mineralization described by Hunger et al. (2017, 2018) be a function of the development of vent facies, which typically includes repeated phases of brecciation and substitution (Goodfellow et al. 1993; Lydon 1995).

9.2. Constraining evidence

9.2.1. Fluid inclusions

Data from fluid inclusion studies on Grota Funda are summarized Appendix 5.1. The main aspects in connection with volcanogenic systems is the interpretation of a deep circulating hypersaline fluid as responsible for the transportation of metals as chloride complexes with accompanying albite and scapolite-hastingsite alteration, a view that may apply, inter alia, to exhalative convective hydrothermal cells with the attending semi-conformable alteration zone.

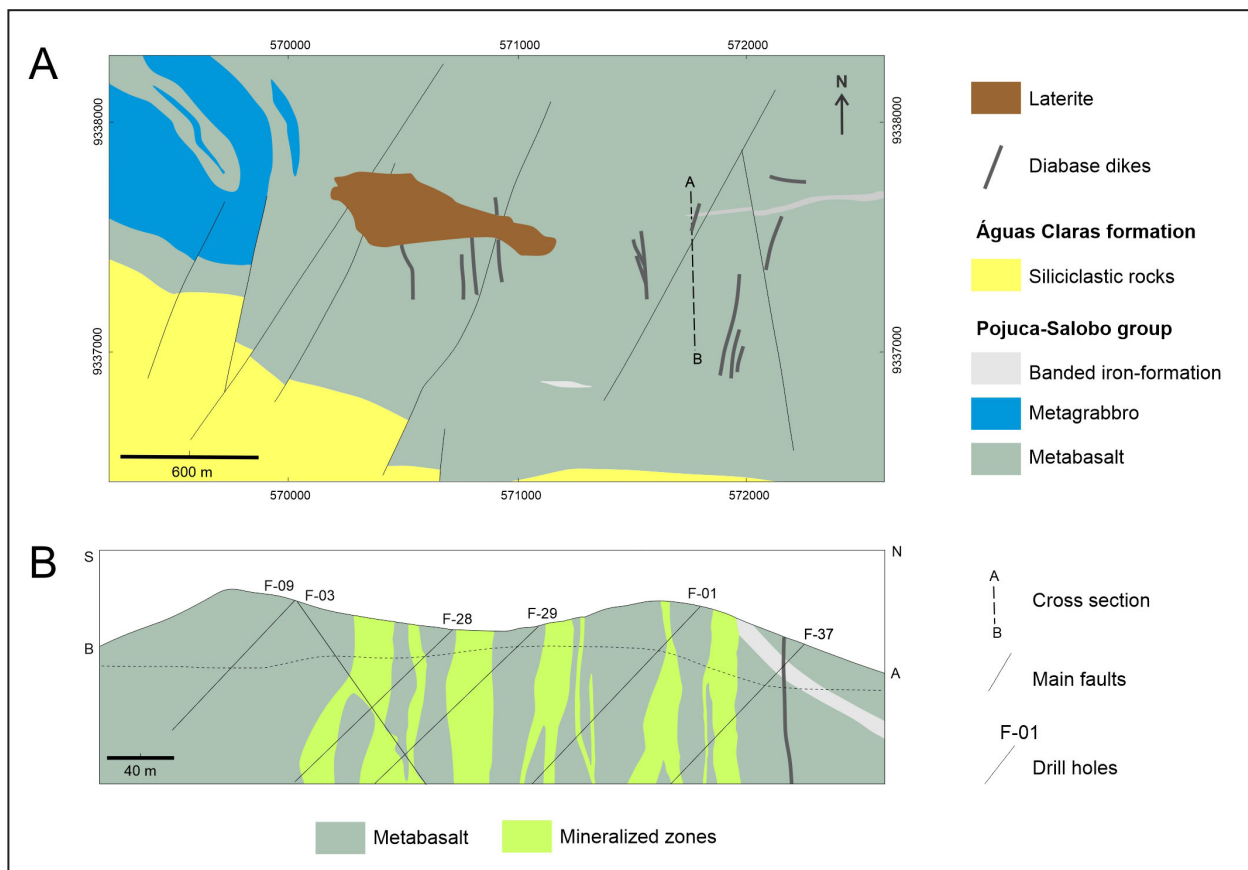


FIGURE 11. A- Simplified map and B- cross-section of the Grota Funda deposit (from Hunger 2017, after a non-specified Vale's source).

9.2.2. Stable isotopes

Stable isotope data on Grota Funda (Appendix 5.1) are restricted to a few determinations of sulfur and boron isotope compositions on chalcopyrite and tourmaline, respectively, which permit the following considerations: (1) Near zero sulfide sulfur isotope composition suggestive of sulfur probably leached from sulfides of the mafic igneous pile that hosts the deposit constituting an interpretation entirely in agreement with synvolcanic convective cells that, characteristically, collect their element budget mainly from the leaching of the underlying dominantly volcanic (i.e., magmatic sulfide-bearing) rock pile. (2) Additionally, the near zero value obtained for chalcopyrite at Grota Funda also in agreement with those obtained from volcanogenic deposits of Archean age (Franklin et al. 2005; Huston et al. 2010). (3) Boron isotope results reinforcing the above picture, being interpreted as not compatible with a fluid of magmatic origin and indicative of sources such as evolved seawater, formation waters, fluids leached from host rocks or even bittern fluids – all of which may be involved in processes associated with the development of synvolcanic hydrothermal systems, precluding an epigenetic origin.

9.2.3. Geochronology

Data on ore geochronology of Grota Funda are also shown in Appendix 5.1 and the following comments apply: (1) Data consisting only of a Re-Os model age of 2530 ± 60 Ma, obtained on molybdenite from grunerite-magnetite veins interpreted as the age of a first stage of mineralization. (2) This stage considered related to iron metasomatism that produced a magnetite-rich quartz-grunerite-almandine fels and considered less important than the second ore stage, associated with biotitic alteration. (3) Alternatively, the possibility that this age of vein molybdenite to represent a younger, perhaps granite-related remobilization, once this, within the error span, is the age of the Neoproterozoic Old Salobo-generation granites of Carajás. (4) For comparison, disseminated molybdenite intergrown with K-alteration biotite of Gameleira returning a Re-Os age of 2614 ± 14 Ma (Marschik et al. 2002, 2005, cf. section 8.2.2) and suggesting therefore that the possibly equivalent main mineralization II of Grota Funda, with similar biotitic alteration, may be at least ca. 100 Ma older than the vein-type mineralization.

10. Igarapé Cinzento (GT-46)

10.1. Synvolcanic features

The GT-46 or Igarapé Cinzento deposit lies in the extreme NW of the northern Carajás Province. Based on geochronology, it was first interpreted as a Paleoproterozoic deposit related to the anorogenic granitic magmatism (Silva et al. 2005), and afterwards considered of Neoproterozoic age formed in connection with the development of the Cinzento shear-zone (Toledo et al. 2017, 2019). Both are epigenetic views. This notwithstanding, the deposit shows the following features, taken mostly from Silva et al. (2005), that can be tentatively ascribed to the volcanogenic model (Fig. 12):

(1) Part of the deposit hosted in the Neoproterozoic volcanic-sedimentary Grão Pará Group with the coeval Igarapé Gelado granite possibly accounting for the sustained heat

source required for the development of robust volcanogenic hydrothermal systems. (2) Reference to regional Ca-Na hastingsite-albite alteration of mafic volcanic rocks (Toledo 2017), which is roughly reminiscent of semi-conformable alteration products of reservoir zone of widespread distribution underneath VMS deposits (Franklin et al. 2005; Santaguida et al. 2002; Paradis et al. 2002). (3) Ore host rocks including biotite amphibolite, amphibole-biotite schist, garnet-biotite-amphibole-quartz-magnetite schist with interlayered grunerite-quartz-magnetite banded iron-formation, and almandine-sillimanite-rich schist and gneiss, this configuring a host package similar to that of the Furnas deposit, and commonly found in metamorphosed volcanogenic deposits. (4) Banded iron oxide-silicate rocks similar to those that host ore in Pojuca, Salobo and, again, Furnas. (5) Specific reference to almandine-sillimanite-rich schists representing a deformed and hydrothermally altered felsic rock subsequently submitted to medium-high grade metamorphic conditions (Silva et al. 2005) and a possible equivalent to synvolcanic alumina alteration of volcanogenic systems. (6) Part of the mineralization described as stringers, veinlets or infillings of chalcopyrite and bornite, as found in chimneys of volcanogenic deposits, and reference also made to the occurrence of massive ore. (7) Part of the ore stretched concordantly to foliation (Silva et al. 2005, p. 128-130; type 1 mineralization of Toledo 2017, p. 91), a situation that can be interpreted in terms of pre-deformation of ore emplacement and, possibly, as indicative of stretched synvolcanic disseminated or stringer ore. (8) Petrographic results also indicating strong deformation of mineralized amphibolite, foliation-concordant mineralization and metamorphic phases in mineralogical assemblage of alteration, this altogether suggesting pre-metamorphic and pre-deformation ore deposition, coherently with syngenetic conditions. (9) Important potassic alteration in the form of biotitization of the mineralized magnetite amphibolites (Silva et al. 2005, p. 104-105), a feature commonly found in volcanogenic deposits. (10) Reference in the same source to amphibolite enriched in cummingtonite, a magnesian grunerite, suggestive of magnesium-rich alteration zone similar to those carrying anthophyllite found in stringer ore chimneys of volcanogenic deposits.

10.2. Constraining evidence

10.2.1. Fluid Inclusions

Appendix 6.1 shows results of fluid inclusion studies of Igarapé Cinzento. The main points in connection with these data are: (1) Silva et al. (2005) – through studying fluid inclusions almost exclusively from granite-associated quartz veins (Appendix 6.1) and considering the salinity of up to 35% eq. NaCl of the widespread type 4 inclusions – concluding that supersaturated fluids were the predominant ones in all the sampled area and that are indicative of magmatic-hydrothermal mineralizing solutions originated from the anorogenic granitic magmatism of 1.88 Ga represented in the deposit area (Fig. 12). (2) Toledo (2017) and Toledo et al. (2019) in contrast - analysing recrystallized quartz from a mineralized quartz-garnet-amphibole schist (1st main mineralization stage) and quartz from a coarse-grained garnet-biotite-chalcopyrite rock representing a late, second stage of alteration and mineralization (Appendix 6.1) – presenting a large spectrum

of interpretation possibilities, which envisages essentially an original hypersaline of evaporitic and/or granitic fluid source with subsequent dilution by shallower, colder and less saline marine or meteoric water. (3) The above interpretation being consistent to a good extent with an evolving synvolcanic hydrothermal cell with coeval evaporitic and/or magmatic fluid input to a predominantly seawater component.

10.2.2. Stable isotopes

Stable isotope studies of Ig. Cinzento are restricted to oxygen, boron and sulfide sulfur as indicated in Appendix 6.2. Main points concerning these studies include: (1) Oxygen and sulfide sulfur isotope interpreted by Silva et al. (2005) and indicative of a Paleoproterozoic granite-source origin for fluids responsible for the mineralization and attending alteration, in conformity with their interpretation of fluid inclusion (above) and geochronological (next item) results. (2) Toledo et al. (2019) in contrast interpreting similar $\delta^{34}\text{S}$ isotope results (Appendix 6.2) of ca. zero per mil for their main mineralization

1 stage (principal, disseminated, strata-bound, ca. 2720 Ma, next item) as indicative of leaching of sulfur from the country rock, an interpretation with a particular appeal for a syngenetic origin for part of the mineralization of Ig. Cinzento and implying a clear-cut departure from the entirely epigenetic interpretation of Silva et al. (2005). (3) Concerning boron isotopes (Appendix 6.2), results interpreted as indicating deposition from metamorphic fluid, in accordance with the nature of the sampled material, viz., tourmaline included in porphyroblastic metamorphic almandine.

10.2.3. Geochronology

Appendix 6.3 summarizes geochronological data available for Igarapé Cinzento and main points concerning the subject are: (1) Paleoproterozoic results obtained particularly with Ar-Ar on alteration biotite by Silva et al. (2005) pointing clearly to an epigenetic mineralization stage for Igarapé Cinzento, with this age probably covering the discordant vein system referred to by these authors. (2) However, the significance of this event

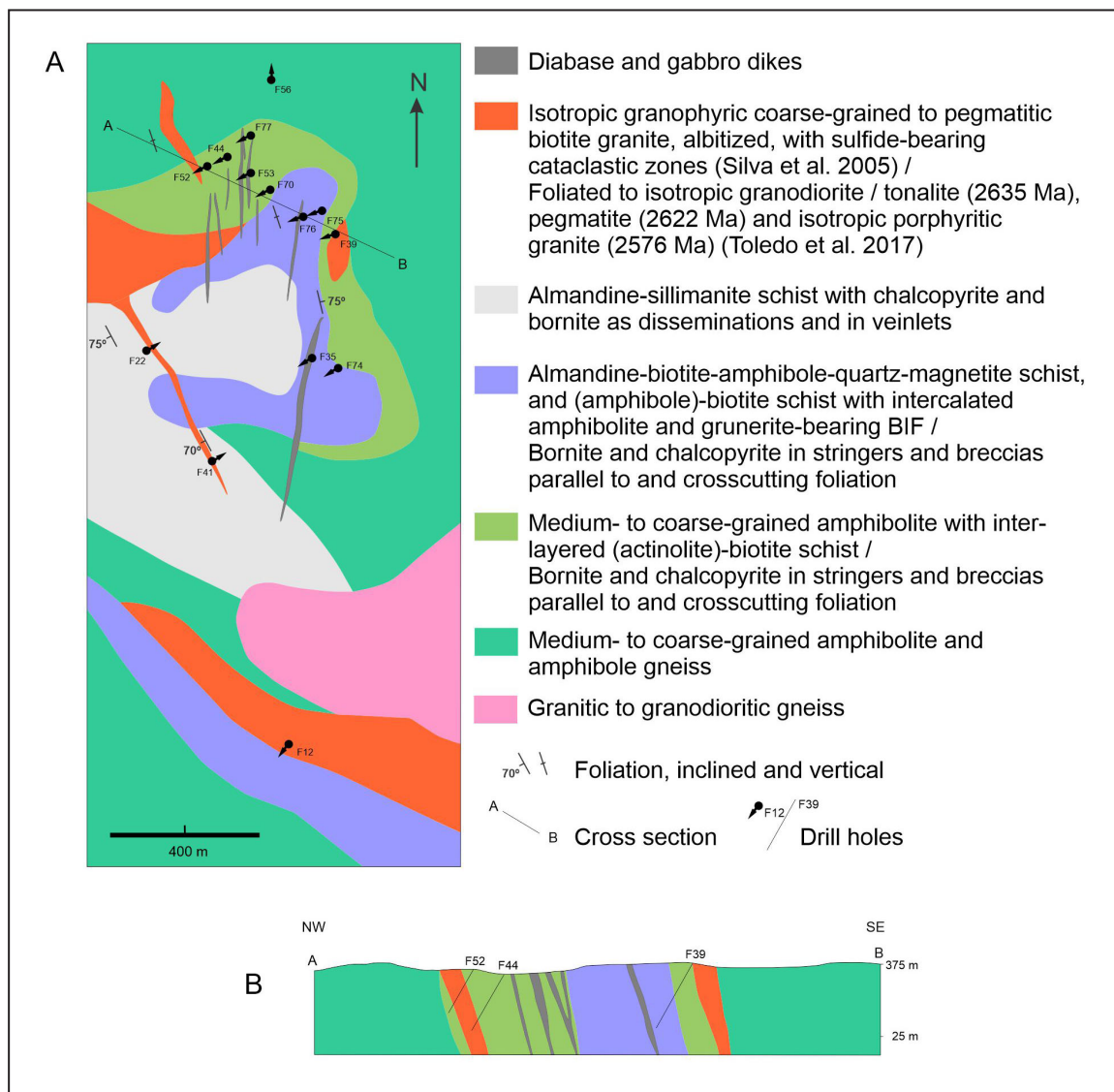


FIGURE 12. A- Geologic map and B- cross-section of the GT-46 / Igarapé Cinzento deposit (from Silva et al. 2005 and Toledo et al. 2017, after Docegeo's Aquiri Project geologists).

in term of the bulk mineralization of the deposit is seemingly pending definition. (3) On the other hand, according to Toledo et al. (2019), molybdenite of the mineralized amphibolite of Igarapé Cinzento returns a Re-Os age of 2718 ± 56 Ma, interpreted as a good estimate of the timing of the first, main, strata-bound, mineralization stage, occurring, for instance, in the form of BIF- and amphibolite-hosted stringers and breccia bodies concordant to foliation (Fig. 12). (4) Comparing this age with that of the ore-hosting amphibolite (2774 ± 19 Ma, U-Pb, zircon, Toledo et al. 2017), there would be an average age gap of 56 Ma between ore and host rock. On the other hand, considering the uncertainty of the results, there is an overlap ca. 20 Ma between the minimum age of host rock (2755 Ma) and the maximum age of the strata-bound ore ($2718 + 56$ Ma, 2774 Ma), implying, rigorously, syngenetic mineralization. (5) Despite this, Toledo et al. (2017, 2019) consider the main, strata-bound mineralization of Ig. Cinzento at ca. 2720 Ma as epigenetic, genetically linked to metamorphic hydrothermalism related to the Cinzento shear zone, with the nearest granitic event in time, cross-cutting strata-bound mineralized bodies, showing a minimum age of ca. 2640 Ma (Fig. 12). (6) Similar average Re-Os ages have also been obtained from ore-related molybdenites of Alemão (2627 ± 11 Ma, Perelló et al. 2023) and Gameleira (2614 ± 14 Ma, Marschik et al. 2002, 2005), with their geological significance being tentatively interpreted by these authors in connection with mafic and granitic intrusive events, respectively (cf. Appendixes 2.5 and 4.2).

11. Summary and discussion

The previous compilations on synvolcanic typological features and constraining evidence of the IOCG deposits of northern Carajás are summarized in tables 1 and 2, respectively.

Regarding typological features (Table 1), it is clear that these deposits share all a series of attributes in the regional and deposit scales that is usually found in deposits of submarine volcanogenic affiliation (Franklin et al. 2005; Gibson et al. 2007; Dubé et al. 2007). Accordingly, in the regional scale, the deposits are all hosted in, and strata-bound to specific units of, a submarine volcanic-sedimentary sequence (the Itacaiúnas Supergroup), which has obviously inherent potential to contain gold and base metals exhalative deposits, particularly given that it presents: (1) adequate structures that were active during the early basin development (e.g., extensional phase of the Cinzento lineament), (2) associated syndepositional robust magmatic heat sources (e.g., Igarapé Gelado batolith) and (3) large metal source hydrothermally altered 'reservoir' zones from which metals may have been possibly scavenged via spilitization and chloritization at Igarapé Bahia and Na-Ca alteration at Igarapé Cinzento.

In the local, deposit-scale, the classical typological volcanogenic attributes are present (Table 1) and include (1) location of deposits at volcanic breaks where waning conditions amenable to exhalative ore deposition occur, (2) syndepositional breccia and slump folds indicative of fluid channelling syndepositional active faults, (3) hydrothermal alteration in the form of dalmatianites as well as of zones of chloritization, biotitization, albitization and alumina alteration, (4) strata-bound deposits confined to oxide-silicate iron-formations and synsedimentary breccias, (5) orebody morphologies consisting mainly of strata-bound

disseminations, but including laminated, massive and stringer ore varieties, (6) associated banded exhalites in the form of oxide iron-formation and a variety of metacherts containing magnetite, tourmaline, actinolite and garnet layers, (7) possible ore-favorable or ore-equivalent horizons represented by linear, stratigraphically controlled breccias and altered zones occurring, for instance, at Pojuca, Igarapé Bahia and Salobo, and (8) particular mineral phases usually found in association with exhalative products, for example, gahnite, dravitic tourmaline, pyrosmalite and Cl-bearing chlorites and amphiboles.

Besides the above generalizations, the following particular synvolcanic-related aspects of the deposits under consideration deserve mention: (1) These various orebody morphologies possibly corresponding to different facies of volcanogenic hydrothermal edifices, namely, subseafloor breccia-hosted disseminations at Igarapé Bahia, massive brecciated vent-facies at Alemão and Grota Funda, proximal, near-seafloor stringers at Pojuca and Furnas, and truly exhalative iron-formation-hosted products at Pojuca, Salobo, Igarapé Cinzento and Gameleira (Hutchinson 1979; Goodfellow et al. 1993; Lydon 1995; Dreher 2004; Santos 2002). (2) A further case of exhalative mineralization represented by strata-bound to stratiform cupriferous intersections hosted in the upper turbiditic section of Igarapé Bahia (Ronzê et al. 2000; Melo et al. 2021). An undeniable evidence of the syngenetic nature of this occurrence is that chalcopyrite occurs as lenses embedded in rip-up clasts of the upper section greywackes (Xavier et al. 2017, Fig. 7). They are undoubtedly products deposited by exhalative fluids that managed to surpass the breccia horizon and vented onto the submarine floor. (3) Additionally, there is the remarkable observation by Santos and Villas (2001) that a conglomerate bed in the overlying sedimentary rocks of Igarapé Bahia contains massive sulfide clasts, which is highly suggestive of early, probably penecontemporaneous, sulfide deposition with subsequent incorporation into the conglomerate. (4) Dreher and Xavier (2001) made a similar point regarding early mineralization in stating that the mineralized breccia of Igarapé Bahia is foliated (Ronzê et al. 2000 as well), i.e., of pre-deformation emplacement, and questioning how could the permeability necessary to mineralize the breccia be restored in epigenetic conditions, in a completely lithified rock.

In conformity with these views, it is worth recalling the characterization of Igarapé Bahia by Dreher and Xavier (2005) as an IOCG hydrothermal system that evolved in a submarine setting, which is in entire agreement with the material compiled in the present article.

The major difference of the IOCG deposits treated herein with respect to classical VMS deposits is the disseminated nature of their sulfides. This departure, however, may be explained in connection with the reviewed constraining evidence.

The evidence indicates that highly saline aqueous fluids were involved (Table 2), which are characteristically poor in sulfur and tend to deposit metals preferentially in the form of oxides. The little sulfur available is readily exhausted through reaction with the chemically more active copper cations to form copper sulfides whereas iron is largely consumed afterwards as magnetite (Dreher 2004). Therefore, this ore characteristic is a function of the fluid involved and does not rigorously preclude volcanogenic sulfide deposits, which in several

TABLE 1. Summary of regional and typological features of IOCG deposits of northern Carajás with data taken from the previous text.

DEPOSIT / Features	POJUCA	FURNAS	IGARAPÉ BAHIA	SALOBO	GAMELEIRA (disseminated)	GROTA FUNDA	IGARAPÉ CINZENTO (GT-46)
Heat source	Igarapé gelado batolith	Furnas granite	Mafic volcanic package	Igarapé gelado batolith	Metagabbro	Metagabbro, dacite	Igarapé gelado granite
Growth faulting evidence	Fragmental rock Slump-induced folds	Breccia with chert clasts	Ore breccia itself, clasts mainly of underlying units	Laterally persistent strata-bound fragmental unit	Near fault breccia Fault-truncated beds	Not reported	Not reported
Deposit-scale alteration	Dalmatianite Chlorite, albitite	Dalmatianite Andalusite, sillimanite	Chlorite, biotite, siderite, tourmaline	Biotite, garnet, albite, chlorite, weak Mg, Al alteration	Biotite	Biotite, chlorite	Biotite, chlorite garnet-sillimanite
Host rock	Banded iron-rich rock Fragmental rock	Oxide-silicate BIF	Strata-bound breccia Lesser turbidite-hosted	Oxide-silicate BIFs (Algoma type)	Oxide-silicate BIF ("hydrothermalite")	Metabasalt	Oxide-silicate BIF
Orebody features	Disseminated, partly banded + stringer ore	Disseminated, partly banded	Strata-bound disseminated + Stratiform (in turbidite) + Partly massive (alemão)	Disseminated, local massive bands + stringer ore	Disseminated in magnetite bands	Massive and brecciated	Stretched along foliation
Associated exhalites	Metachert, oxide BIF Banded chert-amphibole rock	Laminated chert-garnet-tourmaline rock	Not applicable to sub-seafloor orebody/ Nearby oxide BIF	Oxide-facies BIF	Oxide-facies BIF?	Oxide-facies BIF	Not reported
Ore favorable horizon	Corpo 4 Formation itself / Fragmental rock as ore-guide horizon	Chert + BIF / Volcanic-sedimentary contact	Orebody along same volcanic-sedimentary mafic-turbidite contact	BIF + chlorite schist +strata-bound breccia?	Not reported	Not reported	Not reported
Miscellaneous	Metal zonation, gahnite	Chlorite with increasing Fe/(Fe+Mg) ratio towards orebody	Spilitization, Chloritization Fe/(Fe+Mg) chlorite zonation Dravitic tourmaline Cl-bearing phases Mineralized clasts	Strike-parallel shear Local cordierite, gedrite,anthophyllite, sillimanite Cl-bearing pyrosmalite	Dravitic tourmaline Mineralized BIF quoted as quartz-grunerite vein	Dacite with blue quartz Near deposit Fe-chlorite Local Ca-Na alteration with albite + scapolite	Extensive Na-Ca alteration, including albite + epidote Mg-cummingonite as alteration phase ?

instances are rich in magnetite, as reviewed particularly by Kirkham (1979) and Davidson (1992).

Constraining evidence represented by stable isotopes also cannot be used to preclude a volcanogenic affiliation nor to attest a magmatic origin as per the material reviewed in the sections on each deposit (Figs. 13-14 and Table 2).

Particularly illustrative in this respect are the sulfur and boron isotopic signatures. The former commonly cluster around zero (Table 2), this constituting the response usually obtained from Archean volcanogenic deposits due to direct leaching of magmatic sulfide sulfur from underlying volcanic rocks (Franklin et al. 2005; Huston et al. 2010). Boron isotope composition in turn falls in the heavy, positive range, which is shared particularly with marine evaporites and altered oceanic crust (Fig. 15).

According to Marschall and Jiang (2011), high $\delta^{11}\text{B}$ values are in last instance sourced from seawater and may be imprinted in a rock via fluids originated from a subducting slab or from marine carbonates and evaporites or directly from convecting seawater. According to Palmer and Slack (1989), in turn, the most significant control on boron isotopic composition of tourmaline from over 40 globally distributed VMS and sedex deposits and tourmalinites sampled by them seems to be the composition of the boron source, particularly the nature of footwall lithologies, and the boron isotope results

appear particularly sensitive to the presence of evaporites and carbonates in source rocks to the massive sulfides and tourmalinites. The overriding importance of the composition of the boron source as the primary factor responsible for the tourmaline boron isotopic signature of various types of deposits is also recognized by Trumbull et al. (2020).

The above aspects come neatly in support of an evaporitic source for the highly saline fluids involved in the generation of the northern Carajás massive oxide Cu-Au deposits as proposed by Dreher (2004), Dreher and Xavier (2005, 2006) and Xavier et al. (2005b, 2008, 2013), and acknowledged by Trumbull et al. (2020, p. 10). This seawater-related signature suggests strongly that this fluid characteristic was acquired by synvolcanic convective cells and is reinforced by the similar positive boron isotopic range obtained from altered oceanic crust that usually constitutes a significant component of the rock package underlying volcanogenic deposits. Coeval granites in this case would probably play essentially the role of heat engines (Barton and Johnson 2000; Williams et al. 2005; Dreher and Xavier 2005; Xavier et al. 2010) once the related tourmaline light boron signature (Fig. 15) has not been detected in the northern Carajás Cu-Au deposits under consideration.

Another aspect of interest is the wide-range (ca. -20 to + 30 per mil) boron signatures of IOCG deposits indicated

TABLE 2. Summary of reviewed constraining evidence of IOCG deposits of northern Carajás with data taken from appendixes 1 to 6 (Pojuca and Furnas not included due to scarcity of constraining evidence, cf. sections 4.2 and 5.2, respectively.)

DEPOSIT		IGARAPÉ BAHIA	SALOBO	GAMELEIRA	GROTA FUNDA	IGARAPÉ CINZENTO (GT-46)	
CONSTRAINING EVIDENCE				(Mineralized veins)		(GT-46)	
AQUEOUS FLUID INCLUSIONS	SALINITY	Aq Biph: 4-24 wt% eq. NaCl Aq Multiph: 29-45 wt% eq. NaCl Cl/Br ratio ~200-600	Aq low-mod S: 1-26 wt% eq. NaCl Aq high S: 31-58 wt% eq. NaCl Fluorite: 4.6-27.4 wt% eq. NaCl	Aq Biph: 1-23 wt% eq. NaCl Aq Triph: 30-40 wt% eq NaCl	Aq biph: 24-29 wt% eq. NaCl + CaCl ₂ (Na-Ca-rich fluid) Aq biph + solid phases: Highly saline	Aq-carb biph: 0-20 wt% eq. NaCl Triph: 35 / 32->50 wt% eq. NaCl Multiph: up to 35 wt% eq. NaCl Aq-carb biph: Th 150-190 °C Triph: Th 200-300 / 286-420°C Multiph: Th 340°C Carbonic	
	TEMPERATURE	Aq Biph: 100-240 °C Aq Multiph: 131-330 °C	Aq low-mod S: 133-270 °C Aq high S: 334-366 °C (mean 360 °C)				
OTHER FI	NATURE	Monocarbonic & Aq-carb.	Monocarbonic + <10% CH ₄				
STABLE ISOTOPES	SULFUR	Ccp of breccia: -2.1 to +5.6‰ Ccp of turbidite: 0.29 to 1.56‰ $\Delta^{33}\text{S} = -0.11$ to -0.01 ‰	Ccp: -1.28 to +5.04‰ Bornite: -0.37 to +1.63‰ Ccp ($\delta^{33}\text{S}$) = 1.0 to 1.5‰ $\Delta^{33}\text{S} = -0.11$ to -0.01 / 0.15 to 0.56‰	Ccp: 2.0 to 3.08‰ Bornite: 3.74‰ Molybdenite: 4.81‰	Chalcopyrite: 0.9 ± 0.9‰	Cu-sulfides concentrate: 0 to 1‰ Early, main sulfides: 0.01 to 1.99‰ Late, lesser sulfides: 9.75 to 11.25‰	
	OXYGEN	Siderite: 0.7 to 15‰ / -27 to -15‰ Magn, quartz: 6.5 to 10.3‰ Calcite: 5.1 to 7.4‰ Chlorite: 1.9 to 3.2‰	Ore fluid: mode at ca. 7‰ Grunerite: 7.20 to 8.50‰ Garnet: 7.10 to 9.70‰ Tourmaline: 5.07 to 7.37‰ Biotite: 7.23 to 8.03‰ Quartz: 7.52‰	Calcite: 8.91 to 10.03‰ Quartz: 8.8‰		Hydrothermalite / BIF: 6.1 to 7.5‰ Metamafic rocks: 5.3 to 6.4‰	
	HYDROGEN	Tourmaline: -34.02 to -19.74‰ Chlorite: -57.36 to -21.34‰	Tourmaline: -32.13 to +11.60‰ Biotite: -40.94 to -25.94‰				
	CARBON	Siderite: -9.3 to 5.8‰ / -7.3 to 15.8‰ Mostly siderite: -13.4 to -8.3‰ Calcite: -9.32 to -4.93‰	Grunerite: -25.33 to -16.01‰	Calcite: -8.41 to -9.45 ‰			
	BORON	Mg-tourmaline: 12.6‰ to 26.5‰ Mg-tourmaline core: 8.2‰ to 17.2‰ Mg-tourmaline rim: 3.42‰ to 9.8‰	Mg-Fe tourmaline: 14.5 to 24.0‰ Mg-tourmaline core: 8.2‰ to 17.2‰ Mg-tourmaline rim: 3.4 to 9.8‰		Tourmaline: 8.2 to 13.6‰ (from chlorite alteration zone) Mg-tourmaline core: 8.2‰ to 17.2‰ Mg-tourmaline rim: 3.42‰ to 9.8‰	Tourmaline: 5.1 to 6.4‰ (inclusions in porphyroblastic almandine) Mg-tourmaline core: 8.2‰ to 17.2‰ Mg-tourmaline rim: 3.42‰ to 9.8‰	
	CHLORINE			Quartz: +0.28‰ with Cl/Br = 4.071 Quartz: -0.58‰ with Cl/Br = 8.176			
	AGE DATA	Sm-Nd			BIF, whole rock: 1837 ± 30 Ma Vein, whole rock: 1839 ± 15 Ma Vein, whole rock: 1700 ± 31 Ma Vein biotite + sulfide: 1693 ± 30 Ma		Ore conc. 'errorchron': 1752 ± 52 Ma
Ar-Ar				Pervasive biotite: 1734 ± 8 Ma Vein biotite: 1822 ± 4 Ma		Biotite: 1854 ± 5 Ma and 1809 ± 6 Ma Vein biotite: 2506.5 ± 4 Ma	
Pb-Pb		Ccp of breccia: 2769 ± 29 Ma Ccp of breccia: 2772 ± 46 Ma Ccp of mafic volc.: 2756 ± 24 Ma Ccp pyroclastic rock: 2754 ± 36 Ma Gold of breccia: 2744 ± 12 Ma	Magnetite of IF: 2776 ± 240 Ma Chalcocite: 2762 ± 180 Ma Ccp of ore: 2427 ± 130 Ma Tourmaline in ore: 2587 ± 150 Ma Cu-sulfides: 2579 ± 71 Ma		Vein chalcopyrite: 2419 ± 12 Ma Vein chalcopyrite: 2422 ± 12 Ma Ccp concentrate: 2217 ± 19 Ma, 2218 ± 14 Ma, 2180 ± 84 Ma		
U-Pb		Monazite of breccia: 2575 ± 12 Ma Monazite of breccia: 2559 ± 34 Ma	Monazite of ore: 2452 ± 14 Ma Zircon of ore: 2535 ± 8.4 Ma				
		Ore-associated: 2627 ± 11 Ma	Ore-associated: 2576 ± 1.4 Ma				
Re-Os (molybdenite)			Ore-associated: 2562 ± 3.1 Ma		Intergrown with alteration biotite or from a BIF (also referred to as a banded quartz- grunerite vein): 2614 ± 14 Ma		Ore-host amphibolite: 2718 ± 56 Ma Strongly chloritized rock: 2503 ± 51 Ma

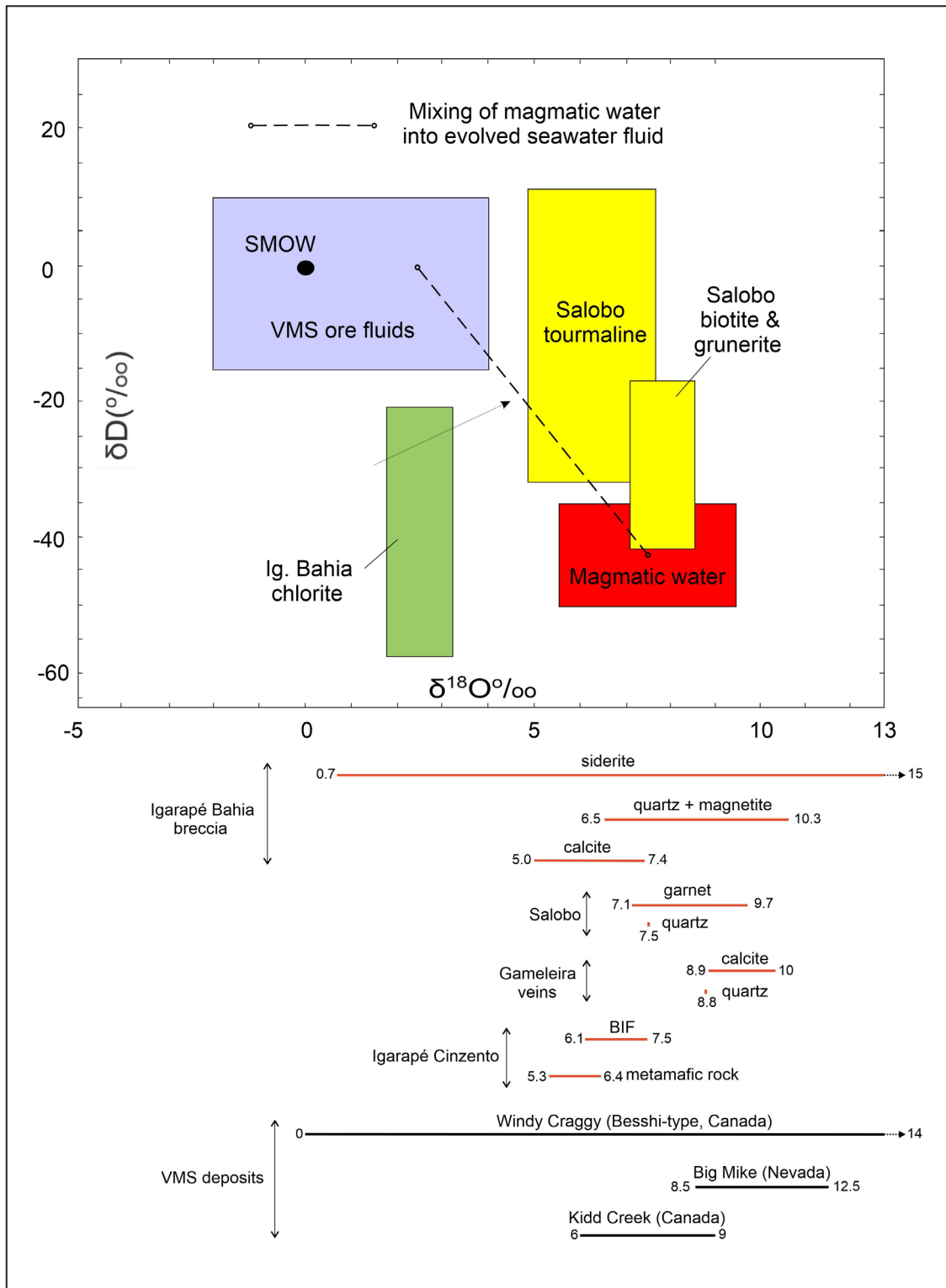


FIGURE 13. Available oxygen-hydrogen isotopic results from the IOCG deposits of northern Carajás (Table 2) compared with the signature of VMS fluids and magmatic water (from Huston 1999), and of specific VMS deposits compiled by Dreher (2004).

in figure 15, actually overlapping the granitic, metamorphic and evaporitic ranges. This certainly reflects the diversity of geological environments to which deposits of the category have been ascribed to (Williams et al. 2005), and points in our opinion to the artificial typological nature of the IOCG grouping. Nevertheless, the IOCG range shown in figure 15 suggests that deposits of this class may actually be metamorphogenic

with fluids having a significant evaporitic component as indicated, for instance, by Cartwright and Oliver (2000) for IOCG deposits of the Mount Isa belt, Australia. Regarding this, mention should parenthetically be made here to the attempt of Winter (1994) to ascribe the high fluid salinity, and the origin itself, of Pojuca to metamorphism (cf. section 4.2). However, though this interpretation could hold for high salinity

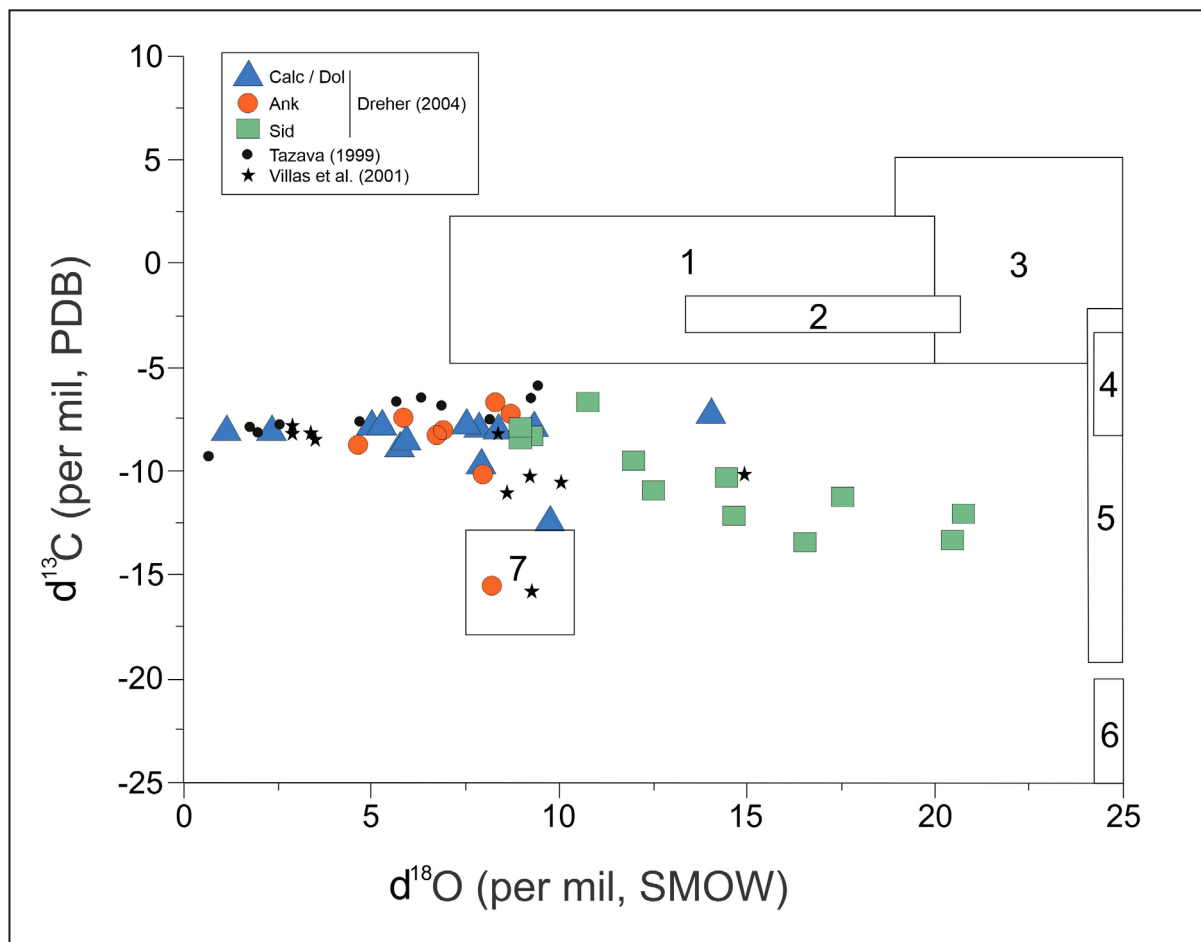


FIGURE 14. Carbon-oxygen isotope compositions of carbonates from Igarapé Bahia (from Dreher 2004, modified). Squared off fields: (1) carbonate from VMS deposits (Huston 1999), (2) siderites from Olympic Dam (Oreskes and Eunadi 1992), (3) marine carbonates, (4) deep-seated carbon, (5) carbonates from Precambrian iron-formations (Perry and Tan 1972; Becker and Clayton 1972; Perry et al. 1973), (6) Carbon from organic origin, (7) carbonates from the amphibolite-grade, VMS Besshi-type Ducktown deposit (Huston 1999). Fields 3, 4 and 6 from Rollison (1993).

base metals systems as Pojuca, as per the above example, metamorphogenic base-metal deposits have been considered very rare and difficult to characterize with respect to genesis (Heinrich et al. 2000). Additionally, the more likely interpretation for metamorphosed base-metals sulfide ores either stratiform or strata-bound within narrow stratigraphic intervals, as is the case of the northern Carajás deposits treated herein, is that they constitute metamorphosed instead of metamorphogenic deposits (Marshall and Spry 2000, p. 50).

Regarding geochronology, evaporation Pb-Pb results (Table 2) back consistently a syngenetic origin for the deposits (e.g., Galarza 2002), some of them showing reasonably low uncertainty (10-20 Ma), whereas the so-called robust methods (U-Pb, Re-Os) fail to define a clear-cut constraining age for the deposits. U-Pb results, particularly on monazite, and part of the Re-Os results on molybdenite point to ca 2550 ages for the mineralization (Tallarico et al. 2005; Requia et al. 2003, Table 2). However, these ages may be problematic due to possible hydrothermal or metamorphic resetting as sustained by Dreher et al. (2008), Melo et al. (2017) and Trunfull et al. (2020).

Literature support for this thesis comes, for instance, from Davis et al. (1994), Ayers et al. (2004), Suzuki et al. (2000, 2001) and Nouzaki et al. (2014). Moreover, the age pattern may also specifically reflect isotopic resetting due to the

long history of development and reactivation of Neoproterozoic shear zones (Pinheiro and Holdsworth 2000; Tavares et al. 2018). Besides this, and perhaps even more important, there is serious geological drawbacks to this mineralization age in the form of sedimentary sequences covering unconformably orebodies and crosscutting mafic dike and sills that are both significantly older than 2550 Ma (Dias et al. 1996; Mougeot et al. 1996a; Dreher 2004; Dreher et al. 2008; Melo et al. 2019a). Additionally, this mineralization event of ca. 2550 Ma has been related to coeval granites (e.g., Old Salobo, Itacaiúnas, Igarapé Geladinho) whose ages have been considered as minimum ones, once the allegedly robust results were obtained from defective zircons (Toledo et al. 2021; Barros et al. 2001). These authors conclude that the crystallization ages are much older than 2550 Ma and that the mentioned granites are actually part of the ca. 2760 Ma main Archean granitic event of Carajás, which includes the Igarapé Gelado batholith (Fig. 1). Pragmatic aspects reinforcing this are the small size and restricted areas of occurrence of these granites.

Another point, made by Dreher (2004), is that the allegedly 2550 Ma-old granites are syntectonic, foliated, implying a compression setting, whereas this was already a time of extension in a cratonic regime as indicated, for instance, by the mafic dike swarm that occurs at Igarapé Bahia. These

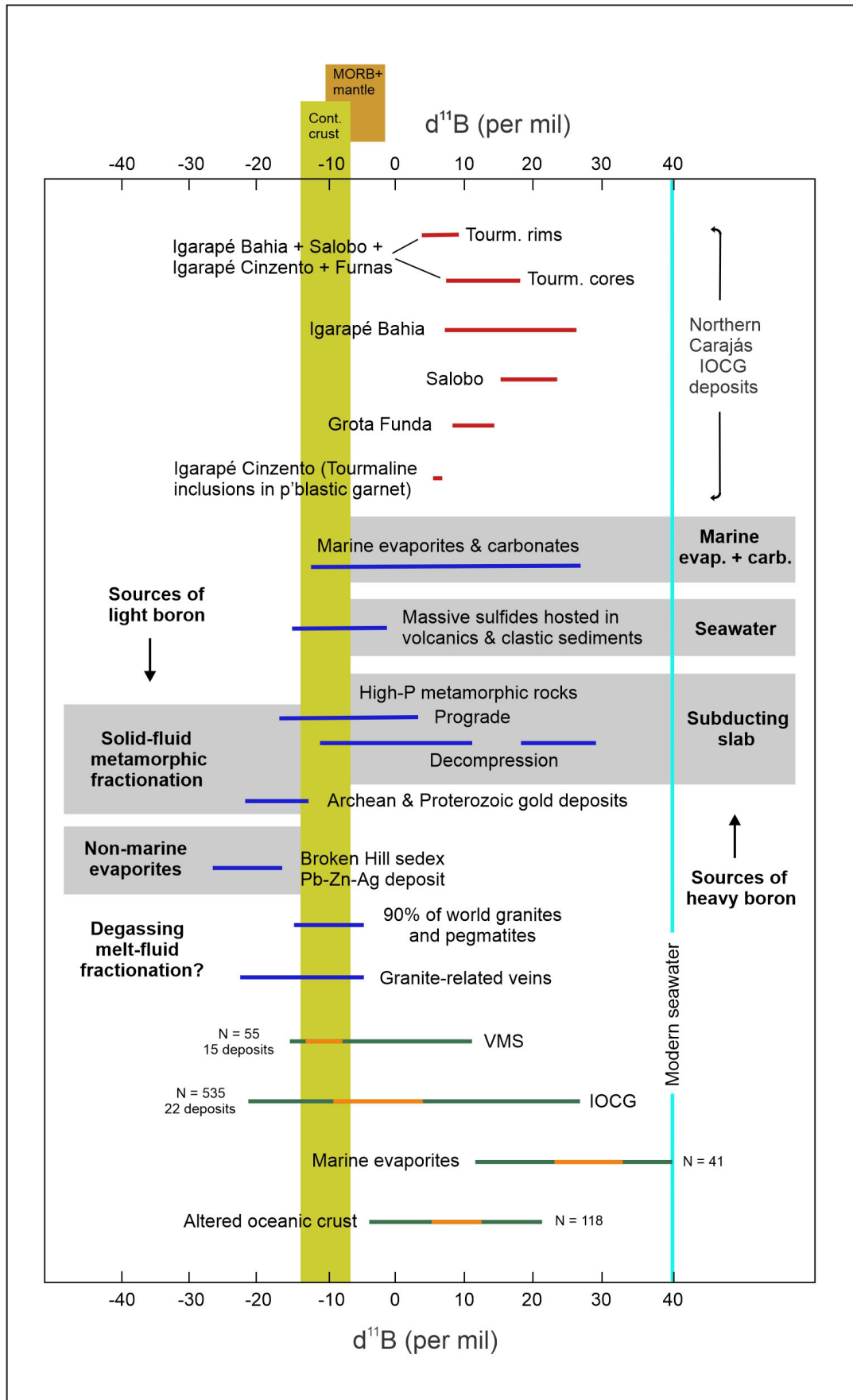


FIGURE 15. Cartoon showing boron isotope signatures of tourmalines of the northern Carajás massive oxide IOCG deposits (red bars, cf. Table 2); of tourmalines as a function of host rock types (dark blue bars) and inferred boron sources (grey bands) (Marschall and Jiang 2011; Shanks III 2014); and from tourmalines of selected deposit types and source rocks (green bars with the 25th-75th percentile range shown in orange) (Trumbull et al. 2020).

views altogether evidently turn down the 2.55 Ga metallogenic event in Carajás and reinforce substantially an Itacaiúnas age for these northern Carajás deposits. Despite this, mention should be made to Re-Os ages on molybdenite that fall in the range of 2600-2700 Ma (Marschik et al. 2002, 2005; Toledo et al. 2017; Perelló et al. 2023, Table 2). These have been used by these authors in the attempt of relating mineralization to regional shearing (Cinzento lineament) or to granitic and mafic magmatism. Alternatively, these ages may be function of partial resetting as mentioned above. At Igarapé Cinzento, the Re-Os age of molybdenite overlaps within error margin with that of the Itacaiúnas itself (cf. section 10.2.3).

12. Final remarks

The set of data presented in this article indicates that the studied magnetitic Cu-Au (IOCG) deposits of north Carajás share many volcanogenic attributes and that the presently available constraining evidence does not prove an epigenetic origin for these deposits. This is further emphasized in Table 3 below showing a qualitative appraisal of the congruity of

attributes and constraining evidence of the northern Carajás deposits with the volcanogenic model.

The table evidently includes various attributes that have been equally utilized as epigenetic characteristics of the IOCG deposits of northern Carajás, with particular reference to metal association, high iron oxide (magnetite) content, hydrothermal alteration and structural control (Xavier et al. 2010, 2017; Pollard et al. 2019). Regarding this apparent dichotomy, we should perhaps appreciate the statement by Williams et al. (2005) that IOCG deposits form a group that is geochemically coherent but geologically very diverse, hinting consequently that the class may encompass deposits of different typology and, possibly, diverse genesis.

To emphasize this, we recall that Hitzmann (2000) envisages three different tectonic settings for IOCG deposits, namely, orogenic collapse (of an originally extensional basin), anorogenic intracontinental and subduction-related continental margin. The first case obviously involves an initial setting that is appropriate for the development of pre-orogenic volcanogenic deposits.

Williams et al. (2005, p. 398) in turn envisage two general geological settings for IOCG deposits, magmatic and non-

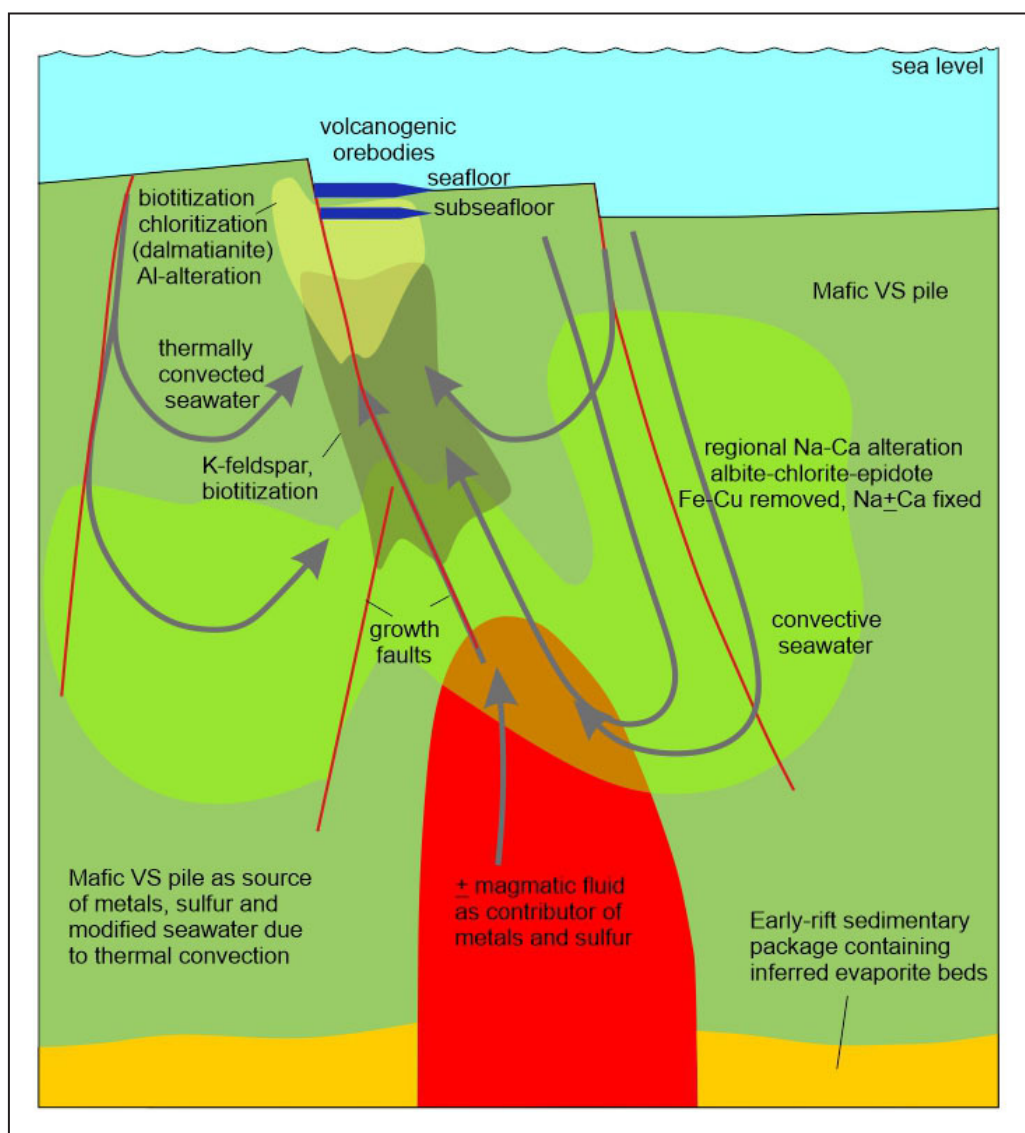


FIGURE 16. A model for seafloor IOCG deposits of north Carajás (based on Williams et al. 2005; see also Barton and Johnson 1996, 2000). Not to scale.

TABLE 3. Degree of congruity between geological attributes and constraining evidence of the massive magnetitic, disseminated Cu-Au sulfide (IOCG) deposits of north Carajás and the volcanogenic model

Volcanogenic attributes (1-8) / Constraining (9-15) evidence	Degree of deposits' adherence / Main aspects
1- Tectonic setting	High / Continental rift, basaltic (tholeiitic) - turbiditic VS sequence
2- Magmatic granitoid heat source	High / A-type foliated granitoids coeval with VS sequence
3- Semi-conformable regional alteration zone	Moderate / Spilitization chloritization (lg. Bahia), Na-Ca alteration(?)
4- Synvolcanic faulting	High / Adequate fault systems, syn-sedimentary breccias, slump folding
5- Deposit-scale hydrothermal alteration zone	High / Dalmatianites, chloritic, biotitic and aluminous alteration zones
6- Volcanogenic orebody proper	High(?) / Disseminated sulfide ore strata-bound in magnetite-rich horizons
7- Exhalite products / Cap rock	High / BIF, metachert, banded quartz-actinolite-tourmaline rocks
8- Favorable / equivalent ore horizon	Moderate / Corpo 4 Fm, extended BIFs and breccias, chloritites
9- Fluid inclusions data	Moderate / High salinity needs magmatic or evaporitic fluid input
10- Sulfide sulfur isotopic signature	High / Close to zero per mil as per Archean VMS deposits
11- Oxygen + hydrogen isotopic signature	Low to moderate / May be interpreted in term of volcanogenic systems
12- Carbon isotopic signature	Low / Ascribed to both magmatic (mantelic) and sedimentary sources
13- Boron isotopic signature	High / Mostly pointing to evaporitic, non-magmatic source
14- Chlorine isotopic signature	Neutral / Applied only to veins but indicative of evaporite-source fluid
15- Ore geochronological data	Low / Syngenetic Pb-Pb with large errors, epigenetic U-Pb (on monazite) and Re-Os either variable or subject to resetting or geologically unsound

magmatic, with the latter further divided into basin-derived and metamorphic-derived. Considering the basin-model (Fig. 16), it becomes quite evident that if the involved brine upflows onto the seafloor, the result would be a syndepositional / synvolcanic product with IOCG characteristics. This is in plain agreement with the view of Dreher and Xavier (2005) that Igarapé Bahia constitutes 'a Fe Oxide (Cu-Au) hydrothermal system evolved in a submarine Archean setting'.

Still according to Williams et al. (2005), the basin-derived model would involve mainly seawater convective fluids in a setting with available non-magmatic chlorine in which the role of intrusions would be primarily to drive thermal convection of the non-magmatic brines (Barton and Johnson 1996, 2000). Fluid salinity could be derived from interaction of convecting seawater with pre-existing marine evaporitic beds (e.g., Red Sea rift, Dreher 2004, Hannington et al. 2005). Evidently, some 'synconvective' magmatic contribution of salt and metals may occur (Huston 1999; Williams et al. 2005; Huston et al. 2011), though not essential. In our view, based on the material compiled in the present exercise, the Cu-Au IOCG deposits of north Carajás fit well the model of a convective hydrothermal system that evolved synvolcanically in an intracratonic extensional basin, with highly saline mineralizing fluids, derived ultimately from lower basin evaporites (Fig. 16), precluding the transportation and deposition of significant quantities of sulfur and sulfides, respectively. Regarding this, Xavier et al. (2010) refer to the Carajás IOCG deposits as generated by granite heat-induced leaching, a process very remindful of a convective exhalative hydrothermal cell scavenging metals from a volcanic-sedimentary pile in a granite-heated environment. Similarly, Schutesky and Oliveira

(2020) suggest that mineralizing fluids may have reached the paleosurface of the Itacaiúnas basin (e.g., mineralized ooids at Alemão) and hint that the IOCG hydrothermal systems developed contemporaneously with the bimodal magmatism (i.e., mafic volcanism and granites) and the world class banded iron-formation-hosted iron ore of the province.

Considering the scenario above – of IOCG deposits with volcanogenic features – it is suggested here, in accordance with Dreher and Xavier (2005), that the deposits dealt with in this paper are products of IOCG hydrothermal systems that evolved as synvolcanic convective cells that upflowed to the (sub)seafloor levels. Complexities brought about by metamorphism and deformation make difficult the unravelling of this metallogenic picture, as they tend to blur detail features and therefore foster misinterpretation, for example, of synvolcanic alteration and syngenetic substitution textures caused by exhalative refining. The larger-scale geological integrity of the deposits, however, was greatly preserved, as per the coherent stratigraphic distribution, strata-bound to stratiform morphology and typological attributes.

Regarding this, Hutchinson (1965; in Lydon 1981, p. 570) pointed out that the small-scale features, on which the hydrothermal replacement theory was based, are the most susceptible to modification by deformation and metamorphism but the larger-scale features are not so susceptible to drastic change. This possibly applies to the northern Carajás deposits, where very detailed, small-scale results provided by laboratory studies have been given more credit than larger-scale, deposit-related geologic features.

Unexpectedly, the deposits consist of disseminated instead of massive sulfides, with magnetite taking the place of

the usual pyrite of volcanogenic deposits. This peculiar aspect is nonetheless shared by other deposits of this affiliation as indicated by Davidson (1992) in what was therein called volcanogenic copper-bearing oxide (VCO) deposits. According to this author, the group includes as potential members - with particularly significant geologic similarities - the Salobo, Granduc (Canada) and Osborne (Australia) deposits.

As a final comment on the copper-gold metallogeny of north Carajás, it may be added that it would be remarkable that in such a world-class mineral province a submarine volcanic-sedimentary sequence – a kind of rock pile that usually develops syngenetic mineralization in several other provinces world over - remained sterile during this stage and would be fertilized only later on via, for instance, granitic magmatic-hydrothermal fluids that failed to mineralize the granites themselves or by metamorphic fluids that in this case failed to generate orogenic gold-only deposits.

Acknowledgements

The authors are grateful to Evandro Klein for his editorial advising and to Roberto Dall'Agnol for his indicating and providing literature items, particularly on granites of Carajás. We fully acknowledge as well the revision work by Avish Kumar, Stephen Munro, and particularly Wilson Scarpelli. Many of their suggestions were incorporated to the manuscript, although any remaining faults should be considered as of the authors' responsibility. Many thanks are also due to Ana Lúcia Borges Fortes Coelho, Nelma Fabrícia da Paixão Ribeiro, Priscila Cristina Ururahy and Flaslendo Vieira Oliveira - librarians at the Geologic Survey of Brazil - for their providing articles and theses particularly difficult to find otherwise. The work on the references by Ana Paula da Silva has been much appreciated as well.

Authorship credits

Author	Study design/Conceptualization	Investigation/Data acquisition	Data Interpretation/Validation	Writing	Review/Editing	Supervision/Project administration
SLM						
AMD						

References

- Almada M.C.O., Villas R.N. 1999. O depósito Bahia: um possível exemplo de depósito de sulfeto vulcanogênico do tipo Besshi arqueano em Carajás. *Revista Brasileira de Geociências*, 29(4), 579-592. Available online at: [10.25249/0375-7536.199929579592](https://doi.org/10.25249/0375-7536.199929579592) / (accessed on 21 April 2022).
- Almeida F.F.M., Hasui Y., Neves B.B.B., Fuck R.A. 1981. Brazilian structural provinces: an introduction. *Earth Science Reviews*, 17(1-2), 1-29. [http://dx.doi.org/10.1016/0012-8252\(81\)90003-9](https://doi.org/10.1016/0012-8252(81)90003-9)
- Alves M.A., Monteiro L.V.S. 2019. Mineralização de cobre do depósito de Furnas, Província Carajás, Brasil. In: *Simpósio Brasileiro de Metalogenia*, 4, 183-184. Available online at: <https://repositorio.usp.br/item/003003552> / (accessed on 1 March 2024).
- Araújo Filho R.C. 2018. O Grupo Águas Claras da Serra dos Carajás, Paleoproterozóico do Cráton Amazônico: fácies, litoestratigrafia e seqüências deposicionais. MSc Dissertation, Instituto de Geociências, Universidade Federal do Pará, Belém, 67 p. Available online at: <http://repositorio.ufpa.br/jspui/handle/2011/10448> / (accessed on 26 January 2023).
- Ayers J.C., Loflin M., Miller C.F., Barton M.D., Coath C. 2004. Dating fluid infiltration using monazite. In: Wanty R.B., Seal II R.R. (eds.). *International Symposium on Water-Rock Interaction*, 11(1), 247-251.
- Barbosa J.P.O., Barros C.E.M., Macambira M.B., Vale A.G. 2001. Geologia e geocronologia do stock granítico Geladinho, região de Parauapebas, Província Mineral de Carajás. In: *Simpósio de Geologia da Amazônia*, 7, 763-766. Available online at: <https://www.sbgeo.org.br/home/pages/44> / (accessed on 1 March 2024).
- Barreira C.F., Soares A.D.V., Ronzê P.C. 1999. Descoberta do depósito Cu-Au Alemão – Província Mineral de Carajás (PA). In: *Simpósio Geologia Amazônia*, 6, 136-139. Available online at: <https://www.sbgeo.org.br/home/pages/44> / (accessed on 1 March 2024).
- Barros C.E.M., Macambira M.J.B., Barbey P. 2001. Idade de zircão do Complexo Granítico Estrela: relações entre magmatismo, deformação e metamorfismo na Província Metalogenética de Carajás. In: *Simpósio de Geologia da Amazônia*, 7, 767-770. Available online at: <https://www.sbgeo.org.br/home/pages/44> / (accessed on 1 March 2024).
- Barros C.E.M., Sardinha A.S., Barbosa J.P.O., Macambira M.J.B., Barbey P., Boullier A.-M. 2009. Structure, petrology, geochemistry, and zircon U-Pb and Pb-Pb geochronology of the synkinematic Archean (2.7 Ga) A-type granites from the Carajás metallogenetic province, northern Brazil. *The Canadian Mineralogist*, 47(6), 1423. <https://doi.org/10.3749/canmin.47.6.1423>
- Barton M.D., Johnson D.A. 1996. Evaporitic-source model for igneous-related Fe-oxide-(REE-Cu-Au-U) mineralization. *Geology*, 24, 259-262. Available online at: https://www.geo.arizona.edu/~mdbarton/MDb_papers_pdf/Barton%5B96_IOC_GEOLOGY.pdf / (accessed on 21 December 2022).
- Barton M.D., Johnson D.A. 2000. Alternative brine source for Fe-oxide (-Cu-Au) systems: implications for hydrothermal alteration and metals. In: Porter T.M. (ed.). *Hydrothermal iron oxide-copper-gold and related deposits: a global perspective*. Adelaide, Australian Mineral Foundation, p. 43-60.
- Beatty D.W., Taylor H.P. 1982. Some petrologic and oxygen isotopic relationships in the Amulet Mine, Noranda, Quebec, and their bearing on the origin of Archean massive sulfide deposits. *Economic Geology*, 77(1), 95. <https://doi.org/10.2113/gsecongeo.77.1.95>
- Becker R.H., Clayton R.N. 1972. Carbon isotopic evidence for the origin of a banded iron-formation in Western Australia. *Geochimica et Cosmochimica Acta*, 36(5), 577-595. [https://doi.org/10.1016/0016-7037\(72\)90077-4](https://doi.org/10.1016/0016-7037(72)90077-4)
- Beisiegel W.R., Farias N.F. 1978. Ocorrências de cobre na Serra dos Carajás. In: *Congresso Brasileiro de Geologia*, 30(4), 1419-1426.
- Bernardelli A.L., Meirelles E.M., Teixeira J.T., Farias N., Saueressig R., Assad R., Beisiegel W.R., Hirata W.K. 1982. Província Mineral de Carajás – Pará: depósitos de ferro, manganês, cobre, ouro, níquel e bauxita. Anexo aos Anais do Simpósio de Geologia da Amazônia, 1, Belém, SBG, 103 p.
- Bhün B., Santos R.V., Dardenne M.A., Oliveira C.G. 2012. Mass-dependent and mass-independent fractionation ($\delta^{34}\text{S}$ and $\delta^{33}\text{S}$) from Brazilian Archean and Proterozoic sulfide deposits by laser ablation multi-collection ICP-MS. *Chemical Geology*, 312-313, 163-164. <https://doi.org/10.1016/j.chemgeo.2012.04.003>
- Blondel F. 1955. Les types de gisement de fer. In: *Chronique des Mines Coloniales*, 231, 226-244.
- Bonnet A.-L., Corriveau L. 2007. Alteration vectors to metamorphosed hydrothermal systems in gneissic terranes. In: Goodfellow W.D. (ed.). *Mineral deposits of Canada: a synthesis of major deposit-types, district metallogeny, the evolution of geological provinces, and exploration methods*. Mineral Deposits Division and Geological Survey of Canada, Special Publication, 5, St. John's, Geological Association of Canada, p. 1035-1049.
- Botelho N.F., Moura M.A., Teixeira L.M., Olivo G.R., Cunha L.M., Santana M.U. 2005. Caracterização geológica e metalogenética do depósito de Cu ± (Au, W, Mo, Sn) Breves, Carajás. In: *Caracterização de depósitos minerais em distritos mineiros da Amazônia*, Brasília, ADIMB. p. 336-389. Available online at: http://www.adimb.com.br/publicacoes/amazonia/Indice/Cap_VI.pdf / (accessed on 4 March 2024).

- Burns N., Gauld C., Alvim M.D., Tagami M. 2019. Geological setting and mineralization. In: Salobo Copper-Gold Mine Carajás, Pará State, Brazil. NI 43-101 Technical Report, Vancouver, Wheaton Precious Metals, p. 22-32. Available online at: https://s21.q4cdn.com/266470217/files/doc_downloads/2020/03/Salobo-Technical-Report-FINAL.pdf / (accessed on 28 July 2023).
- Cartwright I., Oliver N.H.S. 2000. Metamorphic fluids and their relationship to the formation of metamorphosed and metamorphogenic ore deposits. In: Spry P.G., Marshall B., Vokes F.M. (eds.). *Metamorphosed and metamorphogenic ore deposits*. Reviews in Economic Geology, 11, Littleton, Society of Economic Geologists, p. 81-96.
- Chiaradia M., Banks D., Cliff R., Marschik R., Haller A. 2006. Origin of fluids in iron oxide–copper–gold deposits: constraints from $\delta^{37}\text{Cl}$, $87\text{Sr}/86\text{Sr}$ and Cl/Br . *Mineralium Deposita*, 41, 565–573. <https://doi.org/10.1007/s00126-006-0082-6>
- Cordani U.G., Sato K., Teixeira W., Tassinari C.C.G., Basei M.A. 2000. Crustal evolution of the South American Platform. In: Cordani U.G., Milani E.J., Thomaz Filho A., Campos D.A. (eds.). *Tectonic evolution of South America*. Rio de Janeiro, 31st International Geological Congress, p. 19-40. Available online at: <http://rigeo.sgb.gov.br/handle/doc/19419> / (accessed on 4 March 2024).
- CVRD. 2000. Mapa geológico escala 1:12.500 de Igarapé Bahia e seções verticais. Companhia Vale do Rio Doce, unpublished.
- CVRD, SMSA. 2003. Relatório final do Depósito Salobo 3 Alfa. Internal report. Companhia Vale do Rio Doce, Salobo Metais, unpublished.
- Dall'Agnol R., Lafon J.-M., Macambira M.J.B. 1994. Proterozoic anorogenic magmatism in the central Amazonian Province, Amazonian orogen: geochronological, petrological and geochemical aspects. *Mineralogy and Petrology*, 50(1-4), 113-138. <https://doi.org/10.1007/BF01160143>
- Dall'Agnol R., Souza Z.S., Althoff E.J., Barros C.E.M., Leite A.A.S., Jorge João X.S. 1997. General aspects of the granitogenesis of the Carajás Metallogenic Province. In: *International Symposium on Granites and Associated Mineralization*, 2, 135-161.
- Dall'Agnol R., Frost C.D., Rämö O.T. 2012. IGCP Project 510 "A-type granites and related rocks through time": Project vita, results, and contributions to granite research. *Lithos*, 151, 1-16. <https://doi.org/10.1016/j.lithos.2012.08.003>
- Davidson G.J. 1992. Hydrothermal geochemistry and ore genesis of seafloor volcanogenic copper-bearing oxide ores. *Economic Geology*, 87(3), 889–912. <https://doi.org/10.2113/gsecongeo.87.3.889>
- Davis D.W., Schandl E.S., Wasteneys H.A. 1994. U-Pb dating of minerals in alteration halos of Superior Province massive sulfide deposits: syngensis versus metamorphism. *Contributions to Mineralogy and Petrology*, 115(4), 427-437. <https://doi.org/10.1007/BF00320976>
- De Ronde C.E.J., Hannington M.D., Stoffers P., Wright J.C., Ditchburn R.G., Reyes A.G., Baker E.T., Massoth G.J., Lupton J.E., Walker S.L., Greene R.R., Soong C.W.R., Ishibashi J., Lebon G.T., Bray C.J., Resing J.A. 2005. Evolution of a submarine magmatic-hydrothermal system: Brothers volcano, southern Kermadec Arc, New Zealand. *Economic Geology*, 100(6), 1097. <https://doi.org/10.2113/gsecongeo.100.6.1097>
- Dias G.S., Macambira J.M.B., Dall'Agnol R., Soares A.D.V., Barros C.E.M. 1996. Datação de zircões de sill de metagabro: comprovação de idade arqueana da Formação Águas Claras, Carajás, Pará. In: *Simpósio de Geologia da Amazônia*, 5, 376-379. Available online at: <https://www.sbgeo.org.br/home/pages/44> / (accessed on 4 March 2024).
- Dixon C.J. 1979. Introduction. In: *Atlas of economic mineral deposits*. London, Chapman & Hall, p. 5-11. <https://doi.org/10.1007/978-94-011-6511-2>
- DOCEGEO. 1988. Revisão litoestratigráfica da Província Mineral de Carajás. In: *Congresso Brasileiro de Geologia*, 35, 9-54. Available online at: <https://www.sbgeo.org.br/home/pages/44> / (accessed on 4 March 2024).
- DOCEGEO. 1993. Área Pojuca Leste: relatório técnico interno, 24 p.
- DOCEGEO. 1997. Seção geológica vertical 3000SE, Projeto Gameleira. Arquivo L_3000.DWG. Relatório Interno.
- DOCEGEO. 1998. Projeto Gameleira. Relatório Interno, 30 p.
- Dreher A.M. 2004. O depósito de Cu-Au de Igarapé Bahia, Carajás: rochas fragmentárias, fluidos mineralizantes e modelo metalogenético. PhD Thesis, Instituto de Geociências, Universidade Estadual de Campinas, Campinas, 221 p. Available online at: <https://rigeo.sgb.gov.br/handle/doc/102> / (accessed on 13 April 2023).
- Dreher A.M., Xavier R.P. 2001. Provável origem e processo de mineralização das brechas de Igarapé Bahia, Carajás. In: *Simpósio Regional de Geologia da Amazônia*, 7, 151-154. Available online at: <https://www.sbgeo.org.br/home/pages/44> / (accessed on 4 March 2024).
- Dreher A.M., Xavier R.P. 2005. The Igarapé Bahia deposit, Carajás: a Fe oxide (Cu-Au) hydrothermal system evolved in a submarine Archean setting. In: *Simpósio Brasileiro de Metalogenia*, 1, 5 p., CD-ROM.
- Dreher A.M., Xavier R.P. 2006. Geologic and isotopic constraints on fluid source for the Igarapé Bahia Cu-Au deposit, Carajás Mineral Province, Brazil. In: Dall'Agnol R., Rosa-Costa L.T., Klein E.L. (eds.). *Symposium on magmatism, crustal evolution, and metallogenesis of the Amazonian Craton*, Abstracts volume and field trip guide, 17. Available online at: <https://www.sbgeo.org.br/home/pages/44> / (accessed on 7 March 2024).
- Dreher A.M., Xavier R.P., Martini S.L. 2005. Fragmental rocks of the Igarapé Bahia Cu-Au deposit, Carajás Mineral Province, Brasil. *Revista Brasileira de Geociências*, 35(3), 359-368. <https://doi.org/10.25249/0375-7536.2005353359368>
- Dreher A.M., Xavier R.P., Taylor B., Martini S.L. 2008. New geologic, fluid inclusion and stable isotope studies on the controversial Igarapé Bahia Cu-Au deposit, Carajás Province, Brazil. *Mineralium Deposita*, 43(2), 161-184. <http://dx.doi.org/10.1007/s00126-007-0150-6>
- Dreher A.M., Tavares, F.M., Oliveira J.K.M. 2018. Wall rocks and hydrothermal alteration associated with the Pojuca and Furnas deposits, Carajás Province. In: *Congresso Brasileiro de Geologia*, 40, poster. Available online at: <http://cbg2018anais.siteoficial.ws/ST09/st09.htm> / (accessed on 4 March 2024).
- Dubé B., Gosselin P., Mercier-Langevin P., Hannington M., Galley A. 2007. Gold-rich volcanogenic massive sulphide deposits In: Goodfellow W.D. (ed.). *Mineral deposits of Canada: a synthesis of major deposit-types, district metallogeny, the evolution of geological provinces, and exploration methods*. Mineral Deposits Division and Geological Survey of Canada, Special Publication, 5, St. John's, Geological Association of Canada, p. 75-94.
- Eckstrand O.R., Sinclair W.D., Thorpe R.I. 1995. Introduction. In: Eckstrand O.R., Sinclair W.D., Thorpe R.I. (eds.). *Geology of Canadian Mineral Deposit Types*. Geology of Canada, 8, Ottawa, Geological Survey of Canada, p. 1-7. <https://doi.org/10.1130/DNAG-GNA-P1>
- Einsele G. 1991. Submarine mass flow deposits and turbidites. In: Einsele G., Ricken W., Seilacher R. (eds.). *Cycles and events in stratigraphy*. Berlin, Springer-Verlag, p. 313-339.
- Farias N.F., Saueressig R. 1982. Jazida de cobre Salobo 3A. In: Bernardelli A.L., Meirelles E.M., Teixeira J.T., Farias N., Saueressig R., Assad R., Beisiegel W.R., Hirata W.K. *Província Mineral de Carajás – Pará: depósitos de ferro, manganês, cobre, ouro, níquel e bauxita*. Anexo aos Anais do Simpósio de Geologia da Amazônia, 1, Belém, SBG, p. 65-73.
- Farias N.F., Santos A.B.S., Biagini D.O., Vieira E.A.P., Martins L.P.B., Saueressig R. 1984. Jazida de Cu e Zn da área Pojuca, Serra dos Carajás - PA. In: *Congresso Brasileiro de Geologia*, 33(8), 3658-3668.
- Ferreira Filho C.F. 1985. Geologia e mineralizações sulfetadas do prospecto Bahia, Província Mineral de Carajás. MSc Dissertation, Instituto de Geociências, Universidade de Brasília, Brasília, 112 p.
- Fleck A., Lindenmayer Z.G. 2001. Caracterização do minério sulfetado do Alvo Gameleira, Serra dos Carajás. In: *Simpósio de Geologia da Amazônia*, 7, 159-162. Available online at: <https://www.sbgeo.org.br/home/pages/44> / (accessed on 4 March 2024).
- Franklin J.M., Gibson H.L., Jonasson I.R., Galley A.G. 2005. Volcanogenic massive sulfide deposits. In: Hedenquist J.W., Thompson J.F.H., Goldfarb R.J., Richards J.P. (eds.). *Economic geology one hundredth anniversary volume 1905-2005*. Littleton, Society of Economic Geologists, p. 523-560. <https://doi.org/10.5382/AV100.17>
- Galarza M.A., Macambira M.J.B. 2002. Geocronologia e evolução crustal da área do depósito de Cu-Au Gameleira, Província Mineral de Carajás (Pará), Brasil. In: *Geologia USP, Série Científica*, 2, 143-159. <https://doi.org/10.5327/S1519-874X2002000100012>
- Galarza M.A., Macambira M.J.B., Villas R.N. 2006. Age and isotopic characteristics (Pb and S) of the Fe Oxide-Cu-Au-U-REE Igarapé Bahia ore deposit, Carajás Mineral Province, Pará State, Brazil. In: Dall'Agnol R., Rosa-Costa L.T., Klein E.L. (eds.). *Symposium on magmatism, crustal evolution, and metallogenesis of the Amazonian Craton*, Abstracts volume and field trip guide, 19. Available online at: <https://www.sbgeo.org.br/home/pages/44> / (accessed on 7 March 2024).
- Galarza M.A., Macambira J.B., Villas R.N. 2008. Dating and isotopic characteristics (Pb and S) of the Fe oxide–Cu–Au–U–REE Igarapé Bahia ore deposit, Carajás Mineral Province, Pará state, Brazil. *Journal of South American Earth Sciences*, 25(3), 377-397. <https://doi.org/10.1016/j.jsames.2007.07.006>

- Galarza Toro M. A. 2002. Geocronologia e geoquímica isotópica dos depósitos de Cu-Au Igarapé Bahia e Gameleira, Província Mineral de Carajás (PA). PhD Thesis, Centro de Geociências, Universidade Federal do Pará, Belém, 214 p. Available online at: <https://www.repositorio.ufpa.br/jspui/handle/2011/8164> / (accessed on 21 April 2022).
- Galley A.G., Hannington M.D., Jonasson I.R. 2007. Volcanogenic massive sulphide deposits. In: Goodfellow W.D. (ed.). Mineral deposits of Canada: a synthesis of major deposit-types, district metallogeny, the evolution of geological provinces, and exploration methods. Mineral Deposits Division and Geological Survey of Canada, Special Publication, 5, St. John's, Geological Association of Canada, p. 141-161.
- Gibson H.L., Allen R.L., Riverin G., Lane T.E. 2007. The VMS model: Advances and application to exploration targeting. In: Milkereit B. (ed.). Proceedings of Exploration '07: Fifth Decennial Conference on Mineral Exploration, 713-730. Available online at: <http://www.dmecc.ca/ex07-dvd/E07/pdfs/49.pdf> / (accessed on 01 July 2017).
- Goodfellow W.D. 2007. An introduction. In: Goodfellow W.D. (ed.). Mineral deposits of Canada: a synthesis of major deposit-types, district metallogeny, the evolution of geological provinces, and exploration methods. Mineral Deposits Division and Geological Survey of Canada, Special Publication, 5, St. John's, Geological Association of Canada, p 1-2.
- Goodfellow W.D., Lydon J.W., Turner R.J.W. 1993. Geology and genesis of stratiform sediment-hosted (SEDEX) zinc-lead-silver sulphide deposits. In: Kirkham R.V., Sinclair W.D., Thorpe R.L., Duke J.M. (eds.). Mineral deposit modeling, NFL, Geological Association of Canada Special Paper, 40, St John's, Geological Association of Canada, p. 201-251.
- Guimarães I.G. 1987. Petrologia da formação ferrífera na área Salobo 3A, Província Mineral de Carajás – PA. MSc Dissertation, Instituto de Geociências, Universidade de São Paulo, São Paulo, 99 p. Available online at: https://teses.usp.br/teses/disponiveis/44/44135/tde-29092015-101200/publico/Guimaraes_Mestrado.pdf / (accessed on 29 May 2021).
- Hannington M.D., Kjarsgaard I.M. 2002. Mineral-chemical studies of regional-scale hydrothermal alteration in the Central Blake River Group, Western Abitibi Subprovince. Part II: Ben Nevis Volcanic Complex. In: Galley A., Bailes A., Hannington M., Holk G., Katsube J., Paquette F., Paradis S., Santaguida F., Taylor B., Hillary B. Database for CAMIRO Project 94E07: interrelationships between subvolcanic intrusions, large-scale alteration zones and VMS deposits. Open File 4431, Ottawa, Geological Survey of Canada, p. 177-122. <https://doi.org/10.4095/213755>
- Hannington M.D., de Ronde C.E.J., Petersen S. 2005. Sea-floor tectonics and submarine hydrothermal systems. In: Hedenquist J.W., Thompson J.F.H., Goldfarb R.J., Richards J.P. (eds.). Economic geology one hundredth anniversary volume 1905-2005. Littleton, Society of Economic Geologists, p. 111-141.
- Heinrich C.A., Andrew A.S., Knill M.D. 2000. Regional metamorphism and ore formation: evidence from stable isotopes and other fluid tracers. In: Spry P.G., Marshall B., Vokes F.M. (eds.). Metamorphosed and metamorphogenic ore deposits. Reviews in Economic Geology, 11, Littleton, Society of Economic Geologists, p. 97-117.
- Hirata W.K., Rigon J.C., Kadekaru K., Cordeiro A.A.C., Meireles E.M. 1982. Geologia regional da Província Mineral de Carajás. In: Simpósio de Geologia da Amazônia, 1, 100-109. Available online at: <https://www.sbgeo.org.br/home/pages/44> / (accessed on 4 March 2024).
- Hitzman M.W. 2000. Iron oxide-Cu-Au deposits: what, where, when, and why. In: Porter T.M. (ed.). Hydrothermal iron oxide-copper-gold and related deposits: a global perspective. Adelaide, Australian Mineral Foundation, p. 9-25.
- Huhn S.R.B., Nascimento J.A.S. 1997. São os depósitos cupríferos de Carajás do tipo Cu-Au-U-ETR? In: Costa M.L., Angélica R.S. (coords.). Contribuições à geologia da Amazônia. Belém, FINEP, SBG, p. 143-160.
- Hunger R.B. 2017. O depósito de óxido de ferro cobre-ouro (IOCG) Grota Funda, Domínio Carajás (PA): alteração hidrotermal, regime de fluídos e idade da mineralização. Msc Dissertation, Instituto de Geociências, Universidade Estadual de Campinas, Campinas, 92 p. <https://doi.org/10.47749/T/UNICAMP.2017.989415>
- Hunger R.B., Xavier R.P., Moreto C.P.N., Toledo P.I.F., Su Z-K, Zhao X-F. 2017. Fluid evolution in the Grota Funda iron oxide-copper-gold (IOCG) deposit, Carajás Domain, Brazil: evidence from fluid inclusions and boron isotope analyses. In: Simpósio de Geologia da Amazônia, 15, 206-210. Available online at: <https://www.sbgeo.org.br/home/pages/44> / (accessed on 5 March 2024).
- Hunger R.B., Xavier R.P., Moreto C.P.N., Gao J-F. 2018. Hydrothermal alteration, fluid evolution, and Re-Os geochronology of the Grota Funda iron oxide copper-gold deposit, Carajás Province (Pará State), Brazil. Economic Geology, 113(8), 1179-1794. <https://doi.org/10.5382/econgeo.2018.4612>
- Huston D.L. 1999. Stable isotopes and their significance for understanding the genesis of volcanic-hosted massive sulfide deposits: a review. In: Barrie C.T., Hannington M.D. (eds.). Volcanic-associated massive sulfide deposits: processes and examples in modern and ancient settings. Reviews in Economic Geology, 8, Littleton, Society of Economic Geologists, p. 157-179.
- Huston D.L., Pehrsson S., Eglinton B.M., Zaw K. 2010. The geology and metallogeny of volcanic-hosted massive sulfide deposits: variations through geologic time and with tectonic setting. Economic Geology 105(3), 571. <https://doi.org/10.2113/gsecongeo.105.3.571>
- Huston D.L., Relvas J.M.R.S., Gemmel J.B., Driehberg. 2011. The role of granites in volcanic-hosted massive sulphide ore-forming systems: an assessment of magmatic-hydrothermal contributions. Mineralium Deposita, 46, 473-507. <https://doi.org/10.1007/s00126-010-0322-7>
- Hutchinson R.W. 1965. Genesis of massive sulphides reconsidered by comparison to Cyprus deposits. Transactions, 681, Montreal, Canadian Institute of Mining and Metallurgy, p. 286-300.
- Hutchinson R.W. 1977. Report on Docegeo exploration projects and possibilities. Internal report, Goiânia, Docegeo, 112 p.
- Hutchinson R.W. 1979. Report on Docegeo copper projects MM-1 and Salobo and regional geological relationships – Pará, Brazil. Internal report, Goiânia, Docegeo, 17 p.
- Jébrak M., Marcoux É. 2014. Geology of Mineral Resources. St John's, Geological Association of Canada, Department of Earth Sciences.
- Jesus S.S.G.P. 2016. Múltiplos estágios de alteração hidrotermal do depósito de óxido de ferro-cobre-ouro Furnas, Província Mineral de Carajás: evolução paragenética e química mineral. MSc Dissertation, Instituto de Geociências, Universidade de São Paulo, São Paulo, 164 p. Available online at: https://teses.usp.br/teses/disponiveis/44/44137/tde-30032017-081317/publico/Dissertacao_Mestrado_Silvandira.pdf / (accessed on 05 July 2021).
- Kirkham R.V. 1979. Copper in iron formation. In: Current Research, Part B. Paper 79-1B, Ottawa, Geological Survey of Canada, p. 17-22. Available online at: <https://emrlibrary.gov.yk.ca/gsc/papers/79-1B.pdf> / (accessed on 25 July 2023).
- Large R.R. 1992. Australian volcanic-hosted massive sulfide deposits: features, styles, and genetic models. Economic Geology, 87(3), 471-510. <https://doi.org/10.2113/gsecongeo.87.3.471>
- Lindenmayer Z.G. 1998. O depósito de Cu-(Au-Mo) do Salobo, Serra dos Carajás, revisitado. In: Workshop depósitos minerais brasileiros de metais-base, 29-37.
- Lindenmayer Z.G., Teixeira J.B.G. 1999. Ore genesis at the Salobo copper deposit, Serra dos Carajás, In: Silva M.G., Misi A. (eds.). Base metals deposits of Brazil. Belo Horizonte, MME, CPRM, DMPM, p. 33-43.
- Lindenmayer Z.G., Pimentel M.M., Ronchi L.H., Althoff F.J., Laux J.H., Araújo J.C., Fleck A., Baecker C.A., Carvalho D.B., Nowatzki A.C. 2001. Geologia do depósito de Gameleira, Serra dos Carajás, Pará. In: Jost H., Brod J.A., Queiroz E.T. (eds.). Caracterização de depósitos auríferos em distritos mineiros brasileiros. Brasília, DNPM, ADIMB, p. 81-139.
- Lydon J.W. 1981. Genetic Models. In: Skinner B.J. (ed.). Economic Geology: seventy-fifth anniversary volume 1905-1980. Lancaster, The Economic Geology Publishing Company, p. 566-605.
- Lydon J.W. 1995. Sedimentary exhalative sulphides. In: Eckstrand O.R., Sinclair W.D., Thorpe R.K. (eds.). Geology of Canadian mineral deposit types. Geology of Canada, 8. Ottawa, Geological Survey of Canada, p. 130-151.
- Machado N., Lindenmayer Z., Krogh T.E., Lindenmayer D. 1991. U-Pb geochronology of Archean magmatism and basement reactivation in the Carajás area, Amazon shield, Brazil. Precambrian Research, 49(3-4), 329-354. [https://doi.org/10.1016/0301-9268\(91\)90040-H](https://doi.org/10.1016/0301-9268(91)90040-H)
- Marschik R., Mathur R., Ruiz J., Leveille R.A., Almeida A.J. 2002. An Archean Re-Os molybdenite age for the Gameleira Cu-Au-Mo mineralization, Carajás Province, Brazil. Geological Society of America Abstracts and Program, 34(6), 337. Available online at: <https://gsa.confex.com/gsa/2002AM/webprogram/Paper39224.html> / (accessed on 29 July 2023).

- Marschik R., Mathur R., Ruiz J., Leveille R.A., Almeida A.J. 2005. Late Archean Cu-Au-Mo mineralization at Gameleira and Serra Verde, Carajás Mineral Province, Brazil: constraints from Re-Os molybdenite ages. *Mineralium Deposita*, 39, 983-991. <https://doi.org/10.1007/s00126-004-0450-z>
- Marschall H.R., Jiang S-Y. 2011. Tourmaline isotopes: no element left behind. *Elements*, 7(5), 313-319. <https://doi.org/10.2113/gselements.7.5.313>
- Marshall B., Spry P.G. 2000. Discriminating between regional metamorphic remobilization and syntectonic emplacement in the genesis of massive sulfide ores. In: Spry P.G., Marshall B., Vokes F.M. (eds.). *Metamorphosed and metamorphogenic ore deposits. Reviews in Economic Geology*, 11, Littleton, Society of Economic Geologists, p. 39-79.
- Marshall B., Giles A.D., Hagemann S.G. 2000. Fluid inclusions in metamorphosed and synmetamorphic (including metamorphogenic) base and precious metal deposits: Indicators of ore-forming conditions and/or ore-modifying histories? In: Spry P.G., Marshall B., Vokes F.M. (eds.). *Metamorphosed and metamorphogenic ore deposits. Reviews in Economic Geology*, 11, Littleton, Society of Economic Geologists, p. 119-148.
- Martini S.L. 2002. Para cada depósito um possível tipo adequado. Comparação entre conceitos, atributos e tipos de depósitos metálicos das classificações dos Serviços Geológicos do Canadá, dos Estados Unidos e da Colúmbia Britânica. Rio de Janeiro, CPRM. Available online at: http://acervo.cprm.gov.br/rpi_cprm/docreaderNET/docreader.aspx?bib=DiversosCPRM&PagFis=18301 / (accessed on 12 April 2023).
- Martins L.P.B., Saueressig R., Vieira M.A.M. 1982. Aspectos petrográficos das principais litologias da sequência Salobo. In: Simpósio Regional de Geologia da Amazônia, 1(2), 253-262. Available online at: <https://www.sbgeo.org.br/home/pages/44> / (accessed on 5 March 2024).
- McCuaig T.C., Hronsky J.M.A. 2014. The Mineral system concept: the key to exploration targeting. *Society of Economic Geologists, Special Publication* 18(2), 153-175. <http://dx.doi.org/10.1080/03717453.2017.1306274>
- Medeiros Neto F.A. 1986a. Zoneamento químico e mineralógico na jazida de Pojuca, Serra dos Carajás: ferramentas potenciais na exploração mineral. In: Congresso Brasileiro de Geologia, 34(4), 1541-1552.
- Medeiros Neto F.A. 1986b. Mineralizações auríferas da área Pojuca: extração, transporte e deposição a partir de fluidos hidrotermais salinos. In: Congresso Brasileiro de Geologia, 34(4), 1969-1977.
- Mellito K.M., Tassinari C.C.G. 1998. Aplicação dos métodos Rb-Sr e Pb-Pb à evolução da mineralização cuprífera do depósito Salobo 3 α , Província Mineral de Carajás. In: Congresso Brasileiro de Geologia, 40, 119. Available online at: <https://www.sbgeo.org.br/home/pages/44> / (accessed on 5 March 2024).
- Melo G.H.C., Monteiro L.V.S., Xavier R.P., Moreto C.P.N., Santiago E.S.B., Dufrane S.A., Benevides A., Santos A.F.F. 2017. Temporal evolution of the giant Salobo IOCG deposit, Carajás Province (Brazil): constraints from paragenesis of hydrothermal alteration and U-Pb geochronology. *Mineralium Deposita*, 52(5), 709-732. <https://doi.org/10.1007/s00126-016-0693-5>
- Melo G.H.C., Monteiro L.V.S., Xavier R.P., Moreto C.P.N., Arquaz R.M., Silva M.A.D. 2019a. Evolution of the Igarapé Bahia Cu-Au deposit, Carajás Province (Brazil): Early syngenetic chalcocopyrite overprinted by IOCG mineralization. *Ore Geology Reviews*, 111, 102993. <https://doi.org/10.1016/j.oregeorev.2019.102993>
- Melo G.H.C., Monteiro L.V.S., Xavier R.P., Moreto C.P.N., Santiago E. 2019b. Tracing fluid sources for the Salobo and Igarapé Bahia deposits: implications for the genesis of the iron oxide copper-gold deposits in the Carajás Province, Brazil. *Economic Geology*, 114(4), 697-718. <https://doi.org/10.5382/econgeo.4659>
- Melo G.H.C., Monteiro L.V.S., Hunger R.B., Toledo P.I.F., Xavier R.P., Zhao X.-F., Su Z.-L., Moreto C.P.N., Jesus S.S.G.P. 2021. Magmatic-hydrothermal fluids leaching older seafloor exhalative rocks to form IOCG deposits of the Carajás Province: evidence from boron isotopes. *Precambrian Research*, 365, 106412. <https://doi.org/10.1016/j.precamres.2021.106412>
- Mougeot R., Respaut J.P., Briquieu L., Ledru P., Milesi J.P., Macambira M.J.B., Huhn S.B. 1996a. Geochronological constraints for the age of the Águas Claras Formation (Carajás Province, Para, Brazil). In: Congresso Brasileiro de Geologia, 39(6), 579-581.
- Mougeot R., Respaut J.P., Briquieu L., Ledru P., Milesi J.P., Lerouge C., Huhn S.B., Macambira M.J.B. 1996b. Isotope geochemistry constraints for Cu, Au mineralization and evolution of the Carajás Province (Para, Brazil). In: Congresso Brasileiro de Geologia, 39(7), 321-324.
- Nouzaki T., Kato Y., Suzuki K. 2014. Re-Os geochronology of the Hitachi volcanogenic massive sulfide deposit: the oldest ore deposit in Japan. *Economic Geology*, 109(7), 2023-2034. <https://doi.org/10.2113/econgeo.109.7.2023>
- Oreskes N., Enaudi M.T. 1992. Origin of hydrothermal fluids at Olympic Dam: preliminary results from fluid inclusions and stable isotopes. *Economic Geology*, 87(1), 64-90. <https://doi.org/10.2113/econgeo.87.1.64>
- Palmer M.R., Slack J.F. 1989. Boron isotopic composition of tourmaline from massive sulfide deposits and tourmalinites. *Contributions to Mineralogy and Petrology*, 103(4), 434-451. <https://doi.org/10.1007/BF01041751>
- Paradis S., Bailes A., Galley A., Shaw K. 2002. Large-scale hydrothermal alteration systems, Snow Lake area, Manitoba, Canada. In: Galley A., Bailes A., Hanington M., Holk G., Katsube J., Paquette F., Paradis S., Santaguida F., Taylor B., Hillary B. Database for CAMIRO Project 94E07: interrelationships between subvolcanic intrusions, large-scale alteration zones and VMS deposits. Open File 4431, Ottawa, Geological Survey of Canada, p. 281-332. <https://doi.org/10.4095/213755>
- Perelló J., Zulliger G., García A., Creaser R.A. 2023. Revisiting the IOCG geology and age of Alemão in the Igarapé Bahia camp, Carajás province, Brazil. *Journal of South American Earth Sciences*, 124, 104273. <https://doi.org/10.1016/j.jsames.2023.104273>
- Perry E.C., Tan F.C. 1972. Significance of oxygen and carbon isotope variations in Early Precambrian cherts and carbonate rocks of Southern Africa. *Geological Society of America Bulletin*, 83(3), 647-664. [https://doi.org/10.1130/0016-7606\(1972\)83\[647:SOOACI\]2.0.CO;2](https://doi.org/10.1130/0016-7606(1972)83[647:SOOACI]2.0.CO;2)
- Perry E.C., Tan F.C., Morey G.B. 1973. Geology and stable isotope geochemistry of the Biwabik iron-formation, northern Minnesota. *Economic Geology*, 68(7), 1110-1125. <https://doi.org/10.2113/econgeo.68.7.1110>
- Piercey S.J., Peter J.M., Bradshaw G.D., Tucker T., Paradis S. 2000. Geological characteristics of high-level subvolcanic porphyritic intrusions associated with the Wolverine Zn-Pb-Cu volcanic-hosted massive sulphide deposit, Finlayson Lake District, Yukon, Canada. In: Emond D.S., Weston L.H. (eds.). *Yukon Exploration and Geology 2000. Yukon, Indian and Northern Affairs*, p. 335-346. Available online at: https://emrlibrary.gov.yk.ca/ygs/yeg/2000/2000_p335-346.pdf / (accessed on 30 May 2022).
- Pimentel M.M., Lindenmayer Z.G., Laux J.H., Armstrong R., Araújo J.C. 2003. Geochronology and Nd isotope geochemistry of the Gameleira Cu-Au deposit, Serra dos Carajás, Brazil: 1.8-1.7 Ga hydrothermal alteration and mineralization. *Journal of South American Earth Sciences*, 15(7), 803-813. [https://doi.org/10.1016/S0895-9811\(02\)00127-X](https://doi.org/10.1016/S0895-9811(02)00127-X)
- Pinheiro R.V.L., Holdsworth R.E. 2000. Evolução tectonoestratigráfica dos sistemas transcorrentes Carajás e Cinzento, Cinturão Itacaiúnas, no bordo leste do Cráton Amazônico, Pará. *Revista Brasileira de Geociências*, 30(4), 597-606. <https://doi.org/10.25249/0375-7536.2000304597606>
- Pollard P.J., Taylor R.G., Peters L., Matos F., Freitas C., Saboia L., Huhn S. 2019. 40Ar-39Ar dating of Archean iron oxide Cu-Au and Paleoproterozoic granite-related Cu-Au deposits in the Carajás Mineral Province, Brazil: implications for genetic models. *Mineralium Deposita*, 54, 329-344. <https://doi.org/10.1007/s00126-018-0809-1>
- PorterGeo. 2018. Grota Funda: Para, Brazil – Main commodities: Cu Au. Available online at: <https://portergeo.com.au/database/mineinfo.asp?mineid=mn1621> / (accessed on 30 May 2022).
- Quigley P.O. 2016. The spectrum of ore deposit types, their alteration and volcanic setting in the Penokean volcanic belt, Great Lakes region, USA. MSc Dissertation, Colorado School of Mines, Denver, 96 p. Available online at: https://repository.mines.edu/bitstream/handle/11124/170335/Quigley_mines_0052N_11081.pdf?sequence=1&isAllowed=y / (accessed on 30 May 2022).
- Requia K. 1995. O papel do metamorfismo e fases fluidas na gênese da mineralização de cobre de Salobo, Província Mineral de Carajás, Pará. MSc Dissertation, Instituto de Geociências, Universidade de Campinas, Campinas, 152 p. Available online at: <http://repositorio.unicamp.br/Acervo/Detalhe/89053> / (accessed on 20 July 2018).
- Requia K., Fontboté L. 2000. The Salobo iron oxide copper-gold deposit, Carajás, Northern Brazil. In: Porter T.M. (ed.). *Hydrothermal iron oxide-copper-gold and related deposits: a global perspective*. Adelaide, Australian Mineral Foundation, p. 225-236.

- Requia K., Fontboté L. 2001. The Salobo iron oxide copper-gold hydrothermal system, Carajás Mineral Province, Brazil. In: GSA Annual Meeting, 33(6), 8.
- Requia K., Stein H., Fontboté L., Chiaradia M. 2003. Re-Os and Pb-Pb geochronology of the Archean Salobo iron oxide copper-gold deposit, Carajás mineral province, northern Brazil. *Mineralium Deposita*, 38(6), 727-738. <http://dx.doi.org/10.1007/s00126-003-0364-1>
- Rodriguez Y.T.C., Della Giustina M.E.S., Oliveira C.G., Whitehouse M.J. 2019. The giant metamorphosed IOCG Salobo deposit, Carajás Mineral Province: S isotopic constraints and implication for a multi-stage evolutionary model. In: Simpósio de Geologia da Amazônia, 16, 696-700. Available online at: <https://www.sbgeo.org.br/home/pages/44/> (accessed on 6 March 2024).
- Rollison H.R. 1993. Using geochemical data: evaluation, presentation, interpretation. England, Longmans, 352 p.
- Ronchi L. H., Lindenmayer Z. G., Araújo J. C., Baecker C. A. 2001. Assinatura granítica das inclusões fluidas relacionadas ao depósito de Cu-Au de Gameleira, Carajás, PA. In: Simpósio de Geologia da Amazônia, 7, 838-841. Available online at: <https://www.sbgeo.org.br/home/pages/44/> (accessed on 6 March 2024).
- Ronzê P.C., Soares A.D.V., Santos M.G.S., Barreira C.F. 2000. Alemão copper-gold (U-REE) deposit, Carajás, Brazil. In: Porter T.M. (ed.). Hydrothermal iron oxide-copper-gold and related deposits: a global perspective. Adelaide, Australian Mineral Foundation, p. 191-202.
- Routhier P. 1963. Les gisements métallifères. Paris, Masson et Cie.
- Routhier P. 1983. Where are the metals for the future? Orléans Cedex, Éditions du BRGM, p. 1-6.
- Sangster D.F. 1972. Precambrian volcanogenic massive sulphide deposits in Canada: a review. Paper 72-22, Ottawa, Geological Survey of Canada, 44 p. <https://doi.org/10.4095/102291>
- Santaguida F., Gibson D.H., Watkinson D.H., Hannington M.D. 2002. Part I: Semi-conformable epidote-quartz hydrothermal alteration in the central Noranda volcanic complex, Canada: Relationship to volcanic activity and VMS mineralization. In: Galley A., Baines A., Hannington M., Holk G., Katsube J., Paquete F., Paradis S., Santaguida F., Taylor B., Hillary B. Database for CAMIRO Project 94E07: interrelationships between subvolcanic intrusions, large-scale alteration zones and VMS deposits. Open File 4431, Ottawa, Geological Survey of Canada, p. 181-242. <https://doi.org/10.4095/213755>
- Santiago E.S.B. 2016. Elementos traço (in situ LA-ICP-MS) e isótopos estáveis ($\delta^{34}\text{S}$, $\Delta^{33}\text{S}$, $\delta^{56}\text{Fe}$ e $\delta^{18}\text{O}$) em magnetita e sulfetos: origem e evolução de sistemas de Cu-Au neoproterozoicos da Província Mineral de Carajás, Brasil. PhD Thesis, Instituto de Geociências, Universidade Estadual de Campinas, Campinas, 205 p. <https://doi.org/10.47749/T/UNICAMP.2016.979285>
- Santiago E.S.B., Xavier R.P., Monteiro L.V.S., Hagemann S., Cliff J. 2013. The isotopic record of sulphur from Archean and Proterozoic Cu-Au deposits in the Carajás Mineral Province, northern Brazil. In: Society for Geology Applied to Mineral Deposits, Biennial Meeting, 12(3), 1390-1393. Available online at: <https://e-sga.org/nc/publications/sga-biennial-meetings-abstract-volumes/2013-uppsala/> (accessed on 2 May 2023).
- Santos M.G.S. 2002. Estudo de isótopos de Pb e Nd do depósito de Cu-Au (U-ETR) Alemão, Província Mineral de Carajás (PA). MSc Dissertation, Centro de Geociências, Universidade Federal do Pará, Belém, 121 p. Available online at: <http://repositorio.ufpa.br/jspui/handle/2011/12132> (accessed on 5 April 2023).
- Santos M.H.L. 2014. Interpretação, inversão 3D de dados magnéticos e modelagem 3D da susceptibilidade magnética medida, aplicadas à prospecção geofísica de depósitos de óxidos de ferro – cobre – ouro (IOCG iron oxide-copper-gold) – Província Mineral de Carajás, Brasil. PhD Thesis, Instituto de Geociências, Universidade de Brasília, Brasília, 128 p. Available online at: <http://repositorio2.unb.br/jspui/handle/10482/17932/> (accessed on 31 July 18).
- Saueressig R. 1988. Depósito de cobre e zinco do Corpo Quatro, Pojuca. In: Província Mineral de Carajás - Litoestratigrafia e principais depósitos minerais. Anexo aos Anais do Congresso Brasileiro de Geologia, 35, Belém, SBG, p. 115-122. Available online at: <https://www.sbgeo.org.br/home/pages/44/> (accessed on 7 March 2024).
- Schutesky M.E., Oliveira C.G. 2020. From the roots to the roof: an integrated model for the Neoproterozoic Carajás IOCG systems, Brazil. *Ore Geology Reviews*, 127, 103833. <https://doi.org/10.1016/j.oregeorev.2020.103833>
- Schwarz M.R., Frantz J.C. 2013. Depósito de Cu-Zn Pojuca Corpo Quatro: IOCG ou VMS? Instituto de Geociências UFRGS, Pesquisas em Geociências, 40(1), 5-19. <https://doi.org/10.22456/1807-9806.42425>
- Shanks III W.C.P. 2012. Hydrothermal alteration in volcanogenic massive sulfide occurrence model. In: Shanks III W.C.P., Thurston R. (eds.). Volcanogenic massive sulfide occurrence Model - U.S. Geological Survey Scientific Investigations Report 2010-5070-C, Reston, U.S. Geological Survey, p. 169-180. <https://doi.org/10.3113/sir20105070C>
- Shanks III W.C.P. 2014. Stable Isotope Geochemistry of Mineral Deposits. In: Treatise on Geochemistry, 13, 2nd edition. Berlin, Elsevier, p. 59-85. <http://dx.doi.org/10.1016/B978-0-08-095975-7.01103-7>
- Silva M.G., Teixeira J.B.G., Pimentel M.M., Vasconcelos P.M., Arielo A., Rocha W.J.S.F. 2005. Geologia e mineralizações de Fe-Cu-Au do Alvo GT-46 (Igarapé Cinzento), Carajás. In: Marini O.J., Queiroz E.T., Ramos B.W. (eds.). Caracterização de depósitos minerais em distritos mineiros da Amazônia. Brasília, ADIMB, p. 93-151.
- Siqueira J.B., Xavier R.P. 2001. Microtermometria das inclusões fluidas da fluorita e características do depósito Salobo 3A (Carajás/PA). In: Simpósio de Geologia da Amazônia, 7, 226-229. Available online at: <https://www.sbgeo.org.br/home/pages/44/> (accessed on 6 March 2024).
- Siqueira J.B., Rego J.L., Aires Filho B. 2001. Relações entre coberturas siliciclásticas da Formação Rio Fresco e vulcanoclasticas do Grupo Igarapé Bahia (Carajás / PA). In: Simpósio de Geologia da Amazônia, 7, 462-465. Available online at: <https://www.sbgeo.org.br/home/pages/44/> (accessed on 6 March 2024).
- Slack J.F. 1993. Descriptive and grade-tonnage models for Besshi-type massive sulphide deposits. In: Kirkham R.V., Sinclair W.D., Thorpe R.I., Duke J.M. (eds.). Mineral deposit modeling. Special Paper 40, St. John's, Geological Association of Canada, p. 343-371.
- Slack J.F., Trumbull R.B. 2011. Tourmaline as a recorder of ore-forming processes. *Elements*, 7(5), 321-326. <http://dx.doi.org/10.2113/gselements.7.5.321>
- Soares A.D.V., Ronzê P.C., Santos M.G.S., Leal E.D., Barreira C.F. 1999. Geologia e mineralizações do depósito de Cu-Au Alemão – Província Mineral de Carajás – PA. In: Simpósio de Geologia da Amazônia, 6, 144-147. Available online at: <https://www.sbgeo.org.br/home/pages/44/> (accessed on 6 March 2024).
- Souza L.H., Vieira E.A.P. 2000. Salobo 3 Alpha deposit: Geology and mineralization. In: Porter T.M. (ed.). Hydrothermal iron oxide-copper-gold and related deposits: a global perspective. Adelaide, Australian Mineral Foundation, p. 213-224.
- Souza S.R.B. 1996. Estudo geocronológico e de geoquímica isotópica da área Pojuca (Província Mineral de Carajás - PA). MSc Dissertation, Centro de Geociências da Universidade Federal do Pará, Belém, 115 p. Available online at: <https://repositorio.ufpa.br/jspui/handle/2011/15117> (accessed on 06 May 2023).
- Suzuki K., Kagi H., Nara M., Takano B., Nozaki Y. 2000. Experimental alteration of molybdenite of the Re-Os system, infrared spectroscopic profile and polytype. *Geochimica et Cosmochimica Acta*, 64(2), 223-232. [https://doi.org/10.1016/S0016-7037\(99\)00291-4](https://doi.org/10.1016/S0016-7037(99)00291-4)
- Suzuki K., Feely M., O'Reilly C. 2001. Disturbance of the Re-Os chronometer of molybdenites from the late-Caledonian Galway Granite, Ireland, by hydrothermal fluid circulation. *Geochemical Journal*, 35(1), 29-35. <https://doi.org/10.2343/geochemj.35.29>
- Tallarico F.H.B., Oliveira C.G., Figueiredo B.R. 2000. The Igarapé Bahia Cu-Au mineralization, Carajás Province. *Revista Brasileira de Geociências*, 30(2), 230-233. <https://doi.org/10.25249/0375-7536.2000302230233>
- Tallarico F.H.B., McNaughton N.J., Groves D.I., Fletcher I.R., Figueiredo B.R., Carvalho J.B., Rego J.L., Nunes A.R. 2004. Geological and SHRIMP II U-Pb constraints on the age and origin of the Breves Cu-Au-(W-Bi-Sn) deposit, Carajás, Brazil. *Mineralium Deposita*, 39(1), 68-86. <https://doi.org/10.1007/s00126-003-0383-y>
- Tallarico F.H.B., Figueiredo B.R., Groves D.I., Kositsin N., McNaughton N.J., Fletcher I.R., Rego J.L. 2005. Geology and SHRIMP U-Pb Geochronology of the Igarapé Bahia deposit, Carajás Copper-Gold Belt, Brazil: An Archean (2.57 Ga) example of iron-oxide Cu-Au-(U-REE) mineralization. *Economic Geology*, 100(1), 7. <https://doi.org/10.2113/100.1.0007>
- Tassinari C.C.G., Bettencourt J.S., Geraldès M.C., Macambira M.J.B., Lafon J.M. 2000. The Amazonian Craton. In: Cordani U.G., Milani E.J., Thomaz Filho A., Campos D.A. (eds.). Tectonic evolution of South America. Rio de Janeiro, 31st International Geological Congress, p. 41-95. Available online at: <https://rigeo.sgb.gov.br/handle/doc/19419> (accessed on 7 March 2024).
- Tassinari C.C.G., Mellito K.M., Babinski M. 2003. Age and origin of the Cu (Au-Mo-Ag) Salobo 3A ore deposit, Carajás Mineral Province,

- Amazonian Craton, northern Brazil. *Episodes*, 26(1), 2–9. <https://doi.org/10.18814/epiiugs/2003/v26i1/001>
- Tavares F.M., Trow R.A.J., Silva C.M.G., Justo A.P., Oliveira J.K.M. 2018. The multistage tectonic evolution of the northeastern Carajás Province, Amazonian Craton, Brazil: Revealing complex structural patterns. *Journal of South American Earth Sciences*, 88, 238-252. <http://dx.doi.org/10.1016/j.jsames.2018.08.024>
- Tazava E., Oliveira C.G. 2000. The Igarapé Bahia Au-Cu-(REE-U) deposit, Carajás Mineral Province, Northern Brazil. In: Porter T.M. (ed.). *Hydrothermal iron oxide-copper-gold and related deposits: a global perspective*. Adelaide, Australian Mineral Foundation, p. 203-212.
- Tazava E., Gomes N.S., Oliveira C.G. 1998. Significado da pirosmalita no depósito de Cu-Au-(U-ETR) de Igarapé Bahia, Província Mineral de Carajás. In: Congresso Brasileiro de Geologia, 40, 161. Available online at: <https://www.sbgeo.org.br/home/pages/44/> (accessed on 7 March 2024).
- Tazava E., Oliveira C.G., Gomes N.S. 1999. Ocorrência de ferropirosmalita nas brechas mineralizadas do depósito de Au-Cu (+ ETR-U) de Igarapé Bahia, Província Mineral de Carajás. *Revista Brasileira de Geociências*, 29(3), 345-348. <http://dx.doi.org/10.25249/0375-7536.199929345348>
- Toledo P.I.F. 2017. Evolução geológica do depósito de óxido de ferro-cobreado Igarapé Cinzento (GT-46), Província Carajás. MSc Dissertation, Instituto de Geociências, Universidade Estadual de Campinas, Campinas, 135 p. Available online at: <https://doi.org/10.47749/TIUNICAMP.2017.1062732> (accessed on 24 November 2021).
- Toledo P.I.F., Moreto C.P.N., Xavier R.P., Melo G.H.C., Hunger R.B., Gao J-F. 2017. New geological and geochronological data for the GT-46 deposit, Carajás Province: Relationships between the Cinzento shear zone reactivation, mineralization and granite emplacement. In: *Simpósio de Geologia da Amazônia*, 15, 268-272.
- Toledo P.I.F., Moreto C.P.N., Xavier R.P., Gao J-F., Matos J.H.S.N., Melo G.H.C. 2019. Multistage evolution of the Neoproterozoic (ca. 2.7 Ga) Igarapé Cinzento (GT-46) iron oxide-copper-gold deposit, Cinzento shear zone, Carajás province, Brazil. *Economic Geology*, 114(1), 1-34. <https://doi.org/10.5382/econgeo.2019.4617>
- Toledo P.I., Moreto C.P., Melo G.H., Monteiro L.V., Matos F.M., Carvalho J.A., Medeiros Filho C.A. 2021. Breaking up the link between IOCG genesis and granitic magmatism at 2.6-2.5 Ga in the Carajás Province, NW Brazil. In: *Society of Economic Geologists Annual Conference (SEG 100)*, 319.
- Trendall A.F., Basei M.A.S., Laeter J.R., Nelson D.R. 1998. SHRIMP zircon U-Pb constraints on the age of the Carajás Formation, Grão Pará Group, Amazon Craton. *Journal of South America Earth Science*, 11(3), 265-277. [https://doi.org/10.1016/S0895-9811\(98\)00015-7](https://doi.org/10.1016/S0895-9811(98)00015-7)
- Trumbull R.F., Codeço M.S., Jiang S-Y., Palmer M.R., Slack J.F. 2020. Boron isotope variations in tourmaline from hydrothermal ore deposits: a review of controlling factors and insights for mineralizing systems. *Ore Geology Reviews*, 125, 103682. <https://doi.org/10.1016/j.oregeorev.2020.103682>
- Trunfull E.F., Hagemann S.G., Xavier R.P., Moreto C.P.N. 2020. Critical assessment of geochronological data from the Carajás Mineral Province, Brazil: implications for metallogeny and tectonic evolution. *Ore Geology Reviews*, 121, 103556. <https://doi.org/10.1016/j.oregeorev.2020.103556>
- Vale. 2010. Projeto Furnas. Relatório final de pesquisa. Brasília, Departamento Nacional de Produção Mineral.
- Vale. 2012. Projeto Furnas. Relatório final de geologia, Internal report.
- Vasquez L.V., Rosa-Costa L.T., Silva C.G., Ricci P.F., Barbosa J.O., Klein E.L., Lopes E.S., Macambira E.B., Chaves C.L., Carvalho J.M., Oliveira J.G., Anjos G.C., Silva H.R., Jorge João X.S. 2008. Geologia e recursos minerais do Estado do Pará. Texto explicativo dos mapas geológico e tectônico e de recursos minerais do Estado do Pará. Escala 1:1.000.000. Belém, CPRM, 329 p. Available online at: <https://rigeo.sgb.gov.br/handle/doc/10443> (accessed on 20 July 2020).
- Vieira E.A.P., Saueressig R., Siqueira J.B., Silva E.R.P., Rêgo J.L., Castro F.D.C. 1988. Caracterização geológica da jazida polimetálica do Salobo 3A. In: *Província Mineral de Carajás - Litoestratigrafia e principais depósitos minerais*. Anexo aos Anais do Congresso Brasileiro de Geologia, 35, Belém, SBG, 97-114. Available online at: <https://www.sbgeo.org.br/home/pages/44/> (accessed on 7 March 2024).
- Villas R.N., Santos M.D. 2001. Gold deposits of the Carajás Mineral Province: deposit types and metallogenesis. *Mineralium Deposita*, 36(3), 300-331. <http://dx.doi.org/10.1007/s001260100178>
- Villas R.N., Toro M.A.G. 2001. As brechas hidrotermais do depósito Igarapé Bahia, Carajás: dados geoquímicos e de isótopos estáveis de carbono e enxofre. In: *Simpósio Geologia da Amazônia*, 7, 870-873. Available online at: <https://www.sbgeo.org.br/home/pages/44/> (accessed on 7 March 2024).
- Villas R.N., Galarza M.A., Almada M.C., Viana A.S., Ronzê P. 2001. Geologia do depósito Igarapé Bahia / Alemão, Província Carajás, Pará. In: Jost H. (ed.). *Depósitos auríferos dos distritos mineiros brasileiros*. Brasília, DNPMP, ADIMB, p. 215-240.
- Williams P.J., Barton M.D., Johnson D.A., Fontboté L., de Haller A., Mark G., Oliver N.H.S., Marschik R. 2005. Iron oxide copper-gold deposits: geology, space-time distribution, and possible modes of origin. In: Hedenquist J.W., Thompson J.F.H., Goldfarb R.J., Richards J.P. (eds.). *Economic geology one hundredth anniversary volume 1905-2005*. Littleton, Society of Economic Geologists, p. 371-405.
- Winter C.J. 1994. Geology and base-metal mineralization associated with Archean iron-formation in the Pojuca Corpo Quatro deposit, Carajás, Brazil. PhD Thesis, University of Southampton, Southampton, 297 p.
- Xavier R.P., Araújo C.E.G., Dreher A.M., Taylor B.E. 2005a. The Paleoproterozoic intrusion-related Breves Cu-Au-(Mo-W-Bi-Sn) deposits, Carajás Mineral Province, northern Brazil: hydrothermal alteration, ore paragenesis and fluid evolution. In: *Simpósio Brasileiro de Metalogenia*, 1, CD-ROM.
- Xavier R.P., Wiedenbeck M., Dreher A.M., Rhede D., Monteiro L.V.S., Araújo C.E.G. 2005b. Chemical and boron isotopic composition of tourmaline from Archean and Paleoproterozoic Cu-Au deposits in the Carajás Mineral Province. In: *Simpósio Brasileiro de Metalogenia*, 1, CD-ROM.
- Xavier R.P., Dreher A.M., Monteiro L.V.S., Araújo C.E.G., Wiedenbeck M., Rhede D. 2006. How was high salinity acquired by brine associated with Precambrian Cu-Au systems of the Carajás Mineral Province (Brazil)? Evidence from isotope composition of tourmaline. In: Dall'Agnol R., Rosa-Costa L.T., Klein E.L. (eds.). *Symposium on magmatism, crustal evolution, and metallogenesis of the Amazonian Craton*, Abstracts volume and field trip guide, 34. Available online at: <https://www.sbgeo.org.br/home/pages/44/> (accessed on 7 March 2024).
- Xavier R.P., Wiedenbeck M., Trumbull R.B., Dreher A.M., Monteiro L.V.S., Rhede D., Araújo C.E.G., Torresi I. 2008. Tourmaline B-isotopes fingerprint marine evaporites as the source of high-salinity ore fluids in iron oxide copper-gold deposits, Carajás Mineral Province (Brazil). *Geology*, 36(9), 743-746. <http://dx.doi.org/10.1130/G24841A.1>
- Xavier R.P., Rusk B., Emsbo P., Monteiro L.V.S. 2009. Composition and source of salinity of ore-bearing fluids in Cu-Au systems for the Carajás Mineral Province. In: *Society for Geology Applied to Mineral Deposits Biennial Meeting*, 10, 272-274. Available online at: <https://e-sga.org/nc/publications/sga-biennial-meetings-abstract-volumes/2009-townsville/> (accessed on 21 December 2022).
- Xavier R.P., Monteiro L.V.S., Souza Filho C.R., Torresi I., Carvalho E.R., Pestilho A.L.S., Moreto C.P.N., Dreher A.M. 2010. The iron oxide-copper-gold deposits of the Carajás Mineral Province, Brazil: An updated review. In: Porter T.M. (ed.). *Hydrothermal iron oxide-copper-gold and related deposits: a global perspective*. Adelaide, Australian Mineral Foundation, p. 285.
- Xavier R.P., Trumbull R.B., Wiedenbeck M., Monteiro L.V.S. 2013. Sources of mineralizing fluids in Cu-Au systems from the Carajás Mineral Province (Brazil): constraints from in-situ microanalysis of hydrogen and boron isotopes in tourmaline. In: *Society for Geology Applied to Mineral Deposits Biennial Meeting*, 12(3), 1402-1405. Available online at: <https://e-sga.org/nc/publications/sga-biennial-meetings-abstract-volumes/2013-uppsala/> (accessed on 1 May 2023).
- Xavier R.P., Moreto C., Melo G.H.C., Toledo P., Hunger R., Delinardo M., Faustino J., Lopes A., Monteiro L.V.S., Previato M., Jesus S.S.G.P., Huhn S. 2017. Geology and metallogeny of Neoproterozoic and Paleoproterozoic copper systems of the Carajás Domain, Amazonian Craton, Brazil. In: *Society for Geology Applied to Mineral Deposits Biennial Meeting*, 14(3), 899-902. Available online at: <https://e-sga.org/nc/publications/sga-biennial-meetings-abstract-volumes/2017-quebec/> (accessed on 21 December 2022).
- Zang W., Fyfe W.S. 1995. Chloritization of the hydrothermally altered bedrock at the Igarapé Bahia gold deposit, Carajás, Brazil. *Mineralium Deposita*, 30, 30-38. <https://doi.org/10.1007/BF00208874>
- Zhang D., Audétat A. 2023. A plea for more skepticism toward fluid inclusions: Part I. Postentrapment changes in fluid density and fluid salinity are very common. *Economic Geology*, 118(1), 15-41. <https://doi.org/10.5382/econgeo.4966>